275 037

DESIGN AND ANALYSIS OF FOUNDATIONS
FOR PROTECTIVE STRUCTURES

Final Report

TECHNICAL DOCUMENTARY REPORT NO. AFSWC-TDR-62-9

January 1962
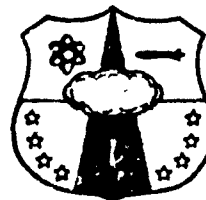
Pesearch Directorate
AIR FORCE SPECIAL WEAPONS CENTER
Air Force Systems Command
Kirtland Air Force Base
New Mexico

Project No. 1080, Task No. 10803

HEADQUARTERS
AIR FORCE SPECIAL WEAPONS CENTER
Air Force Systems Command
Kirtland Air Force Base
New Mexico

ARMOUR RESEARCH FOUNDATION
of
ILLINOIS INSTITUTE OF TECHNOLOGY
Technology Center
Chicago 16, Illinois

SWC
TDR
62-9

ARF Project No. K193
Contract No. AF 29(601)-2561
Project 1080

DESIGN AND ANALYSIS OF FOUNDATIONS

FOR PROTECTIVE STRUCTURES

Final Report

by

K. E. McKee
S. Shenkman

April 8, 1962

for

FOREWORD

This is the final technical report on Contract No. AF29(601)-2561, Project 1030, "Design and Analysis of Foundations for Protective Structures". The objective of this research program is to investigate the problems associated with the design and analysis of foundations for protective structures subjected to dynamic loads from nuclear blast. The current project, initiated at Armour Research Foundation in February 1960, is to a large extent, a continuation of research completed on an earlier contract, AF29(601)1161, of the same title (AFSWC Technical Report 59-56).

The first interim report, dated September 1960, and the second interim report, dated May 1961, cover the technical work up to those dates respectively. This publication reports in detail the research conducted subsequent to these earlier reports and, in addition, summarizes the results over the course of this research study. Since the two earlier reports were published as AFSWC Technical Note 60-36 and AFSWC Technical Note 61-14, it was not felt to be necessary to include details regarding the research reported earlier.

Personnel contributing to the work described in this report include A. Humphreys, T. M. Kiel, K. E. McKee, J. J. Ross, R. D. Roe and S. Shenkman. The authors thank Mr. C. Wiehle of Air Force Special Weapons Center for criticisms and suggestions which have materially aided this project.

ABSTRACT

The behavior of footings subjected to dynamic forces has been the subject of continuing research. Significant contributions have been made to the available knowledge through a combination of theoretical and experimental research.

Prior analytic studies have been based on an "engineering approach" which extended standard soil mechanics approaches to include dynamic behavior. This approach is reviewed and comparisons are made with the experimental results. To improve the theoretical results the influence of soil compressibility was investigated. These studies, which considered the formation of plastic stress waves below the footings, produce improved correlation with the experimental data.

Specific technical results on experimental studies included in this report are three-dimensional static and dynamic tests of footing with overpressure on the surrounding soil surface, two-dimensional static dynamic tests on inclined footings with overpressure on one side (a situation simulating that encountered in footings for arches and/or domes), three-dimensional static and dynamic tests with improved instrumentation to verify earlier results and to provide improved data. Also included is a presentation on the Dynamic Soil Facility, built by Armour Research Foundation and used for portions of this research.

PUBLICATION REVIEW

This report has been reviewed and is approved.

DONALD I. PRICKETT
Colonel   USAF
Director, Research Directorate

JOHN J. DISHUCK
Colonel   USAF
Deputy Chief of Staff for Operations

LIST OF ILLUSTRATIONS

LIST OF ILLUSTRATIONS, cont.

ARMOUR RESEARCH FOUNDATION OF ILLINOIS INSTITUTE OF TECHNOLOGY

LIST OF ILLUSTRATIONS, cont.

LIST OF ILLUSTRATIONS, cont.

LIST OF TABLES

Chapter 1

INTRODUCTION

This publication describes a continuing Armour Research Foundation program dealing with "the design and analysis of foundations for protective structures subjected to dynamic loads from nuclear blast." For all practical purposes, ARF research into the behavior of foundations subjected to dynamic loads represents a single continuing effort initiated in May of 1958. This report discusses the technical results obtained since the last formal report and also summarizes the earlier research. Every attempt has been made to make this report self-contained without undue repetition of previously reported material.

The results of the original study, conducted under Contract No. AF29(601)-1161, are summarized in AFSWC TR-59-54[1]*. More details regarding certain aspects of the research under that contract are found in the three phase reports: Phase Report I, "Recommendations for Full-Scale Tests"[2], issued October 15, 1958; Phase Report II, "Bibliography on Foundations Subjected to Dynamic Loads"[3], issued December 31, 1958; and Phase Report III, "Interim Technical Report"[4], issued January 31, 1959. Technical results on the present contract, No. AF29(601)-2561, have been presented in AFSWC TN 60-36[5] and AFSWC TN 61-14[6]. This report, in addition to serving as a final report on the current contract, includes the detailed technical results obtained since publication of AFSWC TN 61-14[6]. For further details the reader is referred to these earlier reports.

---

* Superscript numbers in parentheses cite references collected on pages 21 - 23.

A. TECHNICAL OBJECTIVES

The objective stated in the contract is "to investigate the problems associated with the design and analysis of foundations for protective structures which are subjected to dynamic loads from nuclear blasts." This general objective really indicates little regarding the technical direction of the program. The more specific goals of the present program are limited to consideration of spread footings (this is contrasted to foundations in general). At least from a qualitative point-of-view, it was postulated in the original program that behavior for all foundations could be explained by an understanding of the behavior of spread footings and pile foundations with other foundations considered as some combination of these two.

With regard to spread footings, the primary research goal has been to achieve an understanding of the behavior of footings on arbitrary soil to an arbitrary time-dependent force. The approach has been a combination of experimental and theoretical research. The theoretical research has attempted to develop analytical models which satisfactorily explain the footing behavior. The experimental research has been directed toward proving or disproving the suitability of the various analytical models. In addition, experiments have been designed to obtain qualitative information to aid in the modification of existing analytical approaches or in the development of new approaches.

B. THE PROBLEMS

The bearing capacity of footings acted on by dynamic loading has been the subject of numerous theoretical and experimental studies. For the most part, previous work has been directed toward the design of foundations for machinery and other equipment. Consequently, these studies, with rare exception, are related to vibratory behavior where the normal assumptions are that the displacements are recoverable and that the soil behaves in an essentially elastic fashion.

Research concerning the effect of loads having arbitrary time histories has not advanced as fast as research relating to time-dependent loading of a vibratory nature. Because of this lack of knowledge, the designers in considering non-vibratory loads have necessarily attempted to be conservative. In some instances, this has lead to extremely complex and costly designs. However, since earlier methods are in certain respects irrational, what is thought to be conservative, may in fact be unsafe. The 1954 work of Landale[7, 8] at MIT represents the only research on footings subjected to non-vibratory dynamic loads known to the authors, which existed prior to the initiation of the research at ARF in 1958. Prior to that time, footings for dynamic loads were designed as if the loads were static with some variations in soil properties being attributed to the dynamic aspects of the loading (see for example OCDM Method A[9]).

Since 1958, a number of agencies have initiated research into this problem area. Related experiments currently are ' q conducted at the Nav': Civil Engineering Laboratory, Port Huene California; University of Illinois, Urbana, Illinois; Massachusetts Institute of Technology, Cambridge, Mass., and the Waterways Experiment Station of the U. S. Army Corps of Engineers, Vicksburg, Mississippi. Analytical studies have also been carried out by American Machine & Foundry, University of Illinois and the Waterways Experiment Station.

C. REPORT ORGANIZATION

This report serves the dual purpose of a final report on the entire project and a detailed technical report on research completed since the last interim report. The organization of this report reflects this dual function.

Chapter 2 contains a general discussion of the behavior of spread footings subjected to static and dynamic concentric vertical forces. Chapter 3 reviews the specific studies which have been completed and which are reported in greater detail in the Appendices. Chapter 4

reviews the project and summarizes the results which have been obtained.

The dynamic soil facility, recently constructed by ARF, is described in Appendix A. Appendices B and C describe experimentation using the dynamic soil facility. Appendix B considers three-dimensional static experiments with and without surface overpressure. Appendix C details three-dimensional dynamic experiments with and without surface overpressure. Appendix D describes two-dimensional experiments conducted in the glass sided container. Of particular interest here are the experiments with inclined footings having static overpressure on one side. In Appendix E, the engineering approach for predicting dynamic footing behavior is considered. The effect of soil compressibility on the behavior of footings subjected to dynamic loads is considered in Appendix F.

Chapter 2

SPREAD FOOTINGS SUBJECTED TO CONCENTRIC VERTICAL FORCES

In general, the concern here is with the behavior of rigid footings on
arbitrary soils subjected to arbitrary time-dependent forces. Assumption
of a rigid footing eliminates any need for considering the actual structural
design of the footing as well as the stress distribution below the footing.
The loads of interest range from those associated with zero footing dis-
placements to displacements the order of the footing size. The basic re-
quirement is to predict the displacement-time response of dynamically
loaded footings.

In reviewing the overall approach to footing behavior adopted during
the course of this program, attention is limited to footings subjected to
vertical concentric loadings since this represents, in a sense, standard
conditions and is the subject of much current theoretical and experimen-
tal research. Chapter 3 will review some of the rese   which has been
aimed at generalizations from this standard. The dyn. .ic loads of inter-
est are a relatively short duration (in order of seconds) and are non-
vibratory in nature. The short load duration means that footing settle-
ments caused by consolidation (long time effects) of the soil as considered
for ordinary footing design are not of interest. The relatively abundant,
though far from conclusive, literature relating to the behavior of footings
subjected to vibratory loads is of little value for this study. Possible
applications of these methods for predicting limited footing displacements
were investigated by Selig[1, 10, 11] in connection with this research and
making use of the available literature. A theoretical approach was devel-
oped and applied to the experimental results. Unfortunately, the correla-
tion was poor. It is sufficient to state that this approach will not be
considered further herein, although further studies should be made along
these lines.

Since emphasis on this project is on theories explaining footing be-
havior, soil properties have been reduced to a secondary role. Soil para-
meters have been used, e.g., cohesion (c), angle of internal friction (ϕ),

and unit weight (γ) from normal soil mechanics, with little concern for how the values would be obtained. It is sufficient for the purposes of this report to assume that realistic values have been or are being obtained by other research. It should be observed that this represents no small task particularly since the dynamic properties are require... Even further it must be recognized that the formulation of the theory depends on the nature (not the values) of the soil parameters and that even the necessary parameters may vary for the dynamic conditions.

A. STATIC BEHAVIOR

The literature provides many analyses for footing failures under static loads caused by shear failure in the soil below the footing. The theory of plasticity includes general methods of approach for such problems. For this research, the methods considered for static loading are the simplified solutions normally used in standard soil mechanics. The one-sided failure modes used were Andersen's[12] analysis and a modification of the Krey analysis developed by Hasson and Vey[13, 14]. For the sided or symmetrical failure patterns, Terzaghi's[15, 16] formula was used.

These three approaches have been found to give similar (within 10 percent of each other) values for bearing capacity, i.e., the first maximum on a static load displacement curve. Over the range of parameters of interest, Andersen's formula gives a load capacity which is essentially that given by the Terzaghi formula, and Hasson demonstrated that his formulation of Krey's method gives capacities similar to those given by Terzaghi's formula.

For static bearing-capacity analyses, the Terzaghi formula is normally accepted. The approximate formula developed by Terzaghi for infinitely long footings with rough bases is:

$$\frac{P_s}{A} = c\,N_c + \gamma D N_q + \frac{1}{2}\,\gamma B N_\gamma \qquad \text{(Eq. 1)}$$

where

B	=	footing width,
c	=	cohesion,
D	=	depth of burial,
$\frac{P_s}{A}$	=	static bearing capacity, and
γ	=	density of soil.

The quantities N_c, N_q and N_γ are dimensionless bearing-capacity factors, depending only on the angle of internal friction, ϕ. The value of each of these factors can be plotted as a function of ϕ[15, 16]. For square or circular footings, the approximate formula is modified by empirical coefficients.

In this research, interest in static footing behavior extends substantially beyond the static bearing capcacity considered above. As a preliminary approach to the dynamic problem, the force-displacement curve under static loads should be known not only up to the initial ·· value (the static bearing c·pacity, but beyond to displacements of the o of magnitude of the footi g s ze. Experimental studies of footing behavior, e.g., Golder[18] and Myerhof[19], have normally considered only the bearing capacities. The only experiment data available for the entire force-displacement history for statically loaded footings are those initiated under this project[1, 5, 6, 17, 20].

Under a constantly increasing static load one might expect that the load-displacement relationship could be idealized as shown in figure 1. From the tests, it has been observed that unloading occurs on a slope steeper than the original. The first portion of the curve would represent settlement which would govern until soil failure. Figures 2 and 3 present typical experimental results obtained on this project for 3 x 3-in. and 4 x 4-in. footings on dense, dry, Ottawa sand. Certain deviations from the idealization of figure 1 will be observed, but basically the experimental results show distinct settlement and soil failure phases. Generally these experimental studies gave satisfactory results. As shown by figures 2 and 3, the data were reasonably reproducible and the measured bearing capacities have been shown to agree with the theoretical values.[17]

Cal ulation of stati . settlements was investigated by Selig[1, 10].
Static stress and settlement solutions[21, 22] are available for a rectangu-
larly loaded half-space. Selig used a truncated rectangular pyramid having
a uniformly stressed horizontal cross section to develop a mathematical
model applicable to soil. The development followed assumptions used for
footing vibration. e.g., work by Pauw[23]. For this project there is no
need to go into detail regarding this study, other than to say that the re-
sulting theory did not correspond to the experimental results[1]. As a
result the only portion of the load-settlement curve which can be predicted
is the bearing capacity, i.e , the first peak. Because of this situation, the
load-displacement. based on the experimental results, as shown in figures
2 and 3, are used in connection with the theoretical research.

Current experimental research using improved apparatus confirms
the earlier results with regard to bearing capacity and load-displacement
curves. As part of the work reported in Appendix B, the earlier tests are
essentially repeated using two linear variable differential transformers (LVDTs)
(with linear ranges ± 0.15-in. and ± 1.0 in.). This instrumentation ver-
ified the earlier results and provided additional improved knowledge re-
garding details of the response.

The influence of overpressure on the surface surrounding the footings
has been incorporated into the earlier analyses. It is only on the recent
research that experimental data taking overpressure into account has be-
come available Using the dynamic soil facility built by ARF (see Appendix
A), tests on three-dimensional footings with overpressure on the surround-
ing surface were conducted (see Appendix B). These experiments were
correlated with theory. Some two-dimensional footings (see Appendix D)
were tested with overpressure on only one side of the footing.

B. DYNAMIC BEHAVIOR

The behavior of footings, or more precisely the soil below the footings,
when subjected to dynamic loads can be considered in a number of ways. In
1958 ARF[2] utilized the standard soil mechanics formulas for statically
loaded footings to include the influence of overpressure on one or both sides

ARMOUR RESEARCH FOUNDATION OF ILLINOIS INSTITUTE OF TECHNOLOGY

of a footing. This extension represented an improvement over the state-of-the-art for footing design in use at that time. Previously footing designs for protective structures had been based on normal static approaches with increases introduced in the cohesion to account for the dynamic effects, e.g., OCDM Method A[9].

Only one earlier study relating to this type of dynamic behavior is known to the authors. Landale[7, 8] conducted a theoretical and experimental investigation at MIT in 1954. Unfortunately this study was limited in scope, therefore, generalizations from these results were difficult. Landale's pioneer efforts have served as the basis for several approaches used in this research.

Earlier in the ARF research[4, 24], an extension to the classic soil mechanics theories was postulated to take into account the dynamic aspects of the behavior, the so-called "engineering approach". This postulation lead to a theory based on an extension to time-dependent loads of Andersen's theory[12] for one-sided failure. The major assumpt   ntroduced for this theory ar :

1. The failure surface under dynamic loads will be the same as the surface determined by application of the initial value of the overpressure as a static surface pressure.

2. The soil is incompressible.

3. The resistance offered to footing movement is a function only of displacement.

4. The behavior of the soil is governed by the density, γ ; cohesion, c and angle of internal friction, ϕ, where c and ϕ may themselves be functions of many parameters relating to the soil and the conditions of loading. By considering the motion of the failure mass of soil, a differential equation was established based on the motion of the footing and the soil mass. Solutions of this equation allow prediction of the footing displacements, investigation of inertia effects, influence of soil parameters, etc.

5. The resistance is rigid plastic in form.

The general statement of this engineering approach and the development of the equations were presented in 1959[1]. This presentation allowed

for overpressure, buried footings, soil with both c and φ, considered primarily a rigid-plastic form of the resistance (assumption 5). The latter restriction was a function of available information and allowed solutions based on knowledge of only the static bearing capacity. For this reason the assumptions listed and the subsequent consideration of the "engineering approach" are more general than the original, since general forms for the resistance were investigated.

Appendix E presents the development of the engineering approach and compares the results with available experimental data. Consideration is limited to concentric vertically loaded footings with equal overpressure over the entire soil surface. This approach has been extended to eccentric loads[5], two-sided failures[5], and failure surface locations, taking into account the inertial effects[1]. However, in Appendix E, attention is limited to the primary formulation of the engineering approach. Utilizing a very similar set of assumptions Triandafildis[25] in 1961 arrived at a similar theory based on one-sided failures for footings on a cohesive soil (i.e., φ = 0). Based on Triandafildis' results Wallace[26,7] developed an approach incorporating two-sided failure.

At the outset of this theoretical research there was essentially no experimental data relating to dynamic loads on footings. During 1959 a series of dynamic tests were conducted at ARF[1,17] as part of this research. These dynamic experiments made use of a dropped weight to apply the loading. These results, although primarily qualitative in nature, suggested the inability of the mathematical models to explain the experimental results.

One attempt to answer those questions under this project was research by Hodge[5, Appendix B] based on a classic plasticity approach to the problem. The possibility of a theoretical approach was established under certain restrictive assumptions and an example was presented. Greater generalization to extend the solution to other problems seems to be possible although the actual labor of obtaining such solutions is expected to increase substantially. The overall results are most interesting since the possibility of this type of theoretical approach was established. Hodge's work was paralleled by Spencer[28] in England who used a different method of solution for the same general formulation of the problem.

ARMOUR RESEARCH FOUNDATION OF ILLINOIS INSTITUTE OF TECHNOLOGY

-10-

A second attempt to answer these questions was the initiation of an experimental study designed to obtain quantitative data suitable for evaluation of the theoretical approach. A dynamic loading apparatus was developed for applying controlled time-dependent forces to small footings. Instrumentation was incorporated into the system to measure the force-time history applied to the footings and the resulting displacement-time history. Detailed descriptions of this apparatus are available[6, 29, 30] but, for the present purposes, interest is limited to the fact that suitable experimental results were developed. Subsequent improvements have been introduced in the experimental approach, and further experiments conducted (Appendix C). These experiments, past and present, resulted in an abundance of quantitative data, i.e., force, displacement, and acceleration records as a function of time, for footings tested under highly controlled conditions. The experiments confirmed the earlier observations regarding the limitations of the engineering approach and indicated that soil compressibility could not be ignored.

A second theoretical approach is reported in Appendix F. Attention there is devoted to consideration of the soil compressibility for vertically loaded footings. With the exception of Landale's consideration[7, 8] soil compressibility under dynamic loads has not been considered previously. There is, however, an abundance of literature relating to plastic stress wave propagation which represents a related problem and a point from which to initiate the theoretical approach.

Chapter 3
SPECIFIC STUDIES

This chapter reports the specific research studies conducted since issue of the interim report in May 1961. Details of this research are reported in the six appendices to this report. In discussing these studies herein, the intent is made to point out their advantages and limitations with particular emphasis on the association with the overall project. Technical details are avoided insofar as possible in the considerations which follow.

A.   DYNAMIC SOIL FACILITY

Appendix A describes the dynamic soil facility built by ARF. This is a multipurpose facility, the potentialities of which have yet to be exploited. Basically the facility is a 48-in. diameter, 300-psi pressure vessel. Static or dynamic pressure can be applied over the su ⁀ of soil filling the vessel Concentrated static or dynamic forces can . applied in arbitrary directions or at arbitrary points within the facility, independently or in combination ith the surface pressures. Provisions have been included for making suitable measurements within the facility. In designing this facility every attempt was made to keep it as versatile as possible so that it will be useful for many problem areas. Appendix A describes the general facility where footing tests represent but one possible application. Specific tests on footings in this facility are described in Appendices B and C.

B.   GENERAL EXPERIMENTAL PROCEDURE

All of the two- and three-dimensional experiments reported in this study were performed on a dense, air-dry Ottawa sand. The grain-size distribution for this sand is shown in figure 4.

Three-dimensional experiments were performed in the dynamic soil facility. Prior to each experiment, the bed was vibrated by inserting an immersion-type concrete vibrator into the bed at a point near the wall of

the sand container. The bed was levelled after three minutes of vibration
and the vibrator withdrawn after an additional one-half minute. Using this
procedure, the average density of the sand bed. based on the volume oc-
cupied by the total weight of sand, was 109.1 pcf. Surface density measure-
ments, using a scoop density device, were made throughout the experimen-
tal program in order to check on the reproducibility of the bed.

Two-dimensional experiments were performed in a glass-sided con-
tainer. These experiments involved the use of both surface and partially
buried footings. In the experiments involving surface footings, the sand
was poured into the glass-sided container and vibrated for two minutes by
attaching a concrete vibrator to the top of the container. The soil con-
tainer was then turned on its side to permit placement of a rectangular grid
of black sand (spaced at 9/16-in. intervals) on one surface. The container was
then returned to its vertical position, and the footing placed on the soil sur-
face. This procedure was slightly modified for the partially buried footings
in that the footing was in position before pouring sand into the container.
Average sand densities for each experiment are listed   ble D-1.

C.   THREE-DIMENSIONAL STATICALLY LOADED FOOTINGS

Appendix B describes the three-dimensional static experiments.
These experiments consisted of vertical loading of surface footings, both
with and without a uniform static overpressure on the surface surrounding
the footing. Load application was provided by a gear box which was manu-
ally operated in the initial experiments, and motor-driven in the later ex-
periments.

Applied loads and resulting footing displacements were measured and
the results plotted in the form of resistance-displacement curves. This
enabled a comparison of bearing capacity with and without surface over-
pressure.

D.   THREE DIMENSIONAL DYNAMICALLY LOADED FOOTINGS

The ARF dynamic loading apparatus[6] was used in applying dynamic
loads to three-dimensional footings. The experiments, reported in Appen-
dix C, consisted of concentrated dynamic loads on surface footings with and
without a uniform static overpressure on the soil surrounding the footing.
Instrumentation. consisted of a high sensitivity force washer, two linear
variable differential transformers, and four accelerometers; transducer
output was recorded on a Consolidated Electrodynamics Corporation oscil-
lograph. The maximum applied loads and resulting footing displacements
are tabulated, and typical force-time, displacement-time and acceleration-
time records are presented in the appendix.

E.   TWO-DIMENSIONAL EXPERIMENTS

Appendix D presents the results of two-dimensional experiments.
These studies were planned as a continuation of the previous two-dimensional
experiment. The present experiments consisted of e   lly loaded sur-
face footings and statically and dynamically loaded partially buried footings.
Sequence photographs for a number of static and dynamic experiments are
presented in the appendix. In addition, high-speed motion pictures are
available for six dynamic experiments.

F.   "ENGINEERING APPROACH" TO DYNAMIC BEHAVIOR OF FOOTINGS

Appendix E presents the "engineering approach" for dynamic footing
response. Much of the information contained in this appendix has been pre-
viously published. The presentation contained in this appendix is somewhat
more general in nature than those previously presented. Attention has been
limited to one-sided failure of footings subjected to vertical loads and the
development carried through for that simple case. Earlier studies have ex-
tended this type of approach to two-sided failure and have considered inclined
and eccentric loads. Presentation of the basic case, i.e , vertical loads;
and comparison with the available experimental data demonstrates the limi-
tation of this approach. Basically, the "engineering approach" alone does

ARMOUR RESEARCH FOUNDATION OF ILLINOIS INSTITUTE OF TECHNOLOGY

-15-

not provide an adequate explanation of footing behavior. As a result of this conclusion, attention has been given to soil compressibility as one means of improving the ability to predict footing behavior.

G.   EFFECT OF SOIL COMPRESSIBILITY

Appendix F presents an attempt to take into account soil compressibility in predicting footing behavior. Several alternate approaches are developed and sample calculations carried out. Assignment of values to the parameters representing physical properties for the soil represents the most difficult problem. The values used in the sample calculations were selected primarily to give reasonable values and variations, without particular attention to the physical significance of the values selected.

Because of the lack of accurate parameters, no quantitative correlation between these theories and the experiments could be anticipated. From a qualitative point of view there were many similarities between the experimental and theoretical results. This type of theoretical approach appears to offer advantages in explaining the initial movement of the footing; however, additional research is required to establish the significant parameters.

Chapter 4
SUMMARY

Numerous detailed investigations, both theoretical and experimental have been conducted since the inception of this research by ARF in May of 1958. This report is one of many publications resulting from this research; the specific studies reported herein are only those conducted since publication of the previous phase report, AFSWC TN-61-14, May, 1961. This chapter will attempt to summarize the entire research effort.

The philosophy of this research has been based on a combined approach, i.e., theory and experiment. Initially, a theory was proposed and used in planning the experiments. Subsequently, the experimental results were used to check the theories and to indicate the direction of future theoretical developments. This partnership has provided considerable insight into the behavior of footings subjected to dynamic loads.

Prior to the initiation of this research, dynamic loaded footings were designed by static formulas with the soil parame modified by a factor to account for the dynamic aspects. The initial theoretical work was based on the assumption that the soil below a dynamically loaded footing would fail along shear surfaces and that the dynamic effects could be introduced by considering the inertia effects. The "engineering approach" is the embodiment of this assumption.

As pointed out, the experimental results demonstrated the inadequacy of the engineering approach to predict dynamic footing behavior—the predicted displacements may be greater or less than the experimental results. To overcome these inadequacies in the engineering approach, the soil compressibility has been considered.

Studies relating to soil compressibility are preliminary in nature. Qualitative comparisons of theory with experiments appear reasonable, although it should be noted that, since much of the suitable experimental data was obtained near the conclusion of this research, the available time precluded making a thorough study of the results.

Intuitively, one might anticipate that the ultimate explanation of the behavior of dynamically loaded footings may be soil compressibility followed by the formation of shear surfaces. Although at the present time there is no proof of this combined theory, it appears to be a reasonable explanation based on observed behavior in the two-dimensional experiments. In any case, continuing research is required to develop an acceptable theory.

The experimental studies have provided data used in evaluating the theoretical approaches considered. Considered independently, the experimental results have made considerable contributions to available knowledge. Suitable quantitative and qualitative data have been obtained for a variety of controlled loadings. The major limitation with regard to these experiments is the relatively small size of footings which can be tested in the laboratory, e.g., for the 4 ft diameter container used for the three-dimensional experiments the size for surface footings has been shown to be limited to less than 1/7 of the container dimensions or 6 in. square. As with any experimental research, certain limitations exist in the approach, e.g., instrumentation, soil placement and test procedures. In reporting spec experimental studies, the attempt is made to provide sufficient detail that the experiments can be reproduced. In addition, an attempt is made to indicate potential limitations.

A general summary can be considered in four parts.

(1) Three-dimensional footing tests for static loads have provided a variety of controlled experimental data not previously available. For example, the data reported in Appendix B represent the only available data for footings with pressure on the surrounding surface.

(2) Two-dimensional static tests in the glass-sided container have provided information regarding footing behavior. Although the quantitative data have been shown to be related to that for long footings, the value of these two-dimensional experiments is primarily qualitative in nature. The mode of failure in the soil below the footing can be clearly observed. This is of particular value for unusual loadings, e.g., eccentric and inclined loads. An example of this application is shown in Appendix D, where inclined footings with overpressure on one side were tested.

-18-

(3) Three-dimensional dynamic footing studies have provided quantitative data against which theories can be evaluated. Measurements of the applied force-time along with the resulting displacements and accelerations have been refined. Appendix C reports the most recent of these experiments where static pressure was applied over the surface.

(4) Two-dimensional footings subjected to dynamic forces have provided demonstrations of the effects of dynamic loading as compared with static loading. The resulting Fastax photography enable the researcher to watch the progress of failure beneath a dynamically loaded footing. The results of Appendix D are pointed out as an example of this type of information.

As a result of research conducted to date, there is substantial information available regarding dynamically loaded footings. This increased knowledge has served to disprove assumptions which appeared reasonable earlier in the program Thus, more questions have been raised than answered. This latter aspect is an important product of a research study. Continuing research i ARF and others can be expected to resul : clear understanding of th dynamic behavior of footings and hence in p. cedures suitable for use by signe

REFERENCES

1. McKee, K. E., Design and Analysis of Foundations for Protective Structures, AFSWC-TR-59-56, October 1959.

2. McKee, K. E., Design and Analysis of Foundations for Protective Structures, Phase Report No. 1, Recommendation for Full Scale Tests, November 1958.

3. McKee, K. E., Design and Analysis of Foundations for Protective Structures, Phase Report II, Bibliography on Foundations Subjected to Dynamic Loads, Armour Research Foundation, Chicago, December 1958.

4. McKee, K. E., Design and Analysis of Foundations for Protective Structures, Phase Report III, Interim Technical Report, Armour Research Foundation, Chicago, January 1959.

5. McKee, K. E., Design and Analysis of Foundations for Protective Structures, Interim Technical Report, AFSWC-TN-60-36, Armour Research Foundation, Chicago, September 1960.

6. McKee, K. E., Design and Analysis of Foundations for Protective Structures, Second Interim Technical Report, AFSWC-TN-61-14, Armour Research Foundation, Chicago, May 1961.

7. Landale, T. S., Investigations into the Dynamic Bearing Properties of Cohesionless Soils, Thesis, Massachusetts Institute of Technology, Cambridge, Massachusetts, September 1954.

8. Massachusetts Institute of Technology, The Behavior of Soils Under Dynamic Loading, AFSWP 118, August 1954.

9. Federal Civil Defense Administration, Recommended FCDA Specifications for Blast-Resistant Structural Design (Method "A"), TR-5-1, January 1958.

10. Selig, E. T., Response of Foundations to Dynamic Loads, Thesis, Illinois Institute of Technology, Chicago, January 1960.

11. Selig, E. T., _Review of Literature Concerning Behavior of Foundations Under Dynamic Loads_, Symposium on Foundation Engineering, Indian Institute of Science, January 1961.

12. Andersen, P., _Substructure Analysis and Design_, p. 81, The Ronald Press Company, New York (1956).

13. Hasson, R. H., and Vey, E., _An Investigation of Krey's Method for Bearing Capacity_, First Pan American Conference on Soil Mechanics and Foundation Engineering, Mexico, Vol. II, 1959.

14. Hasson, R. R. H., _An Analytical Investigation of Krey's Theory of Foundation Failure_, Thesis, Illinois Institute of Techrology, Chicago, June 1959

15. Terzaghi, Karl, _Theoretical Soil Mechanics_, p. 124, John Wiley and Sons, Inc., New York, (1943).

16. Terzaghi, Karl and Peck, Ralph, B., _Soil M ~ nics in Engineering Practice_, John Wiley and Sons, New York, (1 .

17. Selig, E. T., and McKee, K. E., "Static and Dynamic Behavior of Small Footings", _ASCE Proceedings_, Journal of the Soil Mechanics Division, December 1961.

18. Golder, H., "The Ultimate Bearing Pressure of Rectangular Footings", Paper No. 5274, _Institution of Civil Engineering Journal_, London, England, 1942.

19. Meyerhof, G. G., "An Investigation of the Bearing Capacity of Shallow Footings on Dry Sand", Vol. I, _Proc._, Conference of Soil Mechanics and Foundation Engineering, (1948).

20. Mulay, J., "Laboratory Studies of the Bearing Capacity of Footings on Sand", Thesis, Illinois Institute of Technology, 1960.

21. Baussinesq, J., Academic des Sciences, Comptes Rendus, 114, 1465. (1892).

22. Love, A. E. H., "The Stress Produced in a Semi-Infinite Solid
     by Pressure on Part of the Boundary", Trans. Royal Soc.,
     London, England, Series A, 228, 377, (1929).

23. Pauw, A., "A Dynamic Analogy for Foundation-Soil Systems",
     Symposium on Dynamic Testing of Soils, p. 3-34, ASTM Special
     Technical Publication No. 156, (1954).

24. McKee, K. E., "Design and Analysis of Foundation for Protective
     Structures", Proceeding of the Fourteenth Panel Meeting on
     Blast Effects on Building and Structures and Protective Con-
     struction, October 1958.

25. Triandafildis, G. E., Analytical Study of Dynamic Bearing
     Capacity of Foundations, DASA 1189, University of Illinois,
     January 1961.

26. Wallace, W. L., "Displacement of Long Footings by Dynamic
     Loads", Soil Mech. and Foundations Div.,   87 No. SM5,
     October 1961.

27. McKee, K. E., Discussion of Paper, "Displacement of Long
     Footings by Dynamic Loads", by W. L. Wallace.

28. Spencer, A. J. M., "The Dynamic Plane Deformation of an Ideal
     Plastic-Rigid Solid", J. Mech. Phys. Solids, 8, 262-279, (1960).

29. McKee, K. E., "Foundations for Protective Structures", Proc.
     29th Shock Vibration Symposium, 1960.

30. Shenkman, S., and McKee, K. E., "Bearing Capacity of
     Dynamically Loaded Footings", Symposium on Soil Dynamics,
     ASTM, June 1961.

31. Shenkman, S. and McKee, K. E., Report on R5318, Armour
     Research Foundation, 1961.

32. Love, A. E. H., A Treatise on the Mathematical Theory of
     Elasticity, 4th Edition (1927). Dover Publications, (1944).
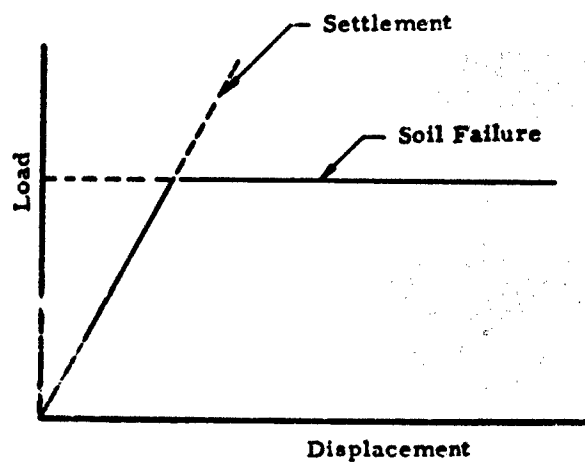
Fig. 1 IDEALIZED LOAD-DISPLACEMENT FOR SPREAD FOOTINGS
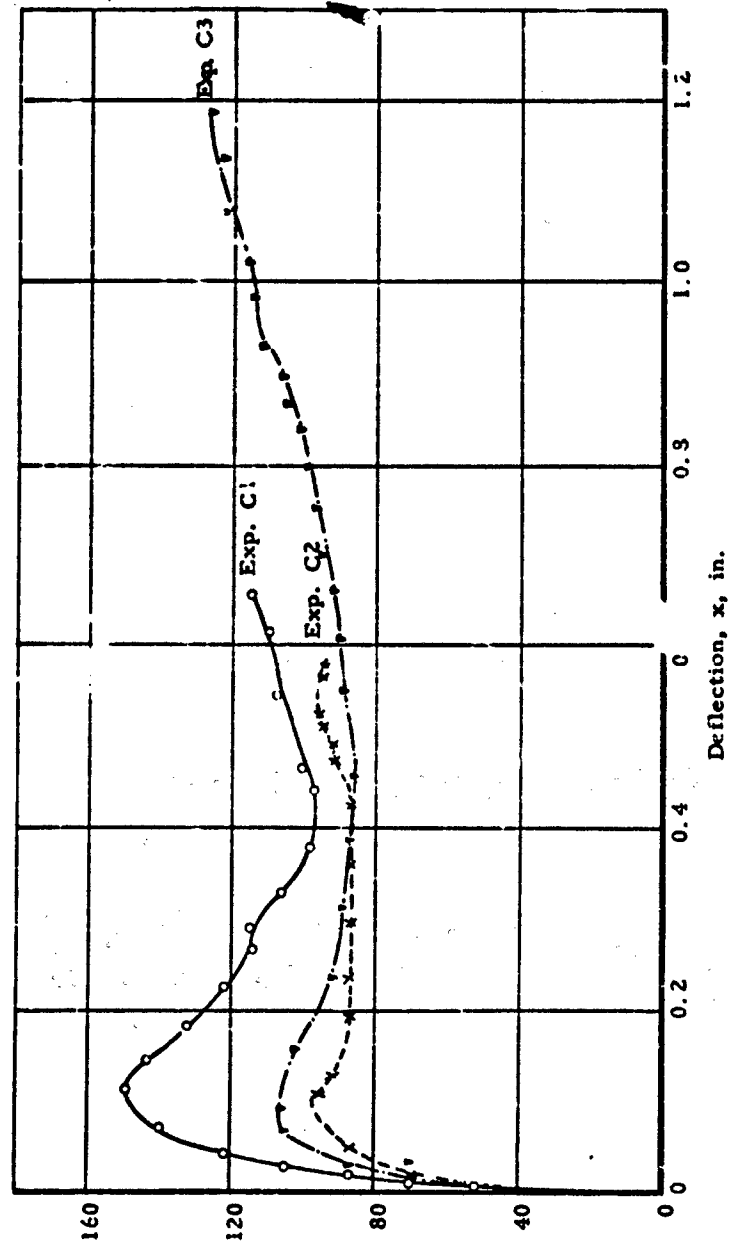
Fig. 2 STATIC LOAD-DEFLECTION FOR 3-IN. SQUARE FOOTINGS
DRY DENSE OTTAWA SAND
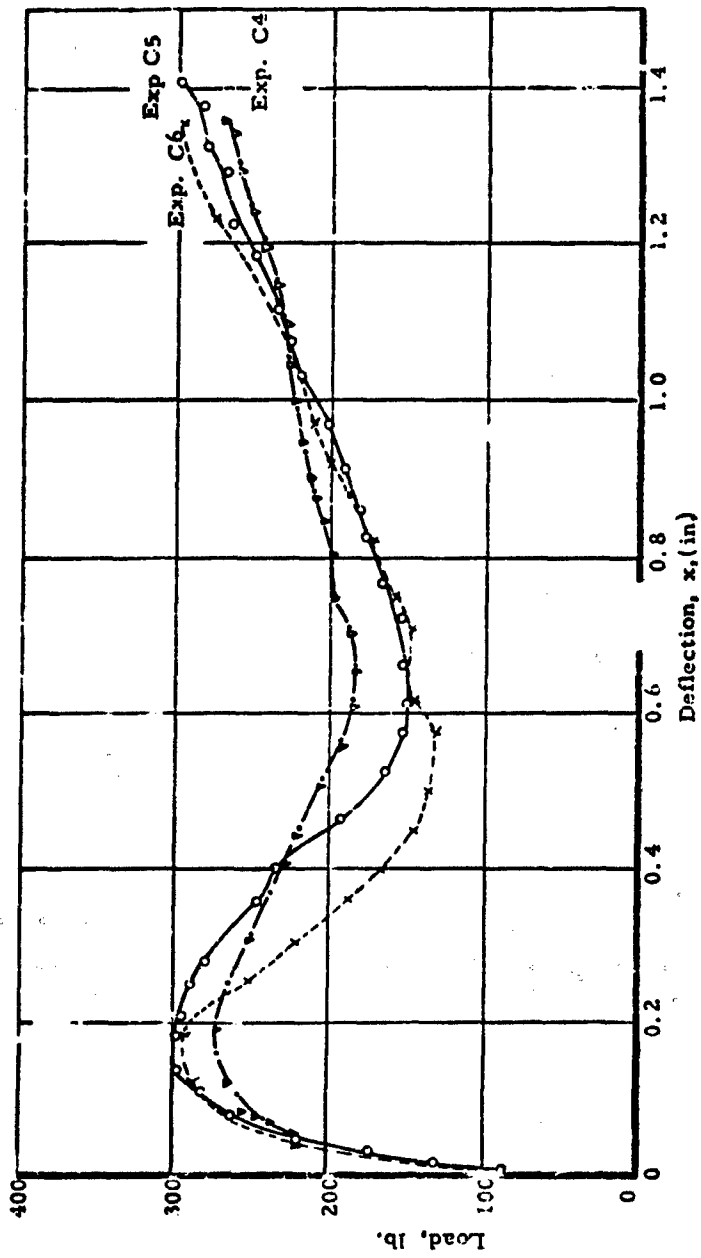
Fig. 3 STATIC LOAD-DEFLECTION FOR 4-IN. SQUARE FOOTINGS, DRY DENSE OTTAWA SAND
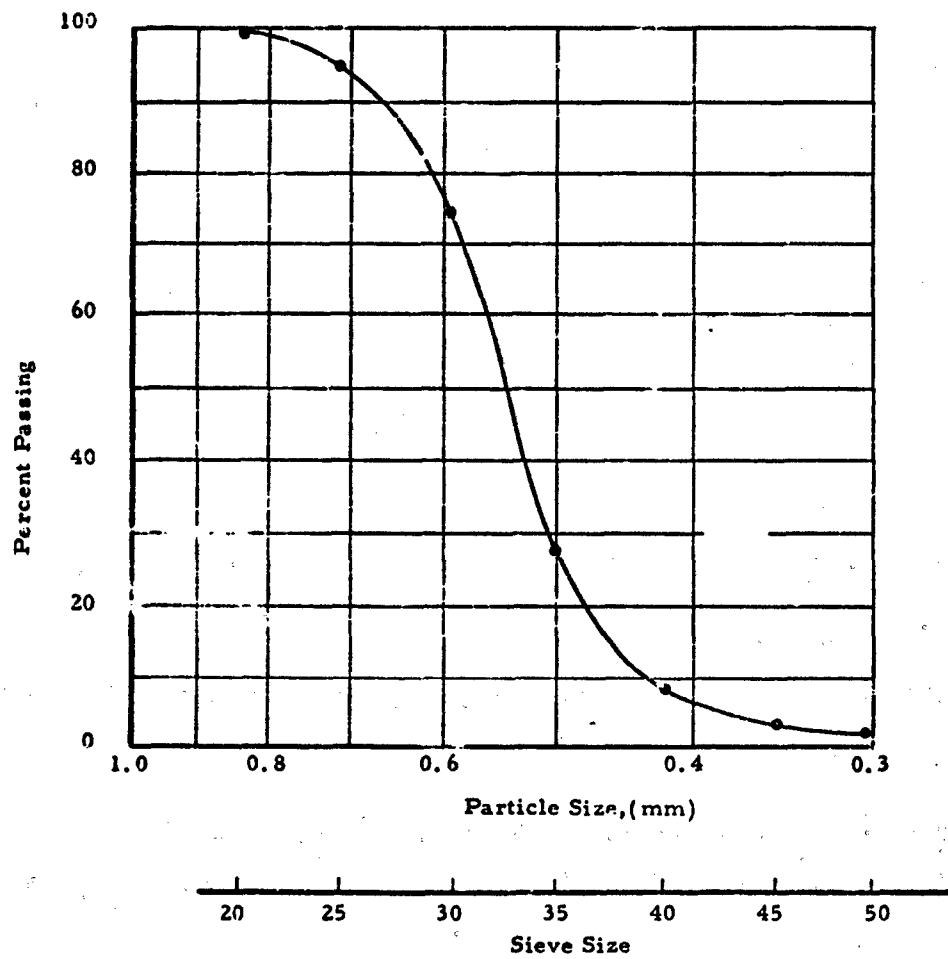
Fig. 4 GRAIN-SIZE DISTRIBUTION FOR OTTAWA SAND

APPENDIX A

DYNAMIC SOIL FACILITY

by

S. Shenkman and K. E. Mckee

APPENDIX A

DYNAMIC SOIL FACILITY

by

S. Shenkman and K. E. McKee

Since 1957 Armour Research Foundation has conducted a number of research programs dealing with soil-structure interaction and dynamic soil mechanics. Primary impetus for an understanding of these areas stems from protective structures -- in particular from the emphasis on hard and superhard facilities which has resulted in "digging in". The least understood aspects of these problems relate to the soil: there is practically no knowledge regarding stress wave transmission or soil-structure interaction.

Research has been severely hampered by the lack of suitable experimental data. This limitation was due, in part, to the conflicting requirements on any experimentation, i.e., control, cost, size, range, scale. A program conducted by ARF for the Office of Civil and Defense Mobilization[A-1]* considered existing experimental tools for such studies an attempt to select the most suitable. This research as well as experience with various experimental studies in the ARF Soil Mechanics Laboratory made certain requirements for a dynamic soil facility apparent to the ARF staff. Such a facility should allow investigation of the effects of static surface overpressures on surface and underground structures, buried cables and mine fuses; and evaluation of soil stress and strain gages.

A proposal for construction of a facility with these capabilities was submitted to ARF in August, 1960[A-2]. In 1961, the Foundation sponsored the design, construction and preliminary testing of the facility.

In the Dynamic Soil Facility, soil control is limited by existing knowledge as well as practical considerations, while control of the loadings is primarily a function of the limitations of the instrumentation used. The experimental setup is felt to be direct enough to reduce second-order effects, permitting proposed theories to be established or disproved.

---

*Superscript numbers in parentheses cite references collected at the end of this appendix.

Description of Facility

Basically, the Armour Research Foundation Dynamic Soil Facility is a pressure vessel fitted with sufficient openings to permit a wide variety of small soil-structure interaction experiments. Design of the pressure vessel is such that an internal pressure up to 300 psi may be applied.

The basic structure, sketched in figure A-1, is a 48-in. OD by 48-in. high cylinder with a fixed dished head on the bottom and a removable flat head on top. Auxiliary portions of the structure include:

1. two 8-in. diameter openings on opposite sides of the vessel intended for investigations of underground tunnel liners;

2. seven 2-in. diameter openings on one side of the vessel to provide for instrumentation connectors;

3. a 6-in. diameter opening on the vessel bottom to allow rapid removal of soil from the vessel;

4. a 10 in. diameter opening on the vessel bottom : studies related to the fluidization of soils and other granular materials;

5. four 6-in. diameter openings in the vessel head intended for dynamic pressure applications or for positioning models on the soil surface;

6. a 12-in. diameter opening in the vessel head for use in applying concentrated static and dynamic loads; and

7. two vertical structural channels connected to opposite sides of the vessel to be used as a loading frame.

In addition, two 1/2-in. openings are provided in the vessel head for static pressure application and an air pressure gage. All of the openings, while primarily intended for these uses, are expected to find numerous additional applications. A photograph of the pressure vessel with the head removed is shown in figure A-2. Figure A-3 shows the vessel with the head in place.

Facility Applications

The overpressure associated with nuclear blast influences the be-
havior of the soil and hence structures set on or in the soil. The facility
enables laboratory studies to be conducted using a pressure over the surface
of the soil bed. This pressure may be time dependent.

Static pressures on the soil surface have been obtained by placing a
rubber diaphragm on the surface of the bed and sealing the edges of the dia-
phragm to the wall of the vessel. For low surface pressure applications
(up to 100 psi), static overpressures have been obtained using a standard
air compressor. Higher pressures (up to 300 psi) have been applied en-
tirely by a nitrogen cylinder, regulated to the desired input, or coupled with
an air compressor.

Dynamic surface pressures are expected to be applied by using water-
filled bags on the soil surface. The hydraulic system designed for the dy-
namic footings experiments on an AFSWC sponsored pr · m(A-3) (Fig. A-4)
should provide controls of load application rate.

A suitable dynamic pressure can be provided by a water-filled bag
covering the soil surface in place of the hydraulic cylinder. Conceptually,
this system should be satisfactory; practically, because of such factors as
the large volume of water and vessel deformation, it may be necessary to
increase the size of the various system components. As for the dynamic
force apparatus, preliminary experimentation will be necessary to establish
the methods of control, ranges of variables, etc.

A motor-driven gear box has been used to apply concentrated static
loads to models on the sand bed surface, with and without a static surface
overpressure. Various rates of displacements may therefore be used, de-
pendent on the capacity of the motor and relative sprocket sizes. A photo-
graph of this type application providing a displacement rate of 0.11 in. per
min is shown in figure A-5.

The use of a static surface overpressure in addition to the concen-
trated load necessitated providing a seal for the rod transferring the dis-
placement from the gear box to the model being loaded. This was

ARMOUR RESEARCH FOUNDATION OF ILLINOIS INSTITUTE OF TECHNOLOGY

accomplished by tapping a hole in the blind flange covering the 12-in. open-
ing on the head, and threading one end of a double-end air cylinder
into the hole, as shown in figure A-6.

Concentrated dynamic loads, using the dynamic loading apparatus
described have been applied to surface models without static surface
overpressure. Figure A-7 shows the dynamic loading apparatus as
used for the footing experiments. A photograph of the instrumentation
used in these experiments, including a force washer, two linear
variable differential transformers (LVDTs), and four accelerometers,
is shown in figure A-8 for experiments without surface overpressure,
and in figure A-9 for experiments with surface overpressure.

When applying concentrated dynamic loads with a surface over-
pressure, the hydraulic cylinder was connected to the pressure vessel
head, as shown in figure A-10, and the remainder of the dynamic load-
ing apparatus was supported by a horizontal channel beam attached
to the vessel loading frame as shown in figure A-11

These applications, with the exception of the dynamic surface
loadings, have been developed and used in ARF Project K193, Design
and Analysis of Foundations for Protective Structures, under Air Force
Special Weapons Center Contract No. AF 29(601)-2561.

REFERENCES

A-1   Ahler, E. B., _Experimental Methods of Determining the Behavior of Underground Structures Under Dynamic Loads_ by Armour Research Foundation for Office of Civil and Defense Mobilization, under Contract No. CDM-SR-47, December, 1961.

A-2   McKee, K. E., _Dynamic Soil Facility_, Armour Research Foundation, Request for Project Support (159-61), August, 1960.

A-3   McKee, K. E., _Design and Analysis of Foundations for Protective Structures_, Appendix A, AFSWC-TN-61-14, Armour Research Foundation, Chicago, May, 1961.

ARMOUR RESEARCH FOUNDATION OF ILLINOIS INSTITUTE OF TECHNOLOGY

1/2-in. Pipe Thread

Four 6-in. diam Flanged Nozzles

12-in. diam Flanged Nozzle

Seven 2-in. diam Extra Heavy Pipe Couplings

Two 8-in. diam Flanged Nozzles (each side)

48-in. diam Shell

6-in. diam Flanged Nozzle

Loading Frame (each side)

ASME Dished Head

10-in. diam Flanged Nozzle
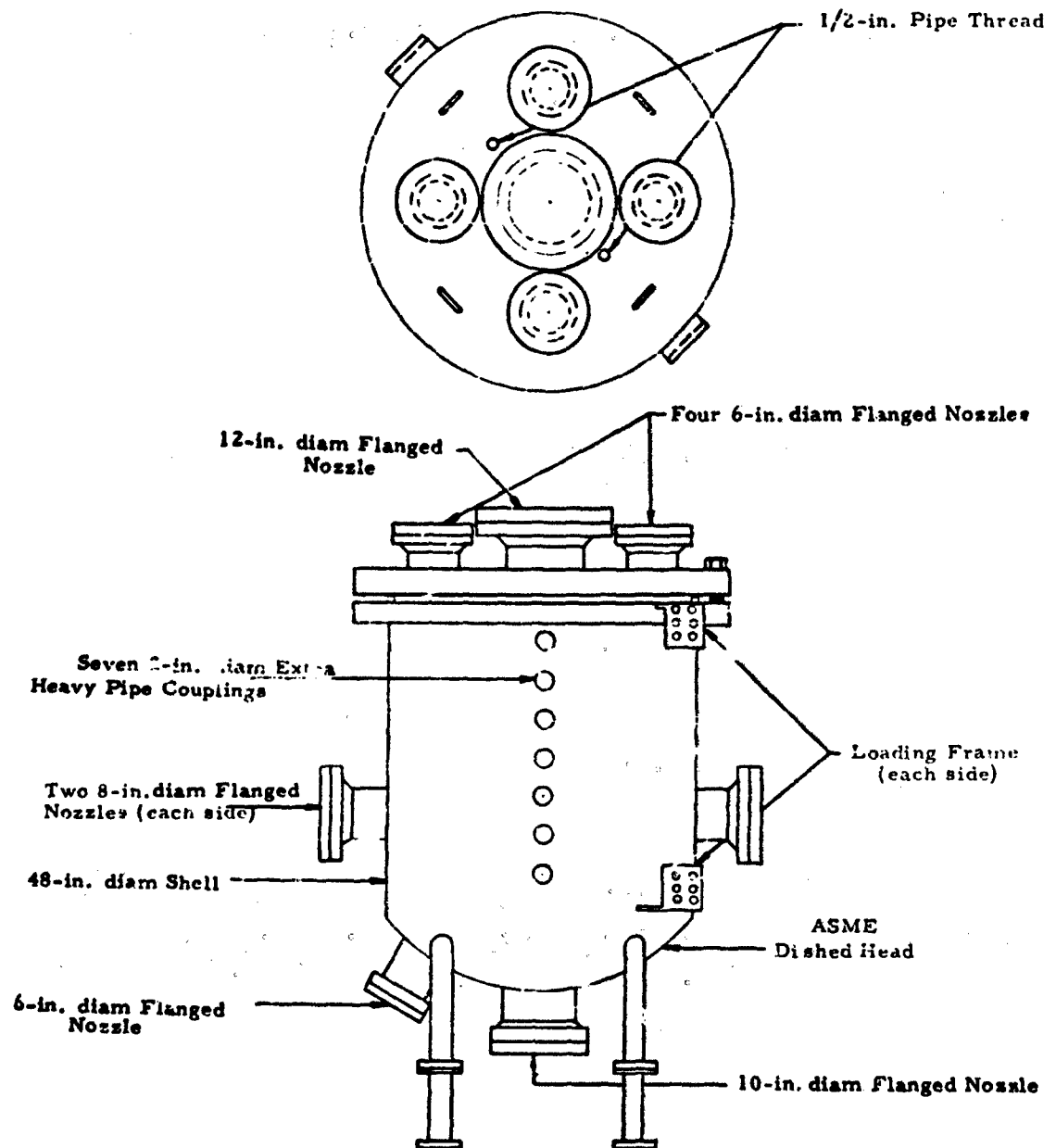
Fig. A-1 __DYNAMIC SOIL FACILITY__

ARMOUR RESEARCH FOUNDATION OF ILLINOIS INSTITUTE OF TECHNOLOGY

A-6

Fig. A-2   PRESSURE VESSEL WITH HEAD REMOVED
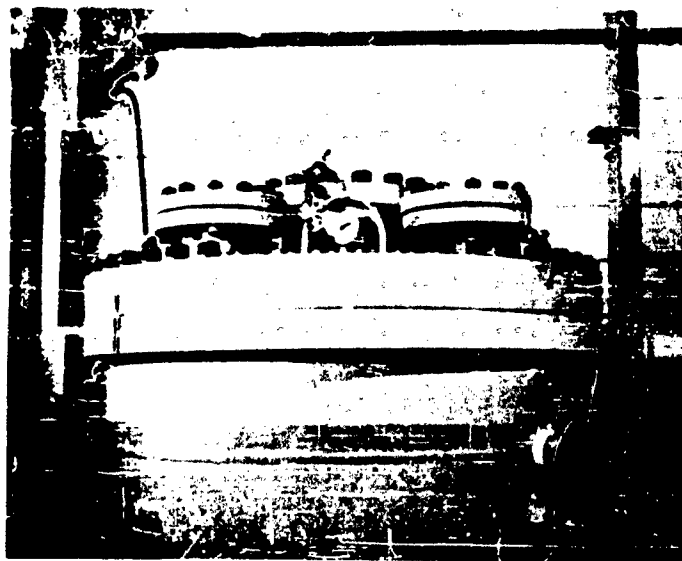
Fig. A-3   UPPER PORTION OF PRESSURE VESSEL WITH HEAD
           IN PLACE

A-7
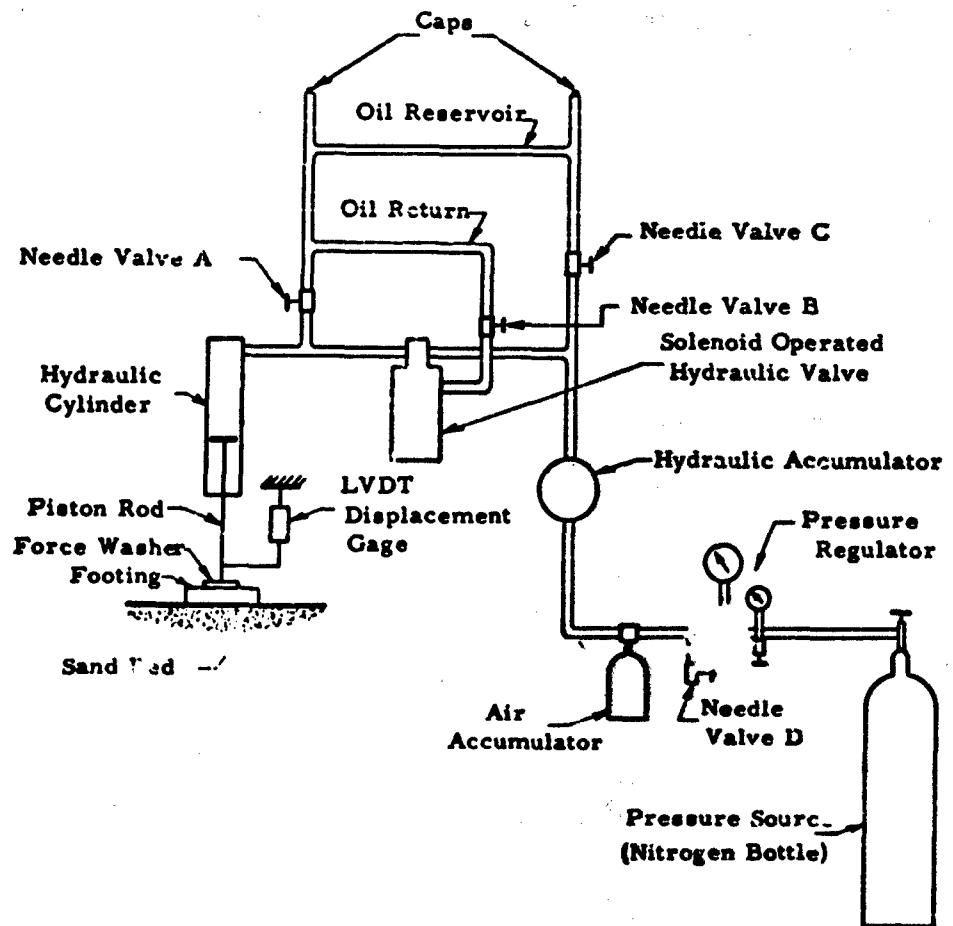
Fig. A-4   DYNAMIC APPARATUS
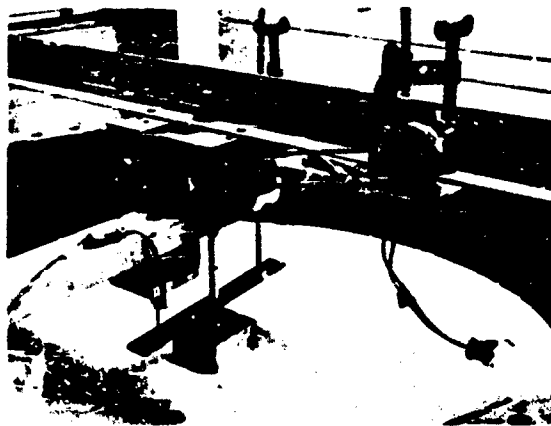
Fig. A-5 MOTOR-DRIVEN GEAR BOX FOR STATICALLY LOADED
FOOTINGS WITHOUT STATIC OVERPRESSURE
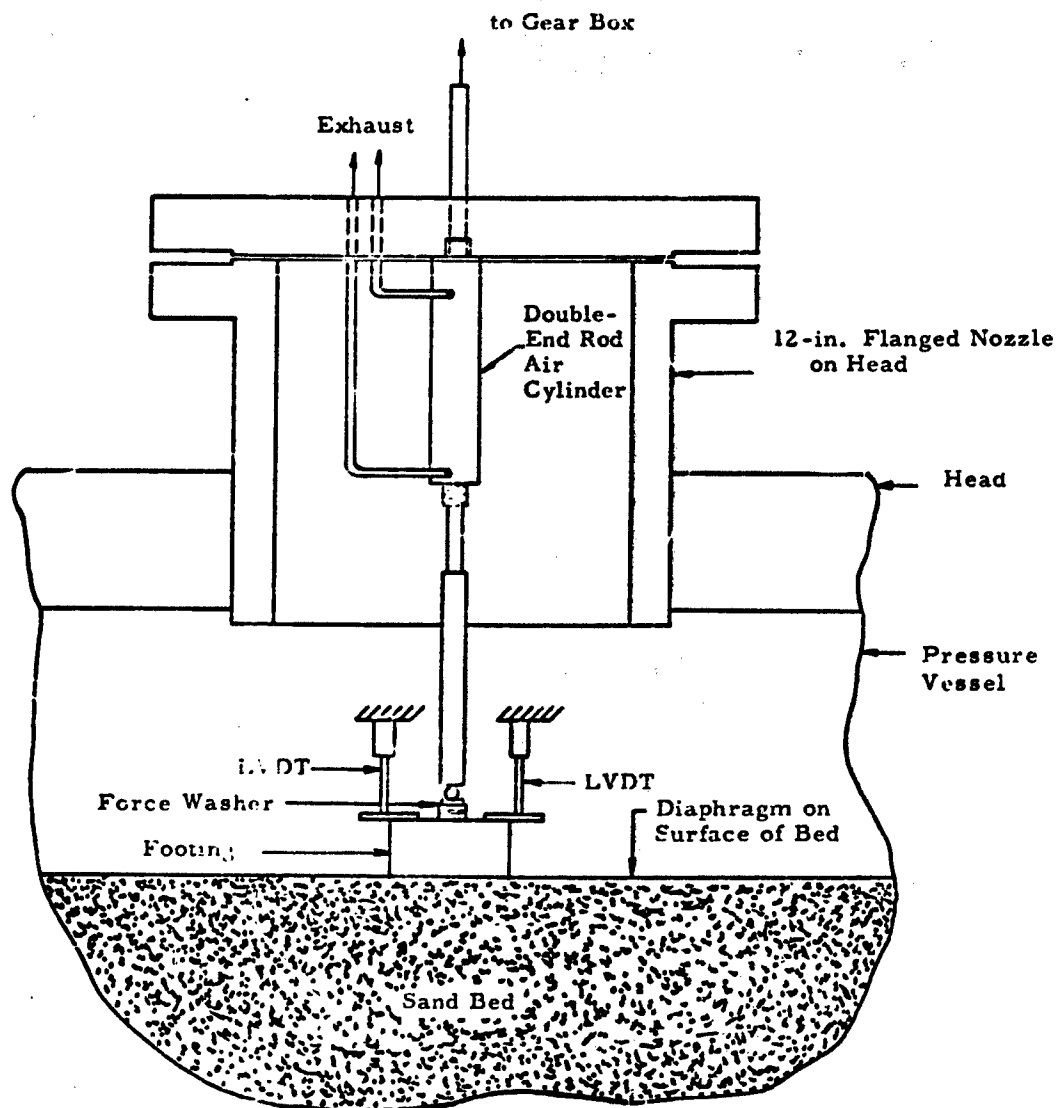
Fig. A-6 EXPERIMENTAL SETUP FOR STATICALLY LOADED
FOOTINGS WITH STATIC OVERPRESSURE

ARMOUR RESEARCH FOUNDATION OF ILLINOIS INSTITUTE OF TECHNOLOGY

A-10
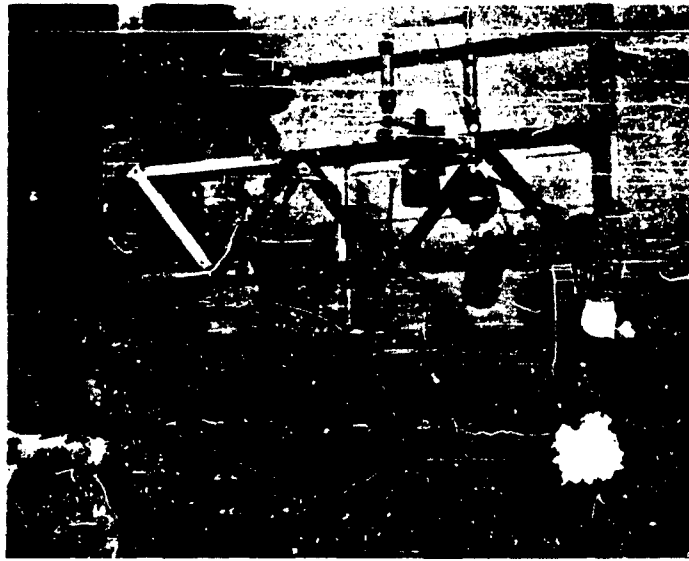
Fig. A-7   HYDRAULIC APPARATUS FOR DYNAMICALLY
LOADED FOOTINGS WITHOUT STATIC OVER-
PRESSURE

A-11
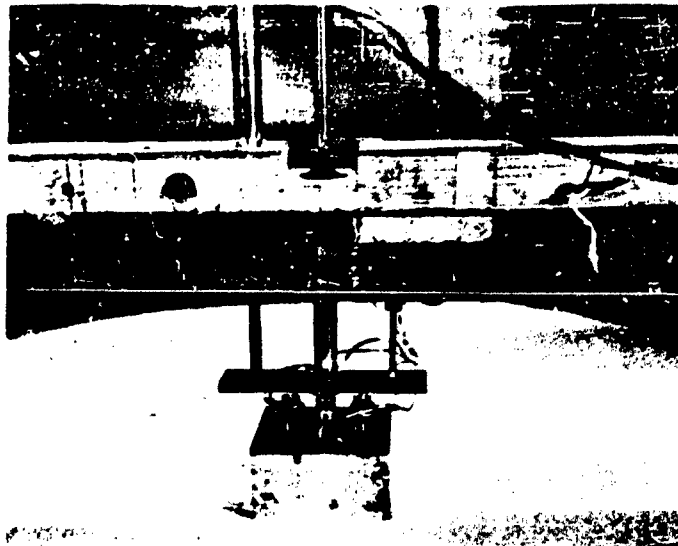
Fig. A-8 INSTRUMENTATION FOR DYNAMICALLY LOADED FOOTINGS WITHOUT STATIC OVERPRESSURE

Fig. A-9 INSTRUMENTATION FOR DYNAMICALLY LOADED FOOTINGS WITH STATIC OVERPRESSURE
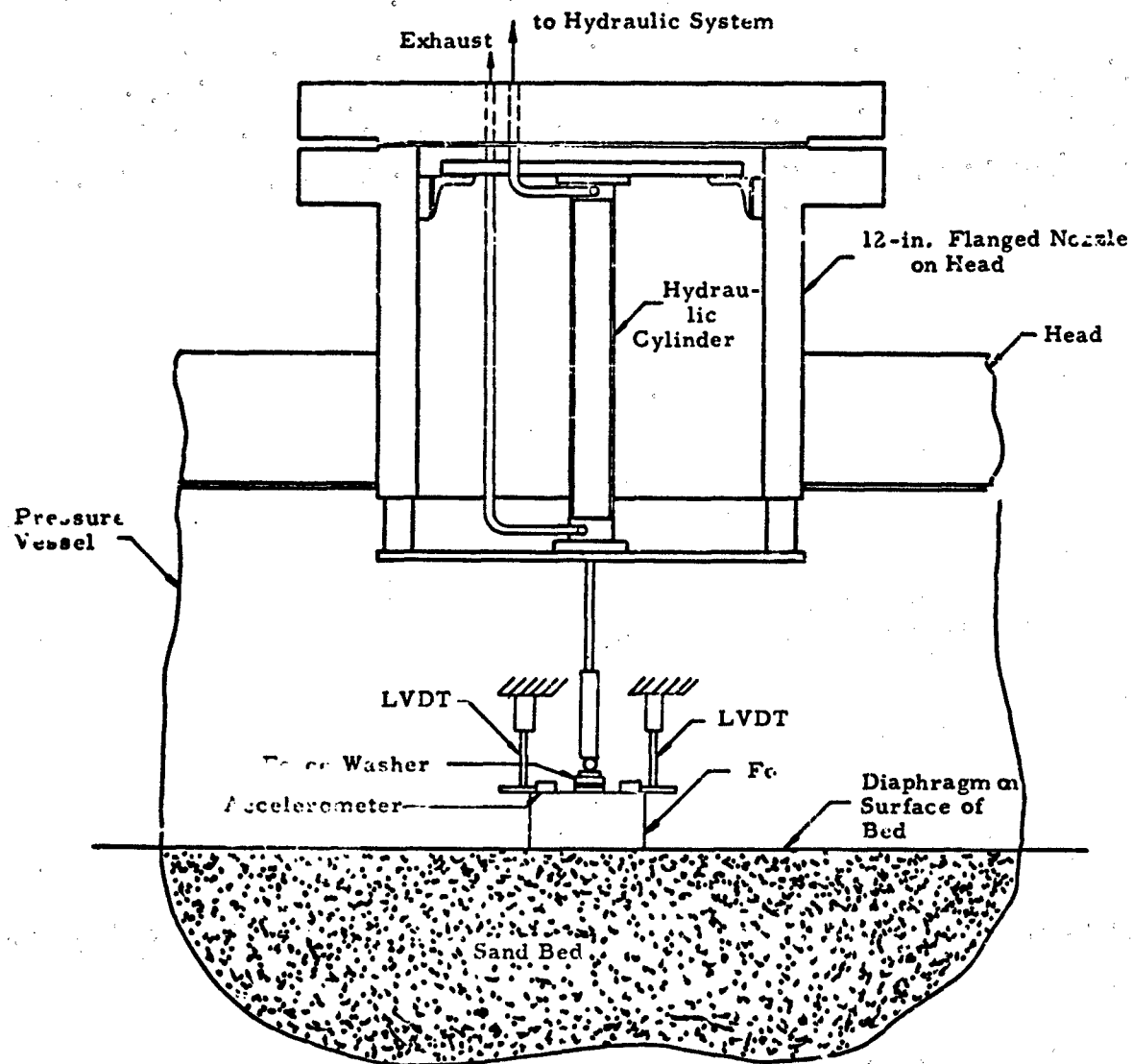
Fig. A-10 EXPERIMENTAL SETUP FOR DYNAMICALLY LOADED
FOOTINGS WITH STATIC OVERPRESSURE
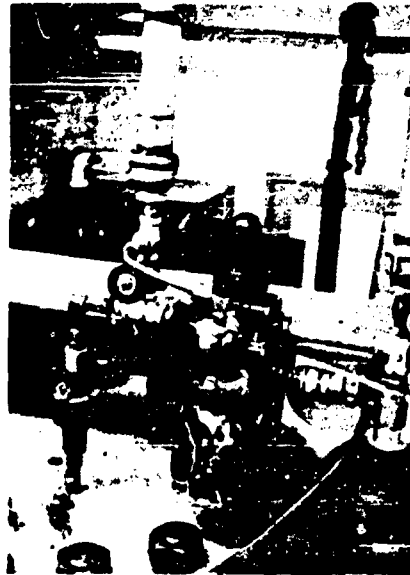
Fig. A-11   HYDRAULIC APPARATUS FOR DYNAMICALLY
            LOADED FOOTINGS WITH STATIC OVERPRESSURE

A-14

APPENDIX B

THREE-DIMENSIONAL STATICALLY LOADED FOOTINGS
by
S. Shenkman

APPENDIX B

THREE-DIMENSIONAL STATICALLY LOADED FOOTINGS

by

S. Shenkman

The three-dimensional static experiments were performed in the dynamic soil facility described in Appendix A. Of primary interest in these experiments is the resistance-displacement characteristics of footings centrally loaded with a concentrated vertical static force and a uniform static overpressure on the surface surrounding the footing. The results of static concentrated loads without overpressure on the surface have been reported under a previous contract[B-1]*. In order to evaluate such factors such as difference in container geometry, grain-size distribution, experimental set-up and techniques. a series of nine experiments were conducted without the overpressure These experiments also provide mea ᶠ comparison with the previous work.

The soil medium used in these experiments was an air-dry Ottawa sand (grain-size distribution shown in figure 4). Prior to each experiment, the bed was vibrated by inserting an immersion-type concrete vibrator into the bed at a point near the wall of the sand container. The bed was leveled after three minutes of vibration and the vibrator withdrawn after an additional one-half minute. Using this procedure, the average density of the sand bed, based on the volume occupied by the total weight of sand, was 109.1 pcf. Surface density measurements using a scoop density device, were made throughout the experimental program to check on the reproducibility of the bed. The footings were 4-in. square by 2-in. high aluminum blocks having a surface in contact with the soil knurled to simulate the roughness generally associated with full-scale footings.

---

* Superscript numbers in parentheses cite references collected at the end of this appendix.

Experiments Without Static Surface Overpressure

Nine experiments were conducted in this series. A gear box, attached to the loading frame, was used to apply the load in each experiment. However, the means of transferring the load to the footing, and the instrumentation used in recording force and deflection were changed a number of times during the series and require further description.

A photograph of a typical setup used in Experiments A1 through A4 is shown in figure B-1. In these experiments, the manually operated gear box was connected to a proving ring, which, in turn, was attached to a 3/4-in. diameter by 16-in. long steel rod. Three dial gages resting on the surface of the footing measured the footing's displacement. Load was applied to the footing through a steel ball resting in a circular indentation in the center of the footing. A similar setup was used in Experiments A5 and A6 except that an electric motor was used to drive the gear box, guaranteeing a more uniform rate of displacement. In Experiments A5 to A6 the rate was 0.055 in. per min.

Instrumentation for Experiments A7 through A9 consisted of a high sensitivity force washer and two linear variable differential transformers (LVDTs). The linear range of the LVDTs was $\pm$ 0.15-in. and $\pm$ 1.0-in., and permitted an accurate tracking of both the initial small- and the final large-displacements of the footing. The $\pm$ 0.15-in. LVDT, a more sensitive transducer for the range considered, was used to verify the general shape of the displacement-time histories for the initial displacements. As shown in figure B-2, the LVDTs were connected to a steel bar which was rigidly attached to a length of pipe transmitting the load. Data for these experiments were recorded on a Consolidated Electrodynamics Corporation (CEC) recorder; paper speed was 1/8 in. per sec. A complete description of the instrumentation is given in Appendix C, and a schematic diagram is shown in figure B-3.

Load sleeves, provided with the force washer, were connected to the footing beneath the washer and to a steel ball above the washer. Load was applied by a pipe connected to the motor-driven gear box, with a ball acting as a roller between the pipe and the force washer. The displace-

ment rate in Experiments A8 and A9 was 0.055 in. per min.

Photographs taken after each experiment, in addition to sketches of failure patterns for a number of experiments, enabled comparison of the failure patterns from test to test. Table B-1 summarizes the results of the nine experiments. Figure B-4 presents resistance-displacement curves averaged for Experiments A1 through A6, A7 through A9, and the results of experiments performed previously, Experiments C4 through C6[B-1]. Noteworthy in this figure is the apparent higher bearing capacity in Experiments C4 to C6. This is understandable since the average bed density for these tests was 112.3 pcf as compared with 109.1 pcf in the present experiments. However, this does not explain the difference in results between Experiments A1 to A6 and A7 to A9. The apparent lower maximum loads for Experiments A7 through A9 may be due to errors in observing the proving ring readings. In the experiments, the proving ring was seen to be jumping, and the observed measurements were made at the upper extremes of these jumps.

The jumping phenomenon was also seen to occur a two-dimensional experiment previously performed[B-2]. A motor-driven gear box was used in this experiment to provide a displacement of 0.00053 in. per min. Proving ring and dial gage readings were recorded with a 16mm movie camera at periodic intervals. Since the jumping was not observed in the force washer records, it appears that this effect is due mostly to the spring-like characteristics of the proving ring.

Experiments with Static Surface Overpressure

The basic static loading apparatus was modified in this series of experiments to provide for a static overpressure. The footing, attached to a diaphragm, used as a pressure seal on the surface of the sand bed, was initially placed on the bed previously vibrated and leveled. This series of experiments is outlined in Table B-2.

A double-end rod air cylinder, connected to the 12-in.
flange, as shown in figure B-5, transferred a constant displacement from
the motor-driven gear box to the footing. The function of the air cylinder
was to provide a seal in the 12-in. flange. Figure B-6 is a photograph of
a typical experimental setup for this series. Instrumentation for the
experiments indicated in Table B-2 was the same as used in Experiments
A7 through A9, except that the LVDTs in this series were connected
directly to the footing rather than cantilevered off the loading rod. This
was done to enable an initial balancing of the LVDTs prior to placing the
head on the pressure vessel. Once the head was placed, the blind flange on one
of the 6-in. openings was removed and final adjustments of the LVDTs
performed.

Four complete bed setups were performed for this series
of experiments. Since there were only small deflections with high over-
pressures, subsequent tests were conducted assuming that the initial con-
ditions were only little different. It should be emphasized that this is an
assumption of the results accepted with this limitation. The experiments
in general, involved a gradual decreasing of the applied overpressure from
test-to-test until failure was reached. It was not possible to reach failure under
an overpressure of 10 psi or greater since the force washer was limited
to a force of 1000 lb. For this reason, a proving ring with a linear range
of 2000 lb was used in Experiments B9 through B11. The proving ring was
connected between the gear box and air cylinder piston rod, as shown
in figure B-7. However, a force of 2000 lb was still not sufficient to cause
failure when the soil surface was subjected to an overpressure of 10 psi.
In these experiments, proving ring measurements were visually recorded
along with corresponding marks on the CEC recorder which recorded
the two LVDTs.

Table B-2 summarizes the results of these experiments.
Since the load generally associated with footing failure was reached in
only two experiments, the peak loads listed in Table B-2 are, with two
exceptions (Experiments B8 and B11) the maximum load obtainable under
a given overpressure, using the available experimental apparatus. Resistance-
displacement curves for the two experiments where failure did occur are

plotted in figure B-8. No attempt is made herein to discuss the shape of these curves.

It was found, in conducting these experiments, that the seal afforded by the surface diaphragm was unsatisfactory in preventing a small, but constant, pressure leakage into the sand bed. Although many attempts were made to remedy the situation, a perfect seal could not be accomplished. An air-pressure gage connected to an instrumentation coupling on the side of the pressure vessel measured this leakage. Therefore, the effective over-pressure listed in Table B-2 for each experiment, is the difference between the air pressure above and beneath the membrane.

A modification of Andersen's analysis for one-sided footing failure, incorporating a uniform static surface pressure, was performed in a past report[B-3]. Further modification of this method assuming a zero depth of burial and a cohesionless soil, results in the two equations:

$$P_s = \left[1 - \frac{\pi \tan \phi}{\gamma \tan \phi} \right] r^2 + \frac{qr\pi}{4\gamma} \qquad \text{(Eq. B-1)}$$

and

$$\frac{B}{r} = (2 - \frac{\pi}{2} \tan \phi) - \frac{8}{3} \frac{\gamma r^2}{P_s} \tan \phi - \frac{qr\pi}{2} \tan \phi \qquad \text{(Eq. B-2)}$$

where

B = width of footing,

P_s = vertical load per unit length,

q = uniform pressure on surface,

r = radius of failure surface,

γ = unit weight of soil, and

ϕ = angle of internal friction.

Using equations B-1 and B-2, we may determine the bearing capacity of the footing as a function of overpressure. With no overpressure

on the surface and an angle of internal friction, ϕ, of 40° (based on past triaxial tests), the maximum footing load is 197 lb; when applying an overpressure of 2 psi, this value is increased to 968 lb. An average maximum load of 216 lb was recorded in Experiments A7 through A9, showing favorable agreement with the theory. An overpressure of 2 psi applied to the surface in Experiment B11, where a maximum load of 1,208 lb was recorded, again agrees, reasonably well with Andersen's formula. It should be noted that the experimental results exceed the theoretical results for both cases. Since the ϕ of 40° was approximate, a better agreement between the analytical and experimental results could be obtained by considering a slight increase in ϕ.

Based on the modified Andersen method, a load of 3,858 lb is required to produce footing failure when applying a surface pressure of 10 psi. Unfortunately, because of the limitations of the experimental apparatus, experimental verification of footing failure subjected to pressures above 2 psi was not possible. In future experimental programs this situation can be corrected.

An experiment, designed to measure the surface displacement under different overpressures, was performed. In this experiment four LVDTs located along a diameter of the pressure vessel as shown in figure B-9, were used in measuring surface displacements. One would generally anticipate the displacement at the center of the bed to be greater than that near its outer boundaries. Records obtained from this experiment did not follow any general pattern as shown in figure B-10. The cause for these inconsistent results has not been definitely determined.

REFERENCES

B-1   K. E. McKee, Design and Analysis of Foundations for Protective Structures, AFSWC-TR-56, Armour Research Foundation, Chicago. October 1959.

B-2   K. E. McKee, Design and Analysis of Foundations for Protective Structures, Appendix E, AFSWC-TN-61-14, Armour Research Foundation, Chicago, May 1961.

B-3   K. E. McKee, Design and Analysis of Foundations for Protective Structures, Appendix E, AFSWC-TR-59-56, Armour Research Foundation, Chicago, October 1959.

Table B-1

MAXIMUM STATIC RESISTANCE WITHOUT OVERPRESSURE

(4-in. Square Footings)

Experiment Number	Maximum Load (lb)	Bearing Capacity (psi)	Displacement at Maximum Load (in.)
A1	240	15.0	0.175
A2	294	18.4	0.185
A3	257	16.1	0.145
A4	241	15.1	0.160
A5	290	18.1	0.190
A6	267	16.7	0.152
A7	239	14.9	0.188
A8	201	12.6	0.160
A9	219	13.7	0.136

Table B-2

STATICALLY LOADED FOOTINGS WITH STATIC SURFACE OVERPRESSURE

Experiment Number	Effective Overpressure (psi)	Maximum Load (lb)	Displacement at Maximum Load (in.)
B1*	10.5	396[a]	0.01
B2	10.0	898	0.03
B3	5.0	1,190	0.042
B4	0	(Illegible record)	
B5*	3.0	943	0.091
B6	2.0	940	0.181
B7	2.0	735	0.052
B8	1.0	293	0.38
B9*	9.8	2,070	0.102
B10	5.0	2,070	0.129
B11*	2.0	1,208	0.258

* Initial bed setup.

[a] Motor, driving gear box failed at this load

NOTE: In all experiments, except B8 and B11, the maximum load and displacement were the highest attainable with the experimental apparatus, rather than the bearing capacity and associated displacement.
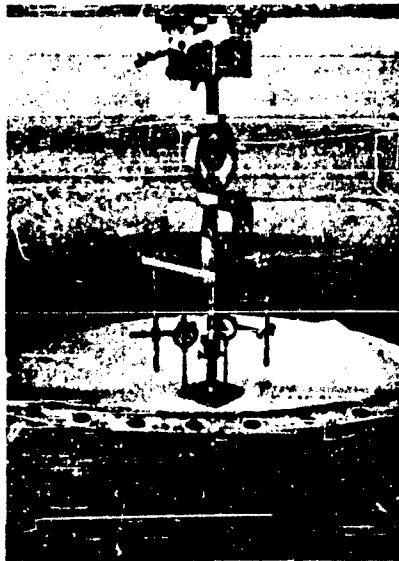
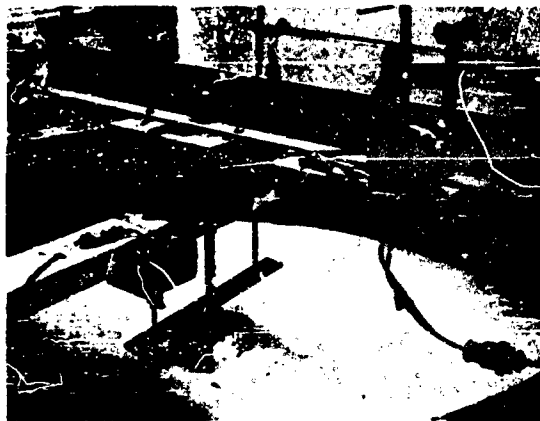Fig. B-1 TYPICAL SETUP FOR EXPERIMENTS A1 TO A4

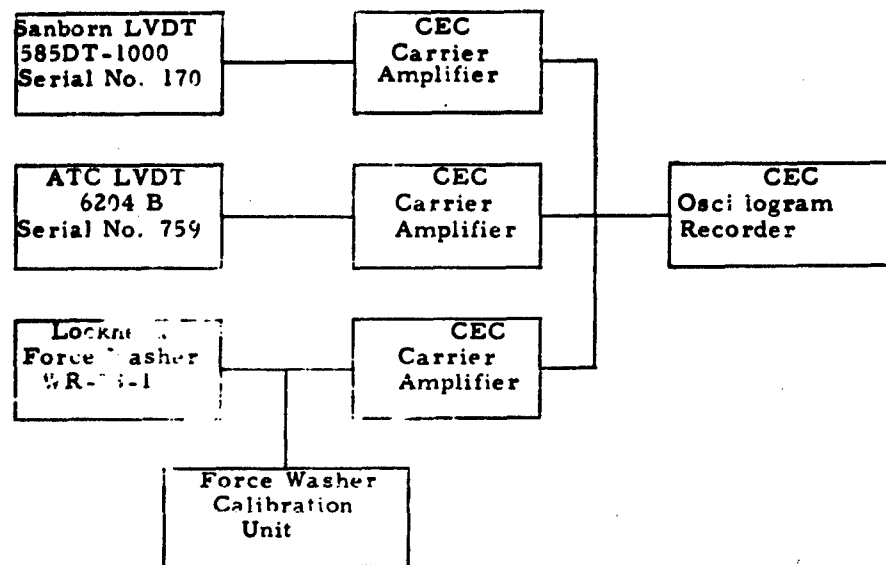Fig. B-2 TYPICAL SETUP FOR EXPERIMENTS A7 to A9

```
┌──────────────────┐      ┌──────────────┐
│ Sanborn LVDT     │      │    CEC       │
│ 585DT-1000       │──────│  Carrier     │─────┐
│ Serial No. 170   │      │  Amplifier   │     │
└──────────────────┘      └──────────────┘     │
                                               │
┌──────────────────┐      ┌──────────────┐     │   ┌──────────────┐
│  ATC LVDT        │      │    CEC       │     │   │    CEC       │
│   6204 B         │──────│  Carrier     │─────┼───│ Oscillogram  │
│ Serial No. 759   │      │  Amplifier   │     │   │  Recorder    │
└──────────────────┘      └──────────────┘     │   └──────────────┘
                                               │
┌──────────────────┐      ┌──────────────┐     │
│  Locknt          │      │    CEC       │     │
│ Force Washer     │──┬───│  Carrier     │─────┘
│  WR-5-1          │  │   │  Amplifier   │
└──────────────────┘  │   └──────────────┘
                      │
              ┌───────┴────────┐
              │ Force Washer   │
              │  Calibration   │
              │     Unit       │
              └────────────────┘
```

Fig. B-3 SCHEMATIC DIAGRAM OF INSTRUMENTATION FOR
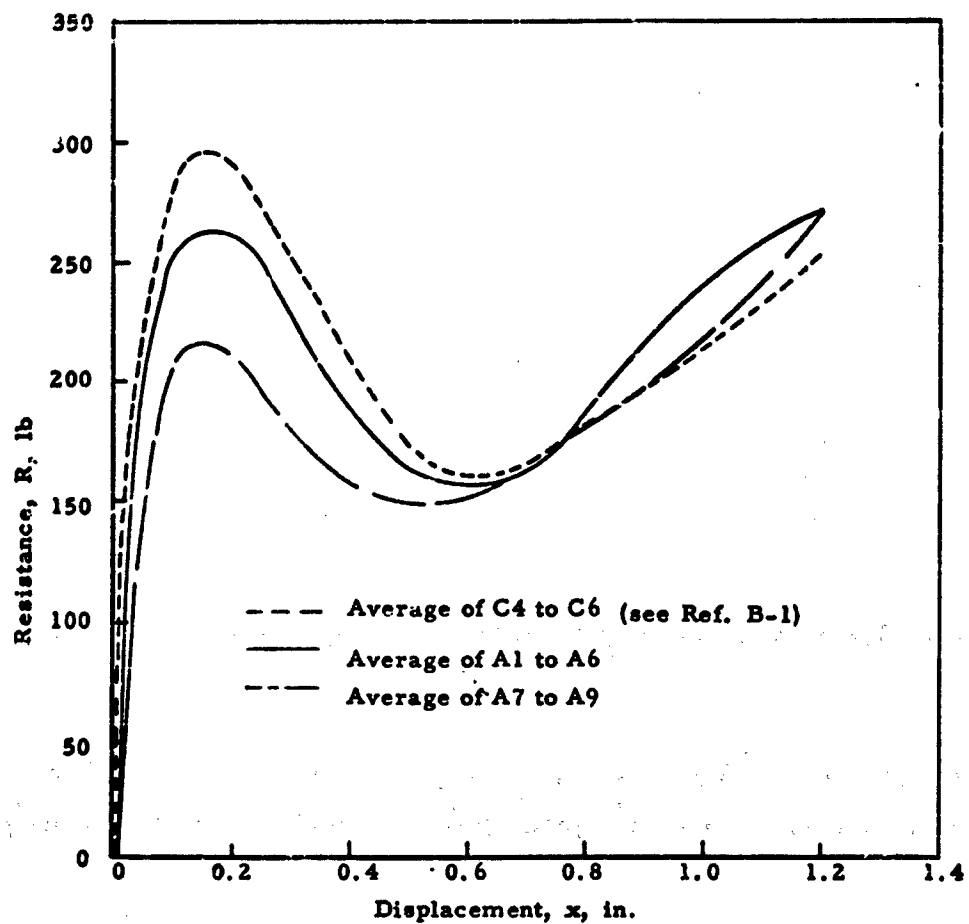   THREE-DIMENSIONAL STATICALLY LOADED FOOTINGS

B-11

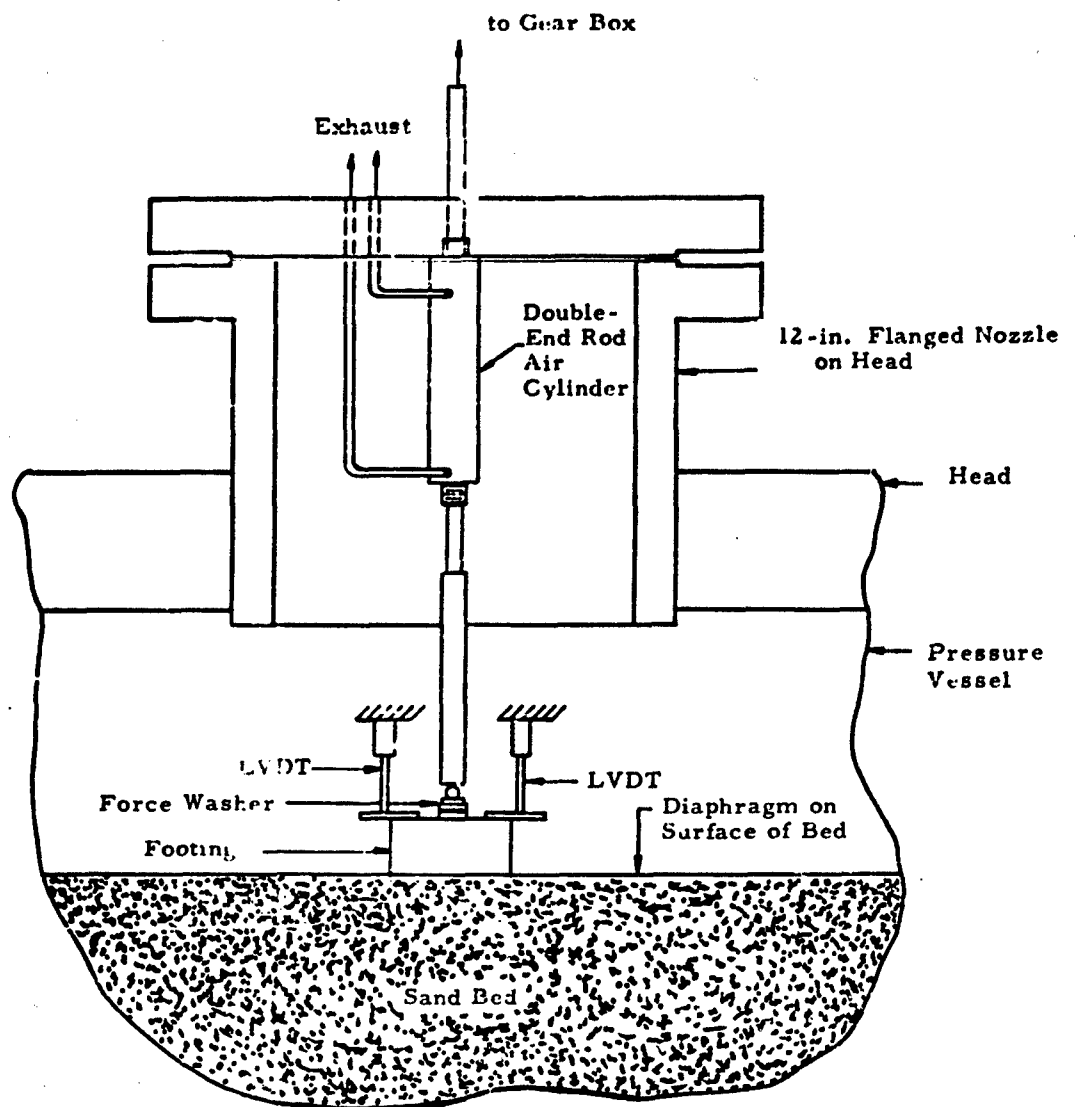Fig. B-4   RESISTANCE-DISPLACEMENT CURVES FOR STATIC EXPERIMENTS WITHOUT OVERPRESSURE

Fig. B-5 EXPERIMENTAL SETUP FOR STATICALLY LOADED
FOOTINGS WITH STATIC OVERPRESSURE

**Fig. B-6 TYPICAL SETUP FOR EXPERIMENTS WITH STATIC
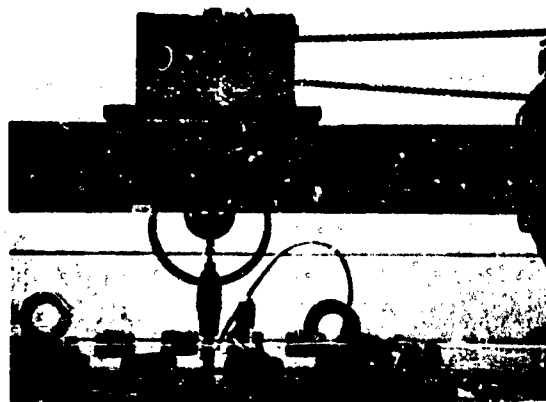OVERPRESSURE**

**Fig. B-7 USE OF PROVING RING AS A FORCE   INDICATOR
FOR EXPERIMENTS B9 TO B11**
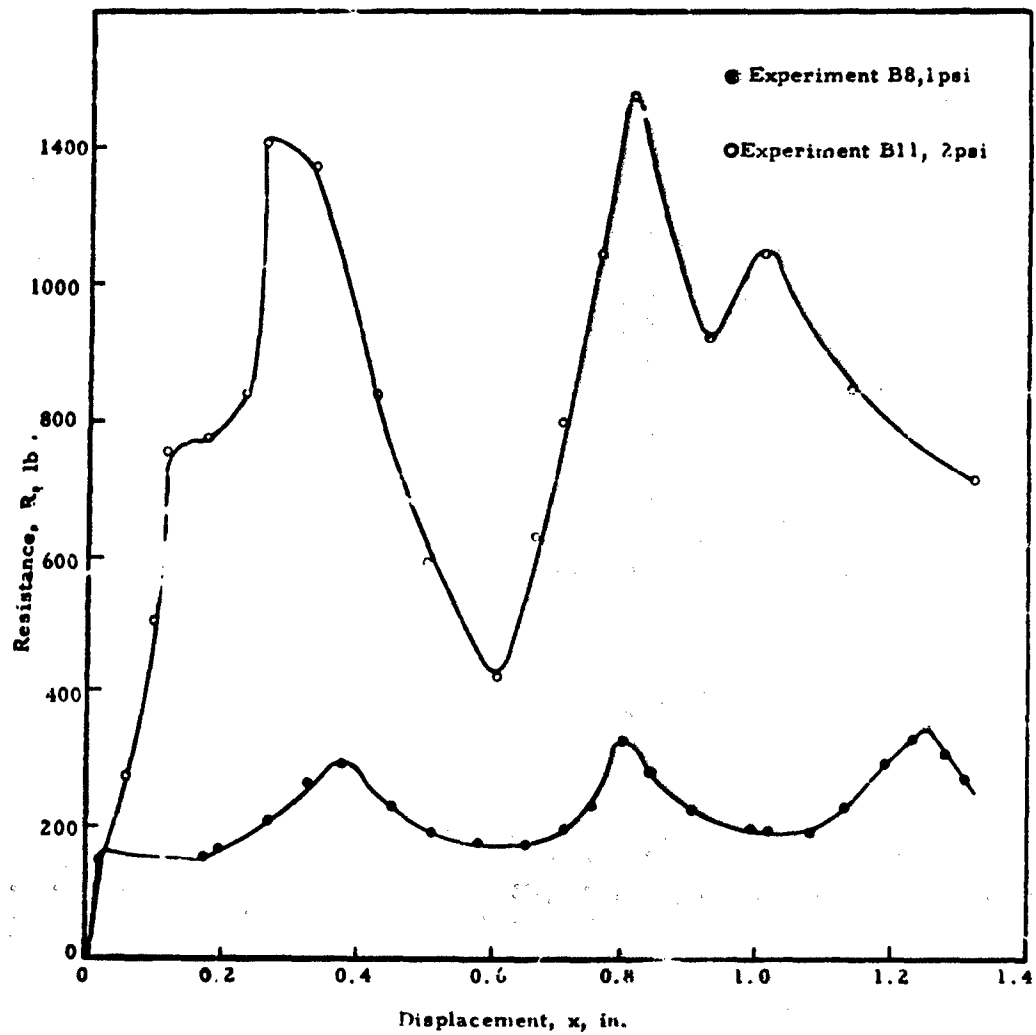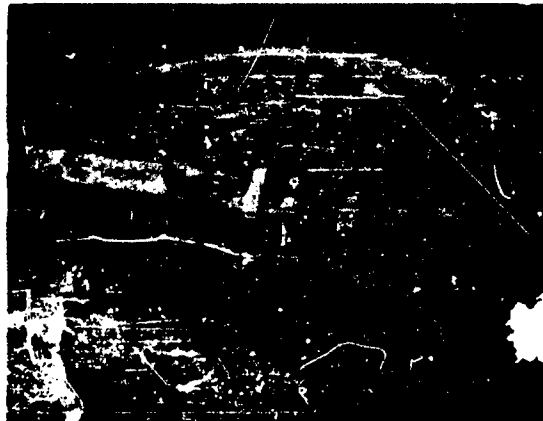
B-14

Fig. B-8   RESISTANCE-DISPLACEMENT CURVES FOR
EXPERIMENTS B8 AND B11

Fig. B-9 DISPLACEMENT GAGES USED IN DETERMINING
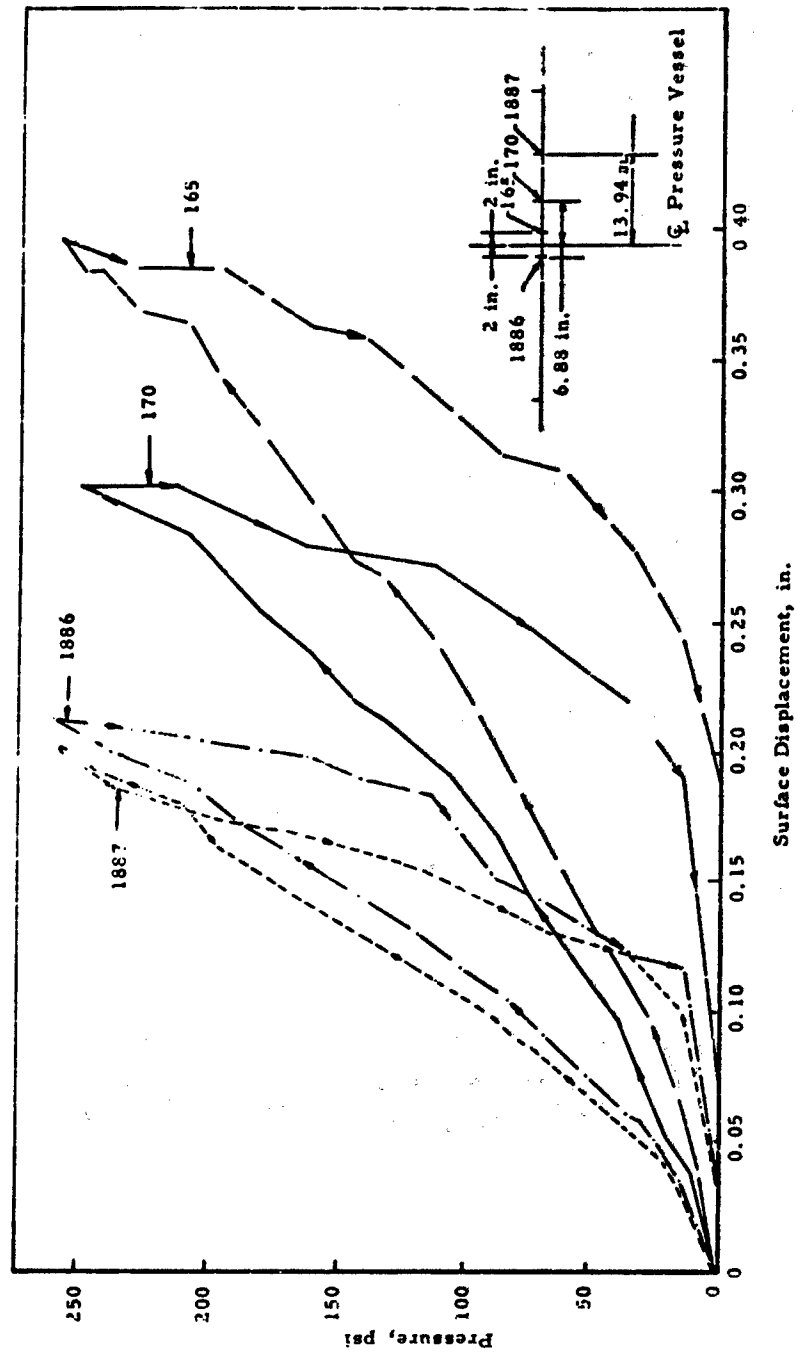SURFACE DISPLACEMENTS UNDER A STATIC
OVERPRESSURE

B-16

Fig. B-10 SURFACE DISPLACEMENTS RESULTING FROM A UNIFORM STATIC OVERPRESSURE

APPENDIX C

THREE-DIMENSIONAL DYNAMICALLY LOADED FOOTINGS

by

S. Shenkman

APPENDIX C

THREE-DIMENSIONAL DYNAMICALLY LOADED FOOTINGS

by

S. Shenkman

Two series of experiments on three-dimensional dynamically loaded footings were performed in the dynamic soil facility described in Appendix A. Initially, concentrated dynamic loads were applied to a 4-in. square by 2-in. high aluminum block placed on the surface of the sand bed (grain-size distribution shown in figure 4. Supplementary experiments were then performed by applying a uniform static overpressure to the surface of the soil surrounding the footing, in addition to the concentrated dynamic load applied to the center of the footing.

Prior to each experiment, the bed was vibrated by inserting an immersion-type concrete vibrator into the bed at a point near the wall of the sand container. The bed was leveled after three minutes of vibration and the vibrator withdrawn after an additional one-half minute. Using this procedure, the average density of the sand bed, based on the volume occupied by the total weight of sand, was 109.1 pcf. Surface density measurements, using a scoop density device, were made throughout the experimental program to check on the reproducibility of the bed.

The dynamic loading apparatus$(C-1)$[*], was used to apply the concentrated dynamic loads. The basic hydraulic system remained similar to that previously used. Three needle valves are shown in figure C-1, a sketch of the dynamic apparatus. The addition of needle valve B to the hydraulic system permits closer control of the force-time history. As shown in figure C-2, an increase in load duration of approximately 10 msec results when the valve is closed. Needle valve B provides an additional function in the experiments using a static overpressure which will be discussed.

[*] Superscript numbers in parenthesis cite references collected at the end of the appendix.

C-1

Instrumentation for the experiments consisted of a high sensitivity force washer, accelerometers, linear variable differential transformers (LVDTs), and air pressure gages.

A Lockheed Electronics Model WR7S high sensitivity force washer, was custom-built to required specifications with a linear range of 0 to 1000 lb. Load sleeves, provided with the washer, connected to the footing beneath the washer and to a steel ball above the washer. The ball acted as a roller between the force washer and a steel pipe connected to the hydraulic cylinder piston rod.

The accelerometers were Columbia Research Model 300 compression-piezoelectric-type gages. The gage sensitivity with the cable lengths and input circuitry used was approximately 30 mv per g acceleration. The dynamic acceleration range of the gages is 0.02 to 40,000 g and their natural frequency is 75 kcps. The accelerometers were attached to the footing, 1-1/4 in. from each corner, with a 10-32 stud.

Two LVDTs, a Sanborn Model 585 DT-1C with a $\pm$ 1-in. linear range and an Automatic Temperature Co. Model 6 ... with a $\pm$ 0.15-in. linear range, were used to measure the footing displacement. In the experiments without surface overpressure, both transformers were connected to a strip of steel center-supported by the loading rod, and did, in fact, measure the deflection of the rod relative to the hydraulic cylinder. However, it was assumed that this motion represented the displacement of the center of the footing. In the experiments with surface overpressure, the LVDTs were connected to each side of the footing in order to simplify adjustment of the gages once the pressure vessel head was placed. Use of the $\pm$ 0.15-in. LVDT enabled accurate tracking of the initial motion of the footing, while the $\pm$ 1-in. LVDT followed the motion of the footing over the larger range. The $\pm$ 0.15-in. LVDT, a more sensitive transducer for the range considered, was used to verify the general shape of the displacement-time histories for the initial displacement.

Static overpressure applied to the surface of the soil was measured by a 0 to 300-psi range United States Gage Co. indicating gage. The gage was attached to the removable head of the pressure vessel and read directly to 1 psi. A J. P. Marsh Corp. zero-psi to 100-psi indicating gage was used for lower pressure application. A Denison Engineering Co. indicating gage was connected to one of the instrumentation couplings on the side of the pressure vessel at a point below the surface of the sand. The prime purpose of this gage was to measure any air pressure leaking through the diaphragm covering the soil bed.

A Consolidated Electrodynamics Corp. oscillograph, a strip chart recorder with a one-msec response time, was used for dynamic recording. As shown in figure C-3, a schematic diagram of control and recording equipment, the recording equipment was run independently of the solenoid valve. The CEC recorder was permitted to reac' full running speed (24 in. per sec for Experiments E1 through E8, and 30 in. per sec for remaining experiments) before the solenoid valve was energized. Photographs of the instrumentation and dynamic load apparatus for experiments without overpressure, are shown in figures C-4 and C-5.

Experiments Without Static Surface Overpressure

In the previous program, force time and displacement time were recorded for footings subjected to concentrated dynamic loads. In attempting to correlate experimental and theoretical results, it was found that experimental acceleration data were necessary in calculating soil resistance beneath the footing. For this reason, four accelerometers were attached to the footing near the corners in the present experiments. It was anticipated that the average of these four accelerometers would define the acceleration of the center of the footing. However, upon running a number of these experiments, the CEC records showed a response by the accelerometers at both the onset and termination of the load. If this response were due solely to the actual force applied to the footing, the acceleration data would provide meaningful results. Subsequent examination of the hydraulic system found these responses to be partly due to the energizing and closing of the solenoid valve. The valve, upon being energized, applied a

concentrated load to the channels supporting the system, thereby deflecting the channels and transmitting a load through the hydraulic cylinder and into the footing. These observations were further verified by examining the results of records taken of the accelerometers, force washer, and ±0 15-in. LVDT, by energizing the solenoid valve without any pressure in the pneumatic system. This situation was remedied by stiffening the channel members supporting the hydraulic system, as shown in figure C-6.

Twenty-nine experiments were conducted in this portion of the program. Table C-1 summarizes the results of these experiments. Typical records obtained for solenoid actuation times of 13, 45, 70 msec and infinite duration, are shown in figures C-7, C-8, C-9 and C-10, respectively. Although considerable variation is noted between the records included on these figures, certain generalizations can be made. The two LVDT records serve to supplement each other. the ± 0.15-in. LVDT is more accurate and should be used for displacements up to 0.15-in., and beyond this range, the ± 1.0-in. LVDT is used. Observation of the acceleration records indicate that at significant disturbances occurred n the solenoid valve is opened and when it is closed. The general nature of the obtainable force-time history for an infinite duration load is shown on figure C-10 - the initial peak is followed by a significant decrease and a subsequent return to essentially the peak force. When the solenoid valve is closed the force drops off and therefore the trough may or may not appear depending on the duration.

Figure C-11 demonstrates the effect of displacement as a function of a load duration. In this figure, peak deflection is plotted against the integral of the force-time history. The force-time history for the infinite duration loading was integrated up to the time of peak displacement. This plot indicates trends, but the scatter is such that the results cannot be considered as conclusive.

Integration of the accelerometer records provided an independent check on the LVDT-measured displacements. In figures C-12 and C-13, double integrations of the accelerometers are plotted along with LVDT displacements for Experiments E26 and E28. There is no apparent reason

C-4

for the consistently lower displacements found through the double integration.
Since the LVDTs could be at least approximately checked after the tests,
the integration techniques must be assumed inaccurate. A check of these
procedures indicated no apparent source for the consistent variations.
It is interesting to note that the velocity-time curves determined as an
intermediate step bears strong similarity to the force time record.

Experiments With Static Surface Overpressure

Application of a surface overpressure necessitated altering the
experimental setup. In this case, the hydraulic cylinder was fixed to
the inside of the 12-in. opening of the pressure vessel head, as shown
in figure C-14. The remainder of the hydraulic system was attached to
a horizontal beam connected to the pressure vessel loading frame, as
shown in figure C-15. Hydraulic fluid was transferred from the hydraulic
system to the hydraulic cylinder through a hole tapped in the blind flange
of the 12-in. opening. A quick-disconnect valve, attached to the flange,
enabled removal of the flange without any loss of oil. Figure C-16 shows
the footing in place on the sand with the diaphragm used to prevent a
static surface overpressure from leaking into the sand bed.

Table C-2 summarizes the experiments performed in this series.
In this table, we define peak displacement as the final displacement of
the footing; the time to peak displacement is the time from initial load
application to the initial peak of the displacement. These definitions
permit better correlation of applied load with displacement, since in a
number of experiments a "bouncing" of the LVDTs was seen to occur, and
there was a degree of uncertainty as to whether this "bouncing" was due
to soil resistance or piston rod vibration.

Six complete bed setups were performed during this phase. In each
setup, the sand bed was vibrated, leveled, and the instrumentation, footing,
and diaphragm were placed in position. However, as shown in Table C-2,
when static surface overpressures of 25 psi or greater were applied, the
peak footing displacements were negligible. Since the apparatus was
limited to a dynamic load of 1000 lb (the linear range of the available

force washer), the majority of experiments yielding measurable displacements were performed with a static surface overpressure of 10 psi or less. initially, pressures greater than 10 psi were attempted, and as a result a number of experiments were performed on the same bed setup. A or B added to the experiment number indicates that the dynamic load was reapplied to the footing without relieving the static surface overpressure.

A number of experimental observations were made in addition to the acceleration, displacement, and force records. The diaphragm used on the sand bed was found ineffective in preventing all pressure leakage into the sand. Various attempts to reduce or eliminate the leakage proved fruitless during the program. However, this shall be remedied prior to any future testing. The pressure buildup in the sand bed was measured by the pressure gage connected to an instrumentation coupling on the side of the pressure vessel. The difference in pressure between the surface and the sand bed for each experiment is listed in Table C-2.

Application of a surface pressure necessitated closi needle valve B. If he needle valve were not closed during the   periments, the pressure within the vessel would be able to force the piston rod up, since the hydraulic fluid would be permitted to exit through the solenoid valve return part. Closing needle valve B, combined with the small footing displacements, resulted in force-time histories which did not decay after approximately 80 or 90 msec as was the case in previous experiments, even though the solenoid actuation time was set at 70 msec. This is presumedly due to friction induced by the overpressure. Typical experiments, are shown in figures C-17, C-18, and C-19. As might be anticipated, the observed footing behavior (accelerations and displacements) increase as the overpressures decrease.

REFERENCES

C-1   McKee, K. E. Design and Analysis of Foundations for
       Protective Structures, Appendix A, AFSWC-TN-61-14,
       Armour Research Foundation, Chicago, (May, 1961).

ARMOUR RESEARCH FOUNDATION OF ILLINOIS INSTITUTE OF TECHNOLOGY

Table C-1

DYNAMIC EXPERIMENTS WITHOUT STATIC OVERPRESSURE

Experiment Number	Impulse (lb x sec)	Duration of Load (msec)	Peak Force lb	Time to Peak Force (msec)	Peak Displacement (in.)	Time to Peak Displacement (msec)
E1	(Illegible record)					
E2	14.24	91.2	263	11.3	1.34	84.0
E3	6.17	77.6	120	8.6	1.28	88.7
E4	11.96	99.4	225	11.4	1.37	93.4
E5	9.81	94.0	190	9.4	>1.5	----
E6	9.65	87.1	246	2.7	1.43	35.5
E7	0.96	32.7	130	3.0	0.03	14.4
E8	2.00	46.5	162	13.3	0.06	24.9
E9	4.29	35.6	317	12.3	0.56	37.0
E10	7.35	39.3	269	5.2	0.56	42.7
E11	7.65	48.8	272	11.0	1.21	55.2
E12	7.60	51.0	255	7.2	1.34	56.2
E13	? ??	58.9	220	16.8	>0.2	----
E14	..26	52.6	228	9.3	0.95	62.3
E15	8.31	56.9	219	7.1	0.68	68.4
E16	10.1?	91.8	190	8.4	1.09	88.
E17	9.76	97.4	190	9.5	1.18	89.0
E18	8.08	93.6	142	5.9	0.76	88.3
E19	8.77	96.0	120	11.2	0.93	95.1
E20	8.99	93.6	199	9.1	1.20	88.2
E21	9.16	90.0	199	5.0	1.17	82.8
E22	18.08	>1000	224	7.2	1.45	114.8
E23	10.03	81.2	252	8.7	1.12	85.1
E24	1.44	17.5	124	2.3	0.07	14.6
E25	17.74	>1000	218	6.5	1.37	119.5
E26	3.06	22.9	319	11.3	0.36	32.2
E27	(Illegible record)					
E28	14.00	78.9	297	10.2	0.92	80.8
E29	12.43	88.1	204	9.3	1.12	87.4

ARMOUR RESEARCH FOUNDATION OF ILLINOIS INSTITUTE OF TECHNOLOGY

Table C-2

DYNAMIC EXPERIMENTS WITH STATIC OVERPRESSURE

Experiment Number	Peak Force (lb)	Time to Peak Force (msec)	Peak Displacement (in.)	Time to Peak Displacement (msec)	Differential Pressure (psi)
F1[*]	75	38.4	0.124	51.9	0
F2[*]	185	14.0	0.605	80.5	0
F2A	196	11.6	1.200	78.4	0
F3[*]	(Illegible record)				106.0
F3A	(Illegible record)				41.0
F4	568	16.7	< 0.001	?	98.0
F4A	512[a]	6.2	< 0.001	?	85.0
F5[*]	871	15.6	0.003	18.0	97.0
F5A	995[a]	8.2	0.005	4.2	102.0
F6	924	8.5	0.012	7.5	55.0
F6A	954	7.4	0.024	8.3	52.5
F7	1030	8.6	0.032	8.6	26.0
F7A	1043	11.8	0.039	10 9	25.0
F8	(Illegible record)		0.056	.	10.0
8A	769	10.3	0.084	10.3	9.0
9	046	10.3	0.113	8.3	4.9
F9A	880	9.8	0.131	11.2	5.0
F10	646	11.6	1.260	66.6	0
F11[*]	943	11.8	0.018	11.8	23.0
F11A	855	10.7	0.025	11.7	23.5
F12	863	9.5	0.064	9.1	5.2
F12A	18	8.2	0.082	5.4	4.8
F13	246	9.6	0.697	70.5	0
F14[*]	993	13.7	0.019	12.0	24.5
F15	961	10.6	0.054	8.8	8.3
F16	935	14.9	0.117	13.0	3.8
F16A	805	9.7	0.193	13.0	2.7
F16B	400	7.2	> 1.2	?	0.8

[*] Initial bed setup
? The time was not apparent in these experiments
[a] Residual static plus applied dynamic load

Note: 1. Displacements are cumulative with respect to the initial bed setup.
2. A or B added to the experiment number indicates that the dynamic load was reapplied to the footing without relieving the static surface overpressure.
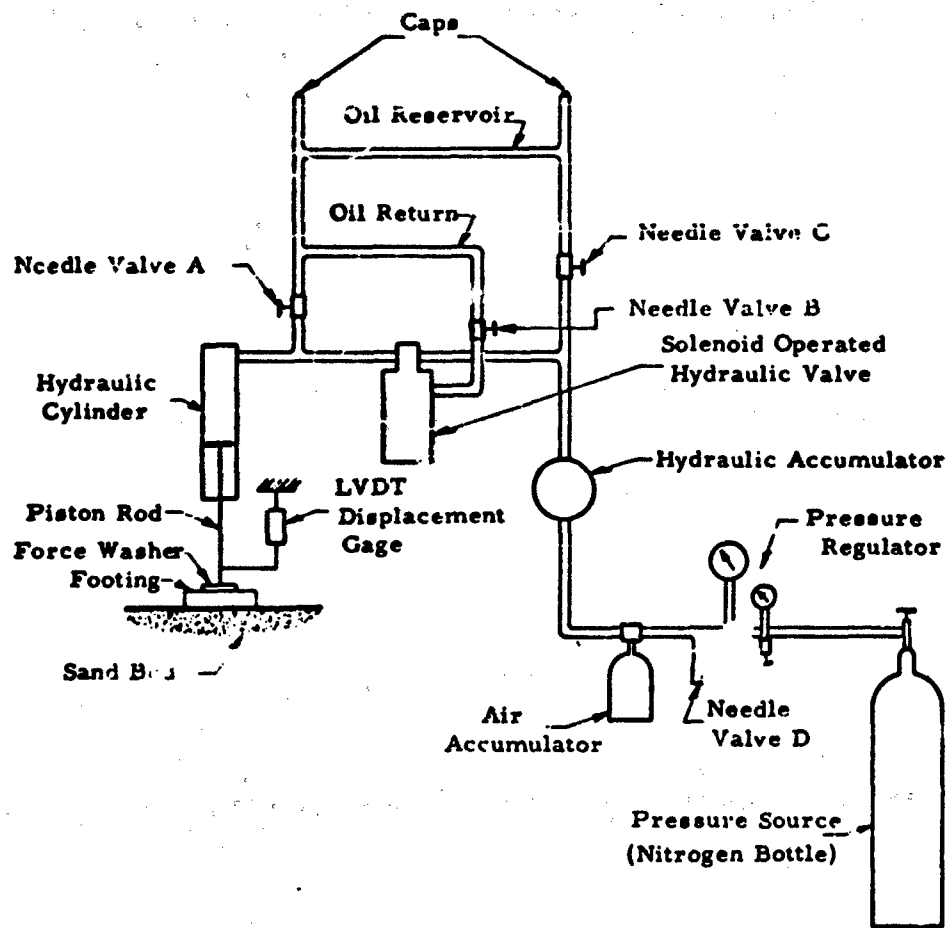
Fig. C-1 DYNAMIC APPARATUS

Time, msec
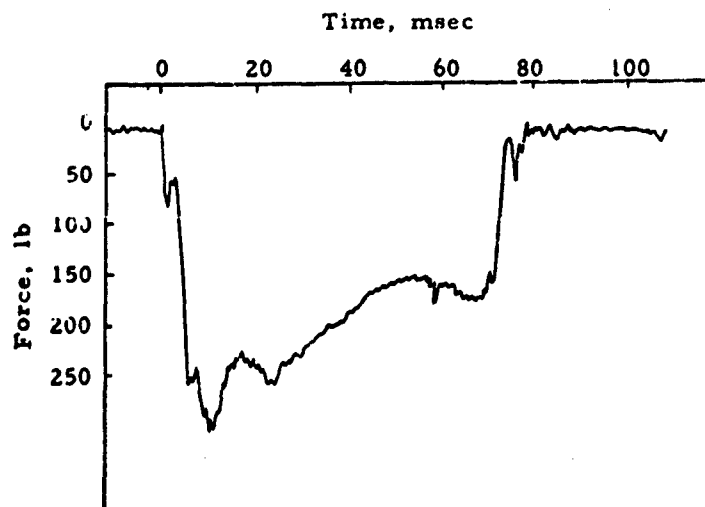
a) Experiment E28, Needle Valve B open.

Time, msec
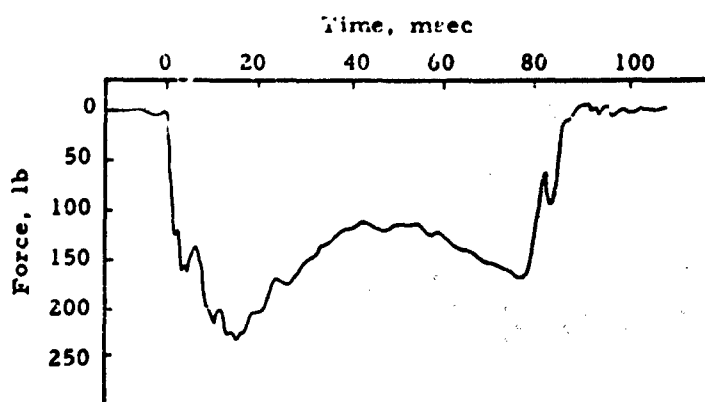
b) Experiment E29, Needle Valve B closed.

Fig. C-2 EFFECT OF NEEDLE VALVE B IN
THE HYDRAULIC SYSTEM

```
        110v    ┌──────────────┐    ┌──────────────┐
         o──────│ Control and Time │──│  Solenoid    │
                │    Delay     │    │    Valve     │
                └──────────────┘    └──────────────┘

                ┌──────────────┐
                │ Accelerometer│
                │Calibration Unit│
                └──────────────┘
  ┌──────────────┐ ┌──────────────┐ ┌──────────────┐
  │     CRL      │ │  Cathode     │ │     CEC      │
  │ Accelerometer│ │  Follower    │ │Linear-Integrate│
  │ Serial No. 164│ │              │ │  Amplifier   │
  └──────────────┘ └──────────────┘ └──────────────┘
  ┌──────────────┐ ┌──────────────┐ ┌──────────────┐
  │     CRL      │ │  Cathode     │ │     CEC      │
  │ Accelerometer│ │  Follower    │ │Linear-Integrate│
  │ Serial No. 165│ │              │ │  Amplifier   │
  └──────────────┘ └──────────────┘ └──────────────┘
  ┌──────────────┐ ┌──────────────┐ ┌──────────────┐
  │     CRL      │ │  Tektronix   │ │              │
  │ Accelerometer│ │ Preamp No. 122│ │  Attenuator  │
  │ Serial No. 166│ │              │ │              │
  └──────────────┘ └──────────────┘ └──────────────┘
  ┌──────────────┐ ┌──────────────┐ ┌──────────────┐   ┌──────────────┐
  │     CRL      │ │  Tektronix   │ │              │   │     CEC      │
  │ Accelerometer│ │ Preamp No. 122│ │  Attenuator  │   │ Oscillogram  │
  │ Serial No. 167│ │              │ │              │   │  Recorder    │
  └──────────────┘ └──────────────┘ └──────────────┘   └──────────────┘
  ┌──────────────┐ ┌──────────────┐
  │ Sanborn LVDT │ │     CEC      │
  │ 585DT-1000   │ │  Carrier     │
  │ Serial No. 170│ │  Amplifier   │
  └──────────────┘ └──────────────┘
  ┌──────────────┐ ┌──────────────┐
  │  ATC LVDT    │ │     CEC      │
  │   6204 B     │ │  Carrier     │
  │ Serial No. 759│ │  Amplifier   │
  └──────────────┘ └──────────────┘
  ┌──────────────┐ ┌──────────────┐
  │  Lockheed    │ │     CEC      │
  │ Force Washer │ │  Carrier     │
  │  WR-7S-1     │ │  Amplifier   │
  └──────────────┘ └──────────────┘
                ┌──────────────┐
                │ Force Washer │
                │Calibration Unit│
                └──────────────┘
```

Fig. C-3   SCHEMATIC DIAGRAM OF INSTRUMENTATION FOR
           THREE - DIMENSIONAL DYNAMICALLY LOADED FOOTINGS

C-12

**Fig. C-4 INSTRUMENTATION FOR EXPERIMENTS
WITHOUT STATIC OVERPRESSURE**
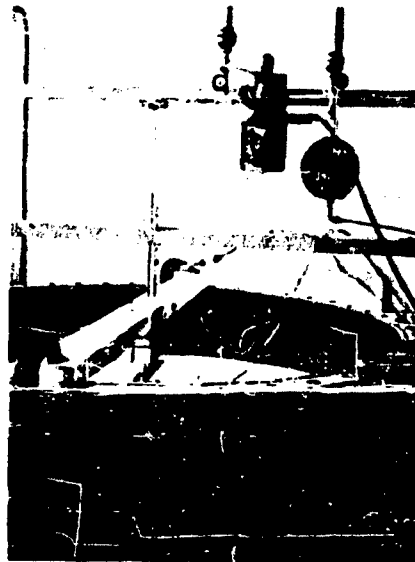
**Fig. C-5 DYNAMIC LOADING APPARATUS FOR EXPERIMENTS
WITHOUT STATIC OVERPRESSURE**
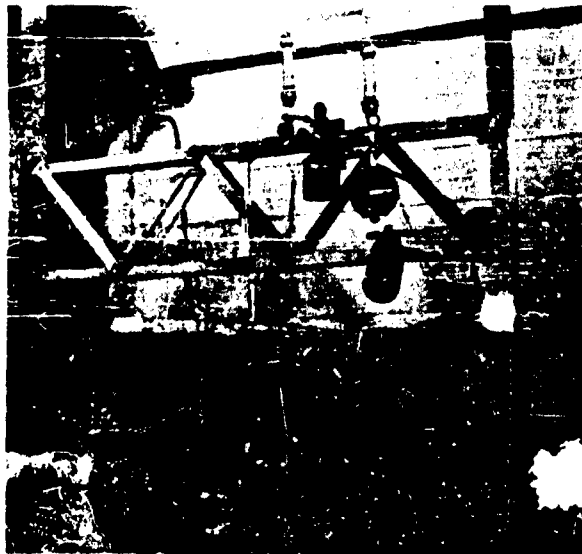
Fig. C-6 TRUSS USED IN STIFFENING CHANNEL MEMBERS
SUPPORTING THE HYDRAULIC APPARATUS
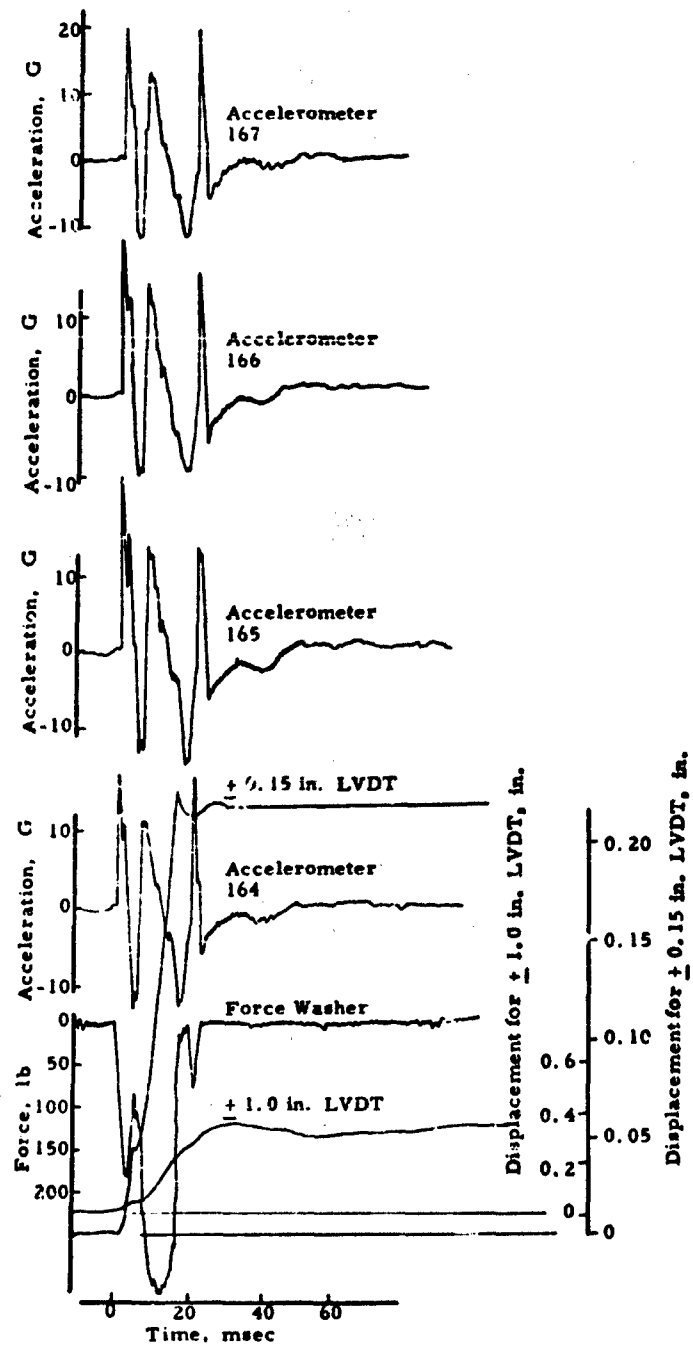
Fig. C-7 EXPERIMENT E26 (13-MSEC SOLENOID ACTUATION)

ARMOUR RESEARCH FOUNDATION OF ILLINOIS INSTITUTE OF TECHNOLOGY

C-15
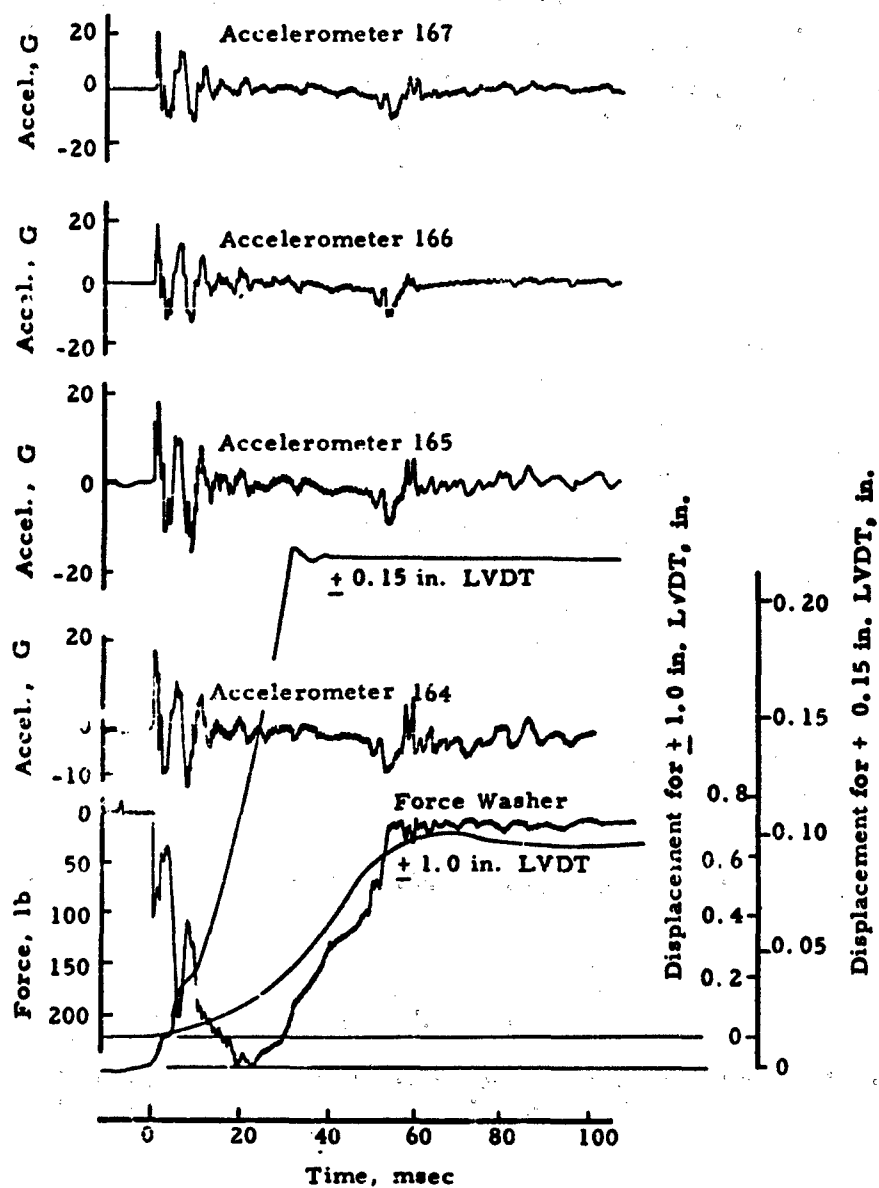
Fig. C-8 EXPERIMENT E15 (45-MSEC SOLENOID ACTUATION)
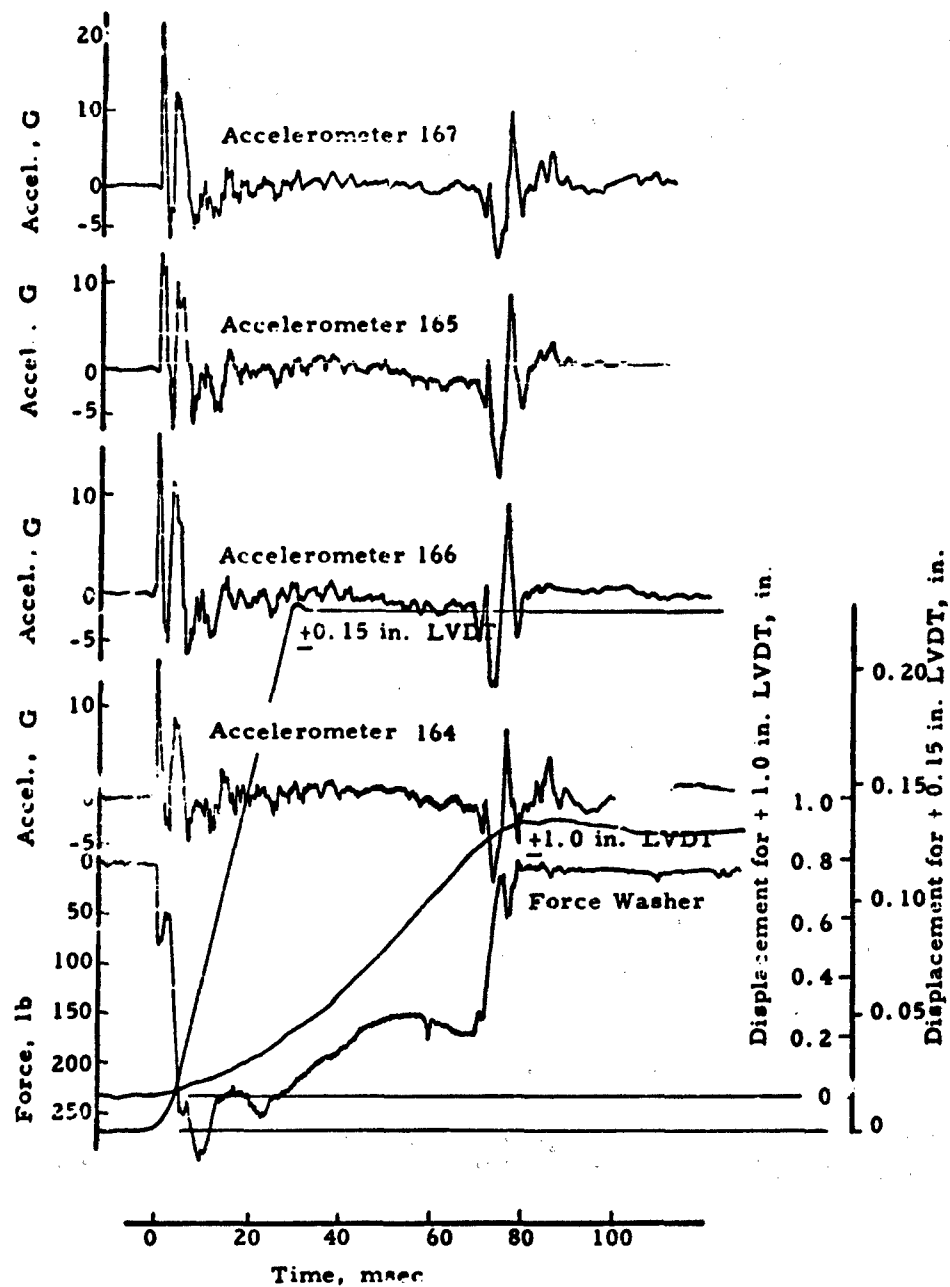
Fig. C-9 EXPERIMENT E28 (70-MSEC SOLENOID ACTUATION)

C - 17
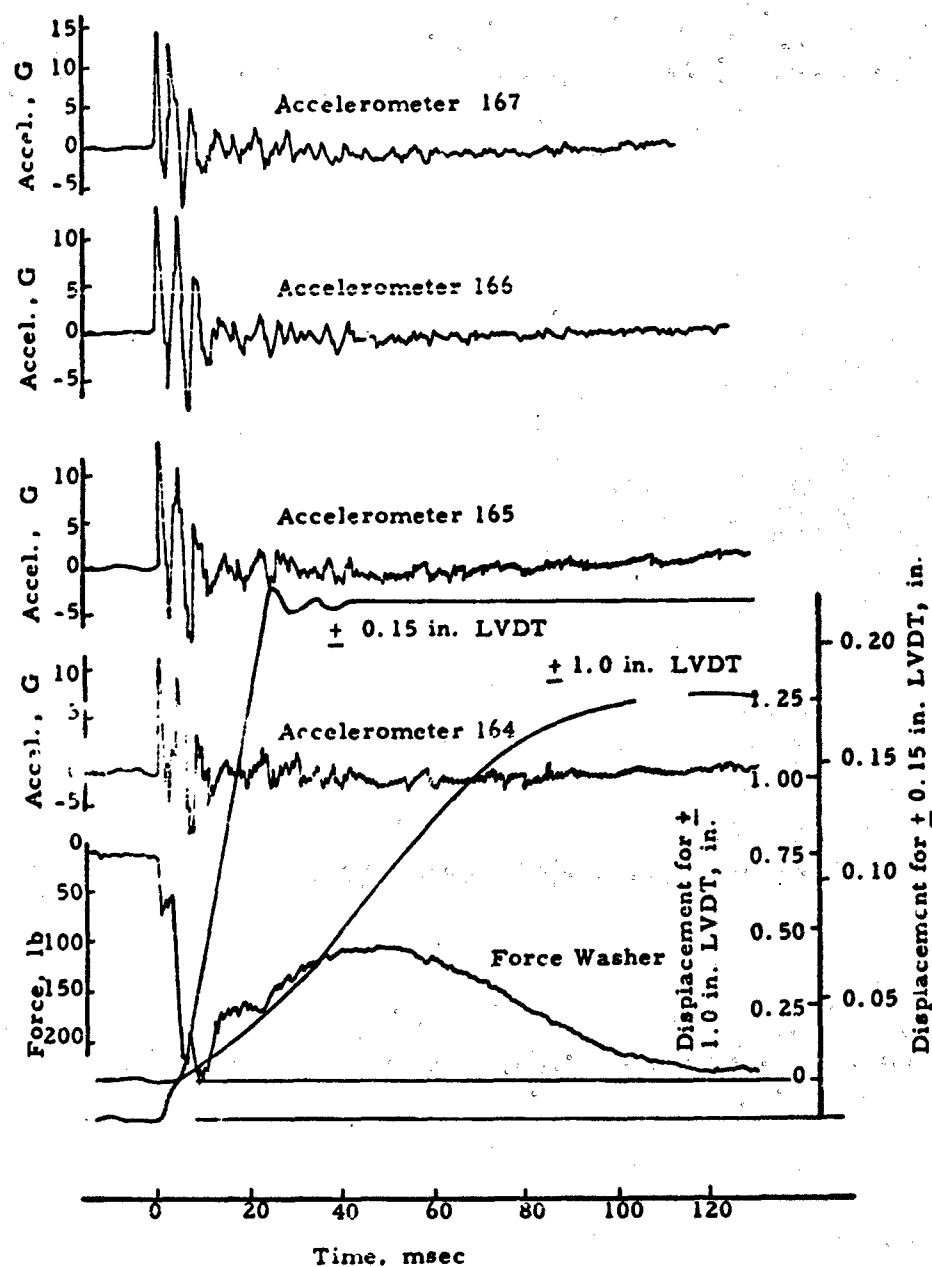
Fig. C-10 EXPERIMENT E25 (INFINITE LOAD DURATION)
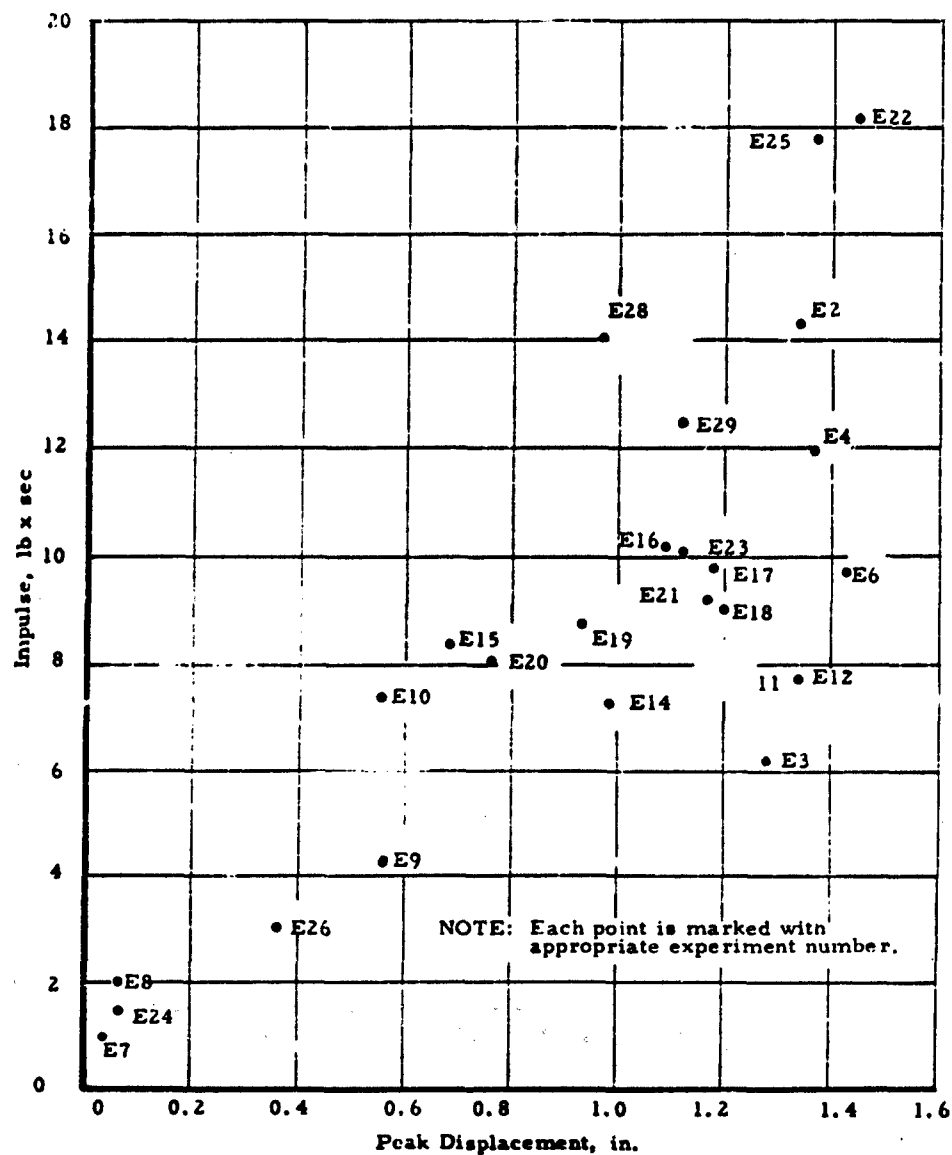
Fig. C-11 PEAK DISPLACEMENT VS. INTEGRAL OF FORCE-TIME
HISTORY FOR DYNAMIC EXPERIMENTS WITHOUT STATIC
OVERPRESSURE
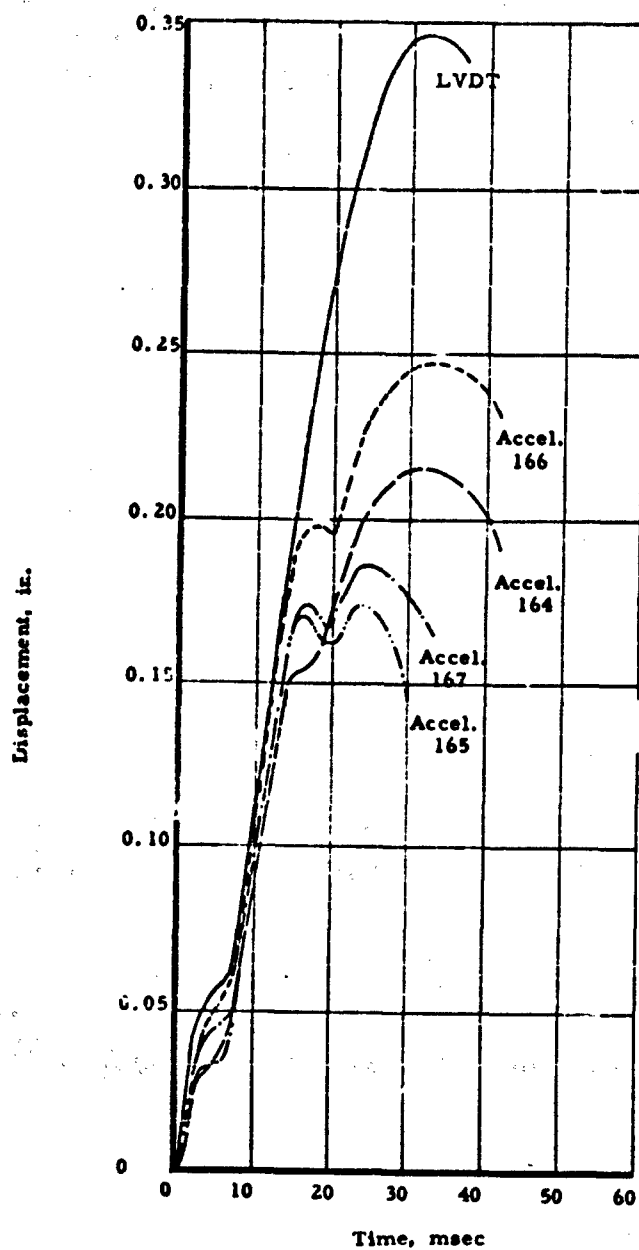
Fig. C-12 EXPERIMENT E26, DISPLACEMENT-TIME HISTORY
USING INTEGRATED ACCELEROMETER RECORDS
AND LVDT RECORDS

Fig. C-13 EXPERIMENT E28, DISPLACEMENT-TIME HISTORY
USING INTEGRATED ACCELEROMETER RECORDS AND
LVDT RECORDS

ARMOUR RESEARCH FOUNDATION OF ILLINOIS INSTITUTE OF TECHNOLOGY

C - 21
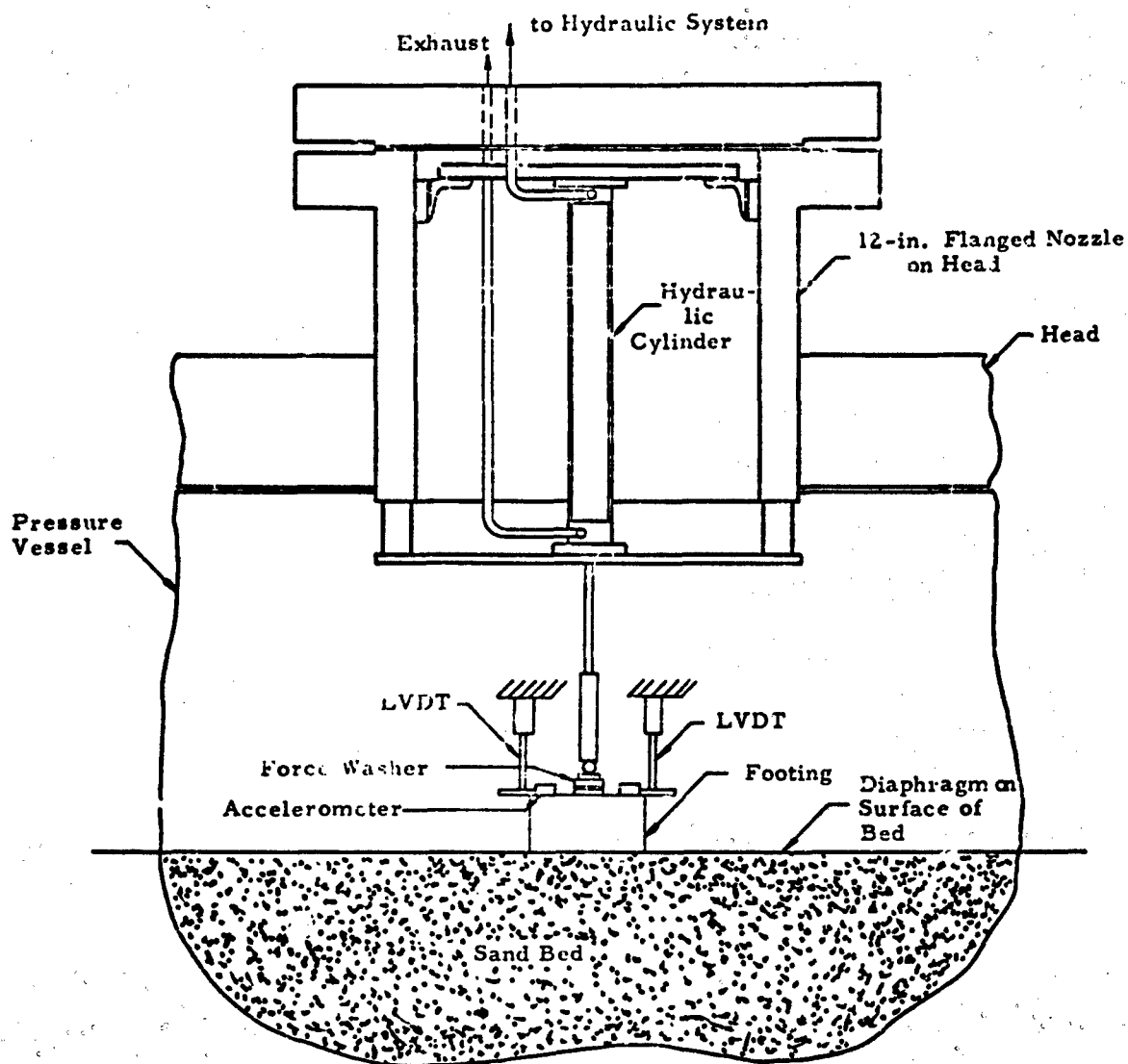
Fig. C-14 CONFIGURATION FOR DYNAMIC EXPERIMENTS WITH
STATIC OVERPRESSURE

ARMOUR RESEARCH FOUNDATION OF ILLINOIS INSTITUTE OF TECHNOLOGY

C - 22
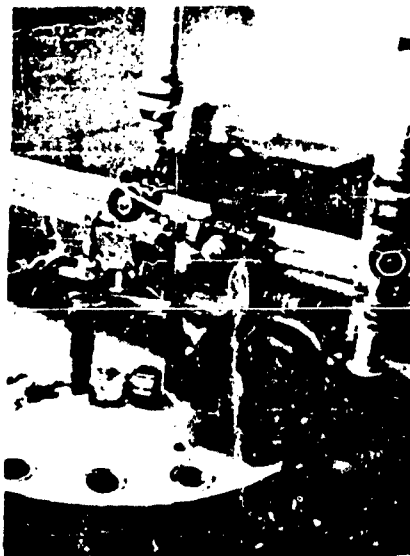
Fig. C-15 HYDRAULIC SYSTEM MOUNTED ABOVE THE 12-IN.
OPENING IN PRESSURE VESSEL HEAD
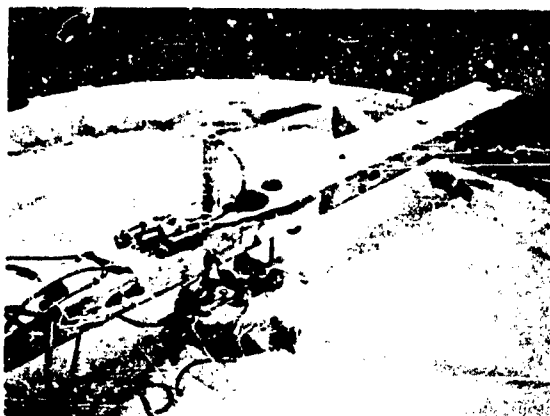
Fig. C-16 TYPICAL SETUP FOR DYNAMIC EXPERIMENTS USING
STATIC OVERPRESSURE
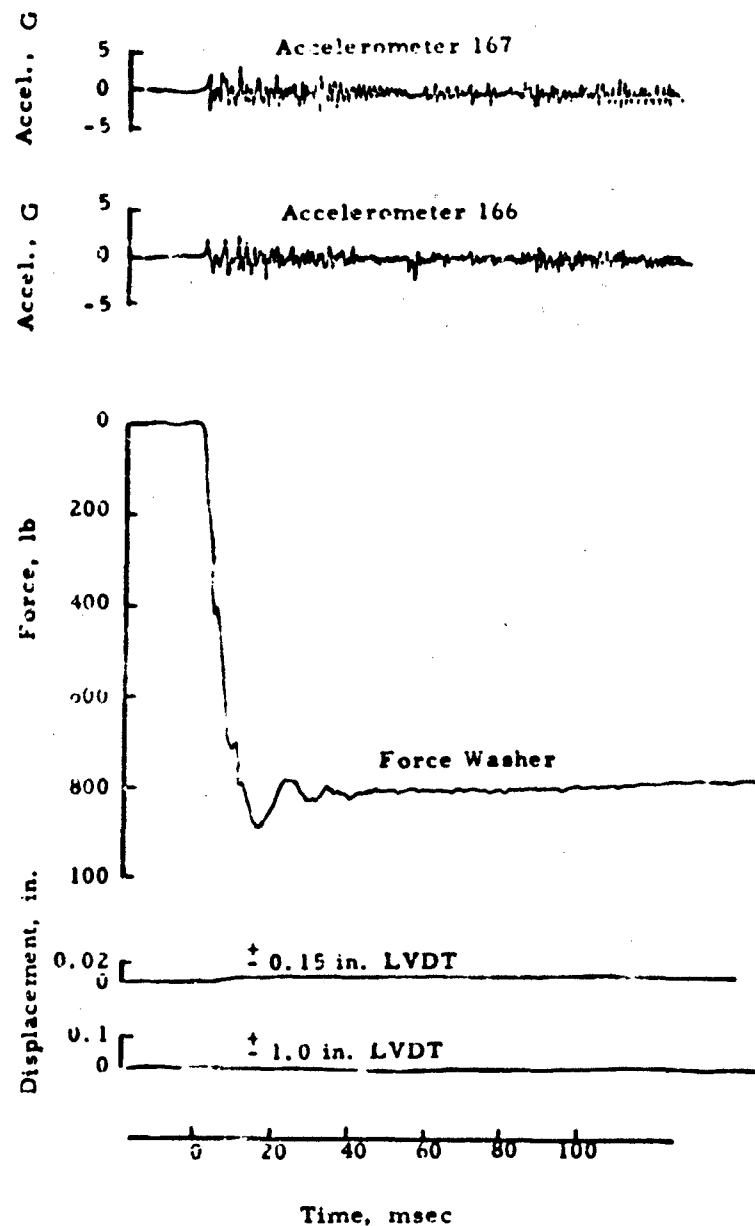
Fig. C-47 EXPERIMENT F5-97-P5 STATIC OVERPRESSURE

ARMOUR RESEARCH FOUNDATION OF ILLINOIS INSTITUTE OF TECHNOLOGY

C - 24
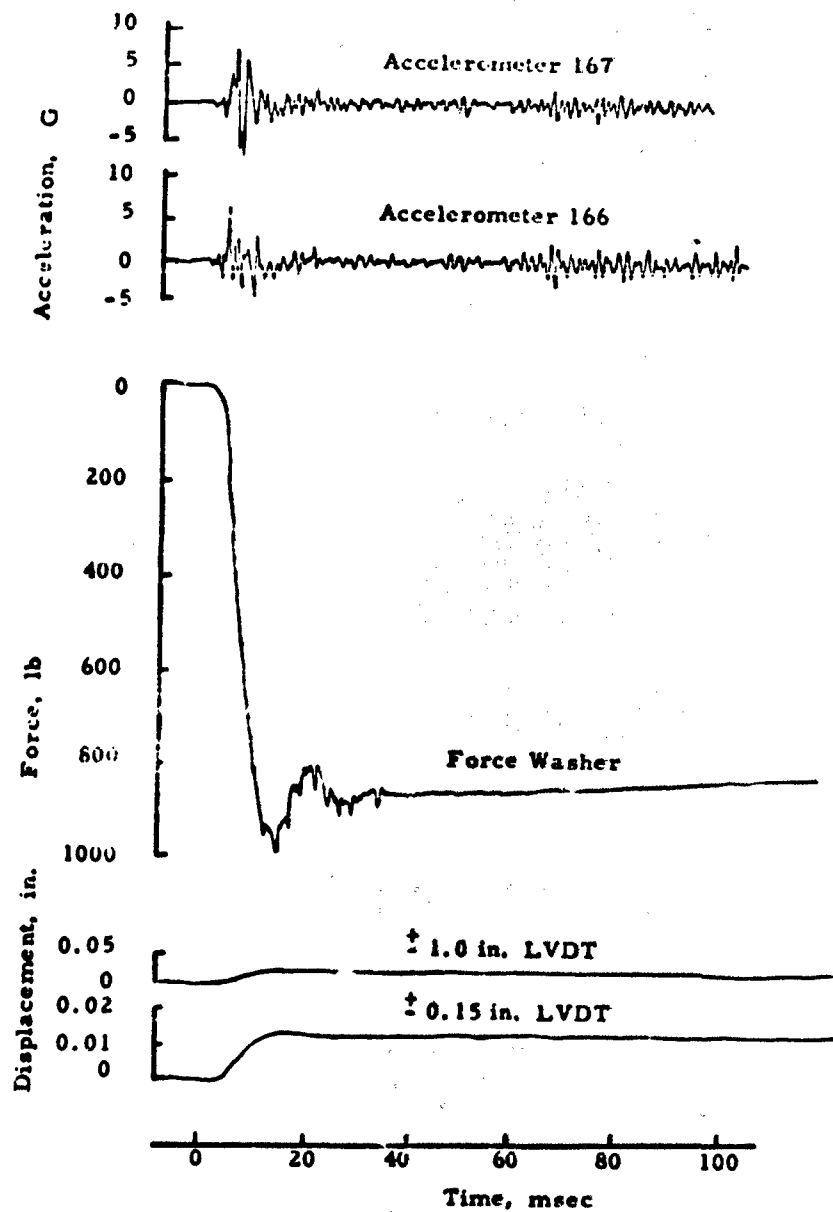
Fig. C-18 EXPERIMENT F14, 24.5-PSI STATIC OVERPRESSURE

C-25
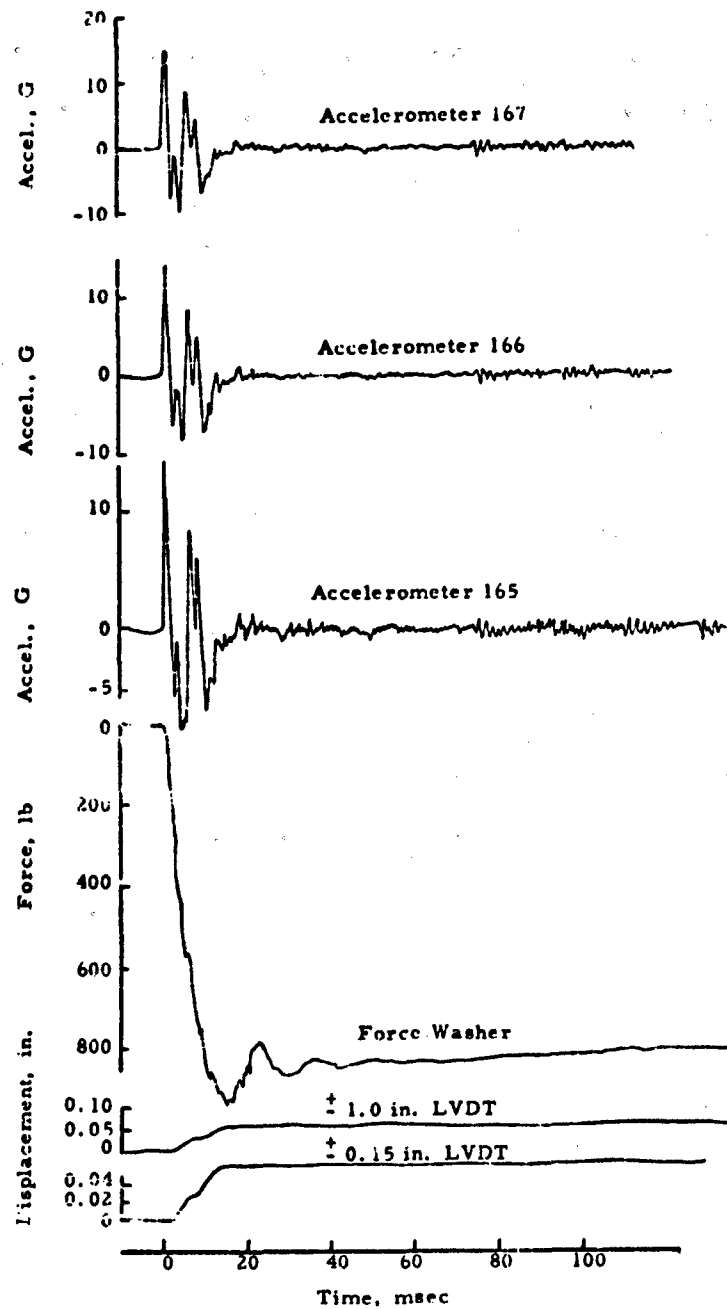
Fig. C-19   EXPERIMENT F16, 3.8-PSI STATIC OVERPRESSURE

APPENDIX D

TWC-DIMENSIONAL STATICALLY AND DYNAMICALLY

LOADED FOOTINGS

by

S. Shenkman

ARMOUR RESEARCH FOUNDATION OF ILLINOIS INSTITUTE OF TECHNOLOGY

APPENDIX D

TWO-DIMENSIONAL STATICALLY AND DYNAMICALLY LOADED FOOTINGS

by

S. Shenkman

Footing behavior was studied qualitatively by two-dimensional experiments. The glass-sided container constructed for the original program [D-1][*] was used in these experiments. The footings were 3-in. by 4-in. and the soil was a dense Ottawa sand (grain-size distribution shown in figure 4). Previous work of this nature was completed on past contracts, including the following series of experiments: a) static concentrated loading, Experiments G1 through G5[D-1]; b) dynamic concentrated loading using dropped weights, Experiments G6 through G8[D-1]; and c) dynamic concentrated loading applied by means of the pneumatic-hydraulic loading apparatus, Experiments G9 through G21[D-2]. Included in these experiments r   vertical static and dynamic loads on surface footings; vertical static loads on buried footings, vertical eccentrically-applied dynamic loadings on surface footings, and inclined dynamic loadings on surface footings.

The present study continues these experiments using both surface and partially buried footings. The numbering system used in the previous studies is continued on this program, since the basic facility remains the same and the qualitative objectives are similar. These experiments are summarized in Table D-1.

---

[*]Superscript numbers in parentheses cite references collected at the end of this appendix.

Surface Footings

Two static experiments, G22 and G23, were performed in this series. In each test, a constant displacement rate was applied to the footing by a motor driven gear box, running at 0.055 in. per min in Experiment G22 and 0.11 in. per min in Experiment G23.

Instrumentation for Experiment G22 consisted of a proving ring which measured the applied load, and a dial gage which recorded the deflection of the footing.

Instrumentation for Experiment G23 consisted of a force washer and two LVDTs (+ 0.15-in and + 1-in. linear range as described in Appendix C) recording on a CEC recorder. Figure D-1 shows the setup for Experiment G23; the setup for Experiment G22 was similar except for the instrumentation. A photograph after failure is shown in figure D-2

Two methods for comparing the results of experiments G22 and G23 with similar previous setups (Experiments G1, G2, and G5)[D-1] would involve either a comparative plot of their resistance-displacement curves, or examination of the resulting bearing capacities. Both methods would of course be desirable, however, the resistances and displacements for Experiments G1, G2, and G5 were tabulated to a point before the peak bearing capacity, and the resulting peak loads recorded without their corresponding displacements. Table D-2 presents a comparison of these experiments, based on their bearing capacity. Also included in Table D-2 is the result of an experiment previously performed in the glass-sided container[D-2] where a static concentrated load was applied to the footing at a "slow" rate (0.00053 in /min).

The comparison attempted is based on the experimental results without any regard to load application techniques or instrumentation. In Experiments G1, G2 and G5, the loads were applied by a hydraulic jack,

whereas in G22, G23, and the "slow" rate loading experiments, the loads were applied by a gear box. Since G22 is similar to G1, G2, and G5, the means of load application does not appear to produce significantly different results.

In observing the proving ring and dial gages while conducting an experiment, the load and deflection seemed to jump in substantial increments This effect has previously been demonstrated in the "slow" rate of loading experiment, where the proving ring and dial gage readings were recorded by a movie camera, the results of which are plotted in Fig. D-3. If we consider the extreme forces recorded by the jumps as defining an envelop, the lower curve of the envelop records a resistance of 224 lb, which is an agreement with Experiment G23 as plotted in Fig. D-4. It is therefore felt that in all static experiments prior to G23, the peak resistances were observed at a point representing the upper curve of the envelop, and do not represent the true bearing capacity of the footing. Very limited jumping was observed in the force washer records. The spring characteristic or time required for recov of load in the proving ing mat explain this jumping.

Partially Buried Footings

An effort to simulate the geometry and type of loadings for arches and domes was made in this series of experiments. Considering the structure (arch or dome) to consist of a concave downward dished head connected to an annular ring or footing of greater width than the thickness of the head, the bearing surface of the footing may either be horizontal or tilted at some angle to the horizontal. The outer surface of the footing would be covered with a layer of soil, dependent on the depth of burial of the footing, while the inner portion of the footing would be at the excavated ground surface. A nuclear detonation, therefore subjects the outer surface of the structures and surrounding soil to an overpressure during the time that the footing is subjected to load. For the purposes of this experimental approach attention has been limited to the two-dimensional problem, although it should be recognized that the real three-dimensional situation may introduce significant variations.

ARMOUR RESEARCH FOUNDATION OF ILLINOIS INSTITUTE OF TECHNOLOGY

Since the object of these experimen s is to supply qualitative result⁃, the actual problem was simplified by applying a static overpressure to one side of a simulated arch or dome footing. The experimental procedure for these experiments considered static and dynamic concentrated loads for vertical footings and footings inclined at an angle of 30° to the vertical   The footings were T-shaped with bearing surface dimensions 3-in. wide by 4-in. deep. Strips of plastic foam covered by a sheet of paper were glued to the sides of the footing to prevent sand from leaking between the footing and glass plates. A rubber membrane contained by the glass box on three sides, and the footing, sand and a steel plate on the other three sides, was inflated and held to a given pressure, simulating a static overpressure on the surface.

Instrumentation, shown schematically in figure D-5, included a force washer, a ± 1.0 in. LVDT, and a ± 0.15 in. LVDT recording on a CEC recorder, (see Appendix C for a complete description of the instrumentation). In addition, a 16 mm Wollen⁃ Fastax camera was used to observe footing failure under dynamic loa

The LVDT were connected to a strip of steel which was center-supported by the loading rod. It was anticipated that these LVDTs would measure the displacement of the center of the footing, regardless of the movement of the footing. However, it was seen that in many cases, the loading rod would bend when the footing started to turn and th displacements recorded   re not those of the center of the footing, but rather, indicative of the motion of a point some distance from the center. It was possible, during the initial displacement of the footing, to average the readings of both LVDTs, since they were on opposite sides of the footings. For this reason, load-displacement curves for the two-dimensional static experiments are plotted until the point where the + 0.15-in. LVDT became nonlinear.

In each of these experiments the force was applied normal to the base of the footing and the deflections measured parallel to the direction of load application.

Table D-3 summarizes the results of the experiments using a concentrated static load. Resistance-displacement curves for these experiments are plotted in figures D-6 and D-7. Typical setups are shown in Figs. D-8 and D-9 for vertical and inclined footings. Each of these experiments used a motor-driven gear box applying the load to the footing at a displacement rate of 0.110 in. per min. A surface overpressure of 5 psi was used in Experiments G29 and G31, however, overpressures as high as 10 psi were attempted in Experiments G24 and G27, but they were found difficult to control for the procedure used, and in both cases caused the rubber membrane to burst. Sequence photographs of footing failure in Experiments G28, G29, G30, and G31 are shown in Figs. D-10, D-11, D-12, and D-13, respectively.

Table D-4 summarizes the results of eight experiments using the dynamic loading apparatus[(D-2)]. In each of three experiments (G32, G34, and G35) the load was applied three times before failure planes were apparent. Repeated application of the load is indicated by A or B in Table D-4 after the experiment number. Repeated t   g was felt to be justified if the displacements on prior tests was small. Footing displacements, listed in Table D-4 for these experiments are cumulative with respect to the initial setup. Typical setups for these experiments are shown in Figs. D-14 and D-15, for vertical and inclined loading application. Force-time and displacement-time records are shown in Figs. D-16, D-17, D-18, and D-19 for Experiments G33, G36, G37, and G39, respectively; sequence photographs taken from the 16 mm movie film are shown in Figs D-20 to D-23 for the above experiments.

Of particular interest in these experiments, both static and dynamic, is the location of the failure plane. While it is not possible to generalize these locations because of the limited number of experiments, the following effects have been observed:

    a) Vertical footings; in all cases failure occurred within the area of the simulated dome.

    b) Inclined footings.

ARMOUR RESEARCH FOUNDATION OF ILLINOIS INSTITUTE OF TECHNOLOGY

D-5

1) Location of the failure plane for static loading was dependent on the applied static overpressure; under ambient pressure, failure occurred outside the structure while an application of 5 psi to the surface caused the shear plane to develop within the structure.

2) Formulation of a failure plane for dynamic loading, under both ambient and overpressure conditions, occurred outside of the structure. In two experiments, G35B and G36, the footing was seen to turn, the initial failure outside the structure formed and followed by a failure plane within the structure.

An important phenomenon observed in the 16 mm movies was the turning or twisting of the footing during load application. As a result, in most cases the final angle of inclination of the footing is different than the original angle of load application. This results in a moment applied to the footing due to the eccentricity, in addition to the applied load. No effort was made to measure this eccentricity during this series of experiments, however, future experiments of a similar nature should attempt to place the point of load application closer to the bearing surface of the footing, thereby minimizing the resulting eccentricity. Of course, the eccentricity may be completely eliminated by rigidly connecting the footing to the loading rod. Any future experiments will weigh this approach against the "roller" type of load application.

REFERENCES

D-1   McKee K. E. Design and Analys s of Foundations for
       Protective Structures, AFSWC-TR-59-56, Armour Research
       Foundation, Chicago (October 1959).

D-2   McKee, K E., Design and Analys .s of Foundations for
       Protective Structures, AFSWC-TN-61-14, Armour Research
       Foundation, Chicago (May 1961).

D-

Table D-1

TWO - DIMENSIONAL EXPERIMENTS REPORTED

HEREIN

Experiment Number	Average Density of Sand in Container (pcf)	Type of Footing	Type of Load	Static Surfac Overpressure (psi)
G22	107.6	Surface	Static	0
G23	107.7	Surface	Static	0
G24	--	Partially buried, vertical	Static	10
G25	106.0	Partially buried, vertical	Static	0
G26	108.8	Partially buried, vertical	Static	0
G27	109.7	Partially buried, vertical	Static	10
G28	108.1	Partially buried, vertical	Static	0
G29	107.2	Partially buried, vertical	Static	5
G30	107.8	Partially buried inclined 30° from vertical	Static	0
G31	110.1	Partially buried, inclined 30° from vertical	Static	5
G32, G32A, G32B*	108.6	Partially buried, inclined 30° from vertical	Dynamic	0
G33*	109.6	Partially buried, inclined 30° from vertical	Dynamic	0
G34, G34A, G34B	112.3	Partially buried, inclined 30° from vertical	Dynamic	5, 5, 3
G35, G35A, G35B*	113.0	Partially buried, inclined 30° from vertical	Dynamic	2, 1, 0, 5
G36*	111.7	Partially buried, inclined 30° from vertical	Dynamic	0.5
G37*	107.4	Partially buried, vertical	Dynamic	0
G38	112.3	Partially buried, vertical	Dynamic	5
G39*	110.3	Partially buried, vertical	Dynamic	5

*Movies of these experiments are available.

ARMOUR RESEARCH FOUNDATION OF ILLINOIS INSTITUTE OF TECHNOLOGY

Table D-2

TWO-DIMENSIONAL STATIC EXPERIMENTS OF
SURFACE FOOTINGS

Experiment Number	Maximum Load (lb)	Bearing Capacity (psi)
G1	264	22.0
G2	300	25.0
G5	344	28.7
"Slow" rate of loading	275	22.9
G22	329	27.
G23	234	19.5

Table D-3

TWO-DIMENSIONAL STATIC EXPERIMENTS OF
PARTIALLY BURIED FOOTINGS

Experiment Number	Static Surface Overpressure (psi)	Maximum Load (lb)	Deflection at Maximum Load (in.)
G25	0	625	0.127
G26	0	605	0.234
G28	0	547	0.123
G29	5	782	0.112
G30	0	468	0.152
G31	5	940	0.328

ARMOUR RESEARCH FOUNDATION OF ILLINOIS INSTITUTE OF TECHNOLOGY

Table D-4

TWO-DIMENSIONAL DYNAMIC EXPERIMENTS

OF PARTIALLY BURIED FOOTING

Experiment Number	Position of Footing	Peak Force (lb)	Time to Peak Force (msec)	Peak Displacement (in.)	Time to Peak Displacement (msec)	Over-pressure (psi)
G32	inclined	391	10.9	0.063	13.8	0
G32A	inclined	495	10.3	0.153	13.7	0
G32B*	inclined	519	10.9	0.742	76.6	0
G33*	inclined	455	10.6	1.593	80.9	0
G34	inclined	803	----	----	----	5
G34A	inclined	793	----	----	----	5
G34B	inclined	916	13.2	----	----	3
G35	inclined	969	19.9	0.372	19.6	2
G35A	inclined	918	13.8	0.553	15.8	1
G35B*	inclined	776	16.2	1.53	83.8	0.5
G36*	inclined	940	15.2	0.66	74.5	0.5
G37*	vertical	552	12.2	1.308	73.3	0
G38	vertical	755	13.1	1.410	97.9	5
G39*	vertical	773	12.1	1.165	90.8	5

*Movies of these experiments are available. Repeated application of the load on a given setup is indicated by the letters A or B after the experiment numbers.
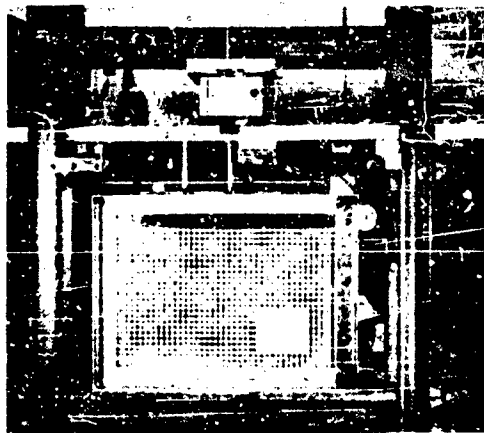
Fig. D-1 SETUP FOR EXPERIMENT G23
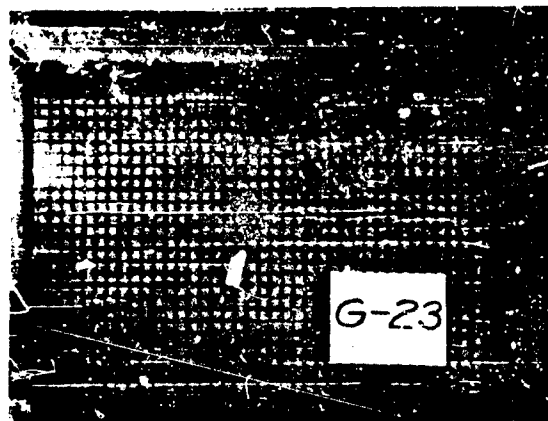
Fig. D-2 EXPERIMENT G23 AFTER FAILURE
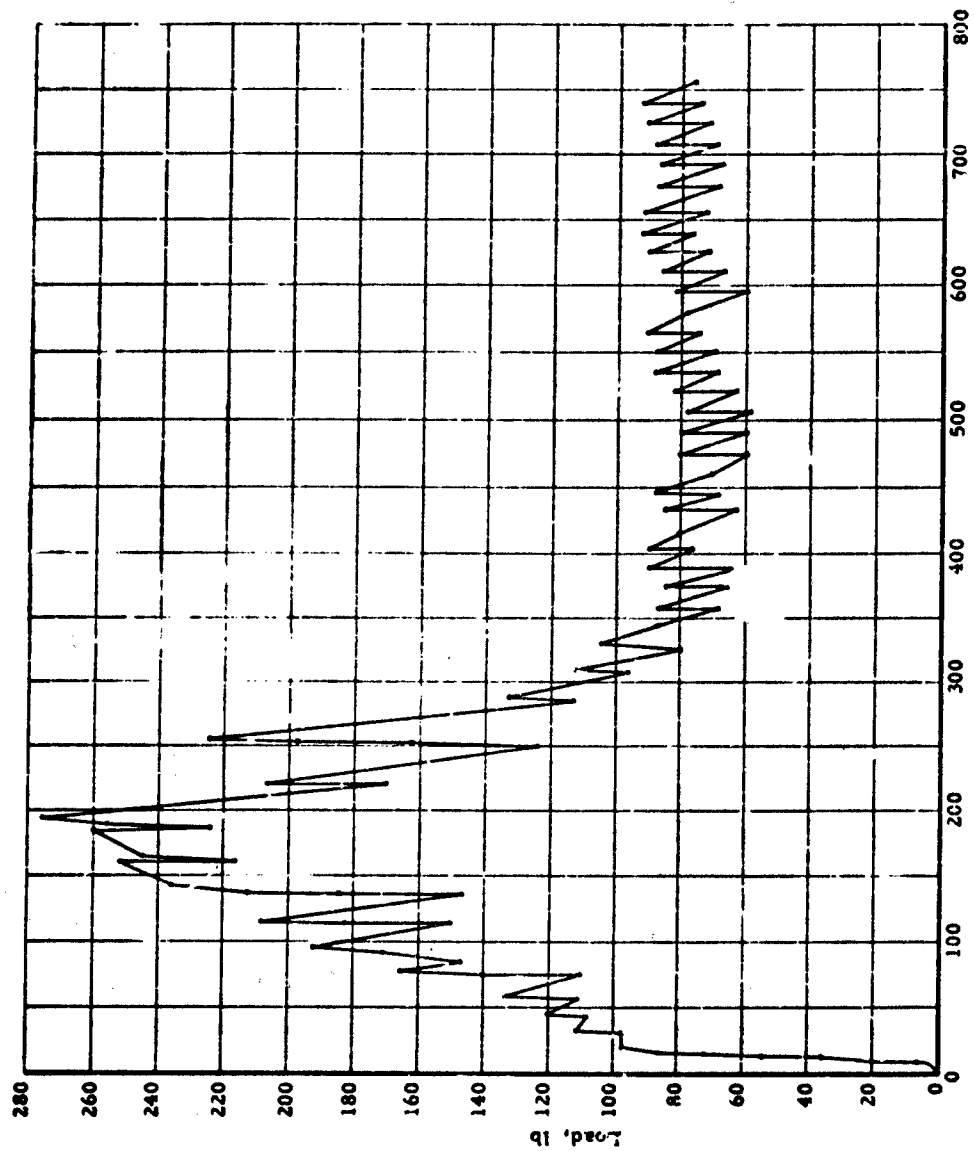
Displacement, in. x 10⁻³

F & D. EXPERIMENT U.NG .... R.TE OF LONDING
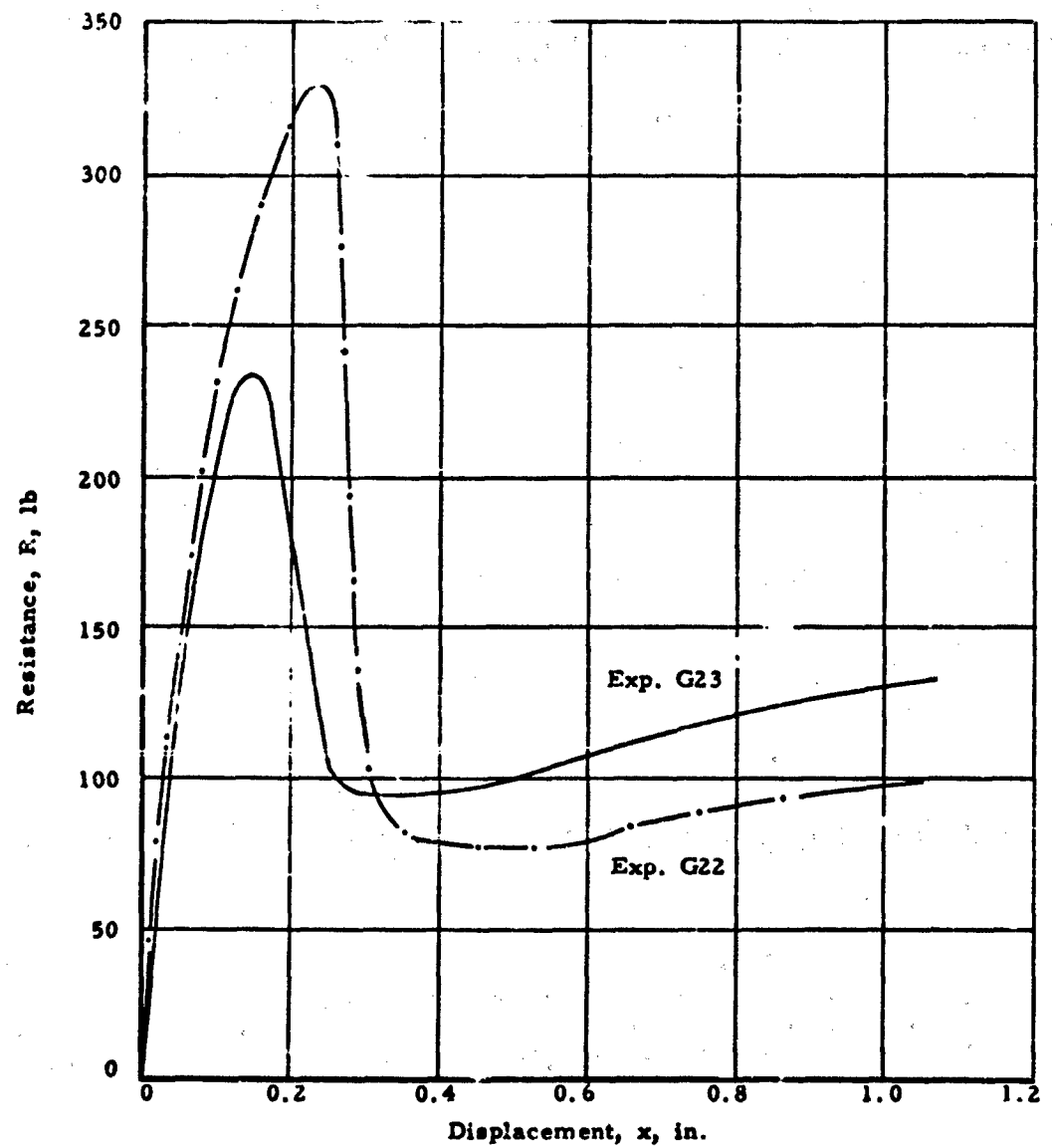
Fig. D-4 RESISTANCE-DISPLACEMENT CURVES FOR
EXPERIMENTS G22 AND G23

```
                    ┌─────────────────┐
                    │ Force Washer    │
                    │ Calibration     │
                    │ Unit            │
                    └─────────────────┘
                            │
┌─────────────┐     ┌─────────────────┐
│ Lockheed    │     │      CEC        │
│ Force Washer│─ ─ ─│ Carrier Amplifier│
│ WR-7S-1     │     └─────────────────┘
└─────────────┘                         │
                                        │
┌─────────────┐     ┌─────────────────┐ │   ┌──────────────┐
│ Sanborn LVDT│     │      CEC        │ │   │     CEC      │
│ 585 DT-1000 │─────│ Carrier Amplifier│─────│ Oscillogram  │
│ Serial No. 170│   └─────────────────┘     │  Recorder    │
└─────────────┘                             └──────────────┘
                                        │
┌─────────────┐     ┌─────────────────┐ │
│ ATC I DT    │     │      CEC        │ │
│ 6204-B      │─────│ Carrier Amplifier│─┘
│ Serial No. 759│   └─────────────────┘
└─────────────┘
```

Lockheed
Force Washer
WR-7S-1

Sanborn LVDT
585 DT-1000
Serial No. 170

ATC I DT
6204-B
Serial No. 759

CEC
Carrier Amplifier

CEC
Carrier Amplifier

CEC
Carrier Amplifier

CEC
Oscillogram
Recorder

110 vac ○────── ┌─────────────┐   ┌──────────┐
                │ Control and │   │ Solenoid │
                │ Time Delay │─────│ Valve   │
                └─────────────┘   └──────────┘

110 vac ○────── ┌─────────────┐   ┌─────────────────┐
                │   Variac   │─────│   16 mm   │
                │   │   │Wollensak Fastax │
                └─────────────┘   │   Camera   │
                                    └─────────────────┘
                                            │
                                            ○ Timing
                                              110 vac
                                              60 cps

Fig. D-5 SCHEMATIC OF INSTRUMENTATION FOR
          TWO-DIMENSIONAL EXPERIMENTS

D-14
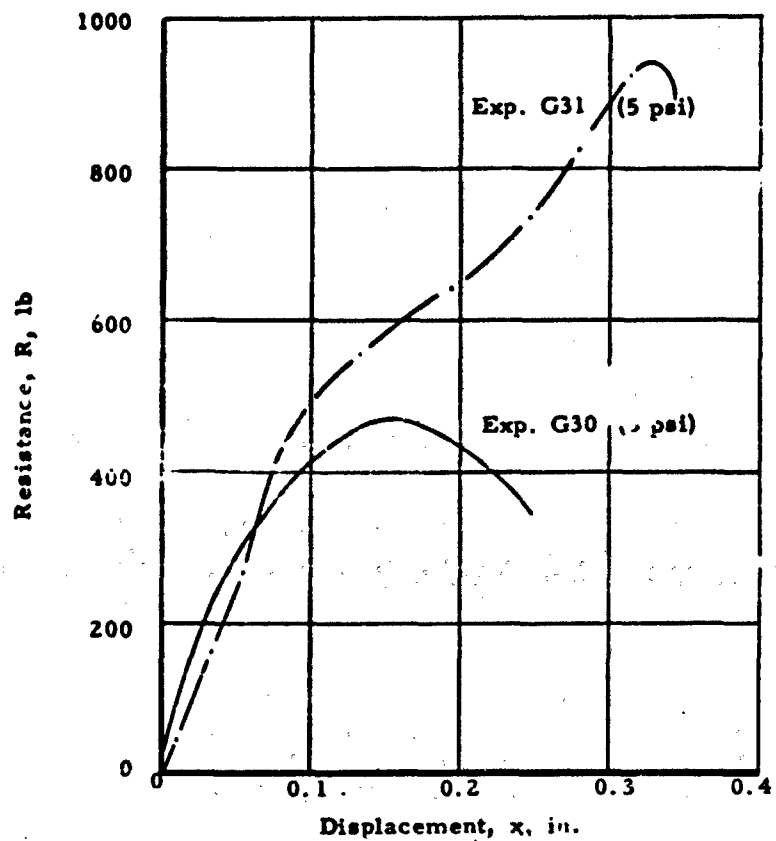
Fig D-6 RESISTANCE-DISPLACEMENT CURVES FOR
INCLINED PARTIALLY BURIED FOOTINGS
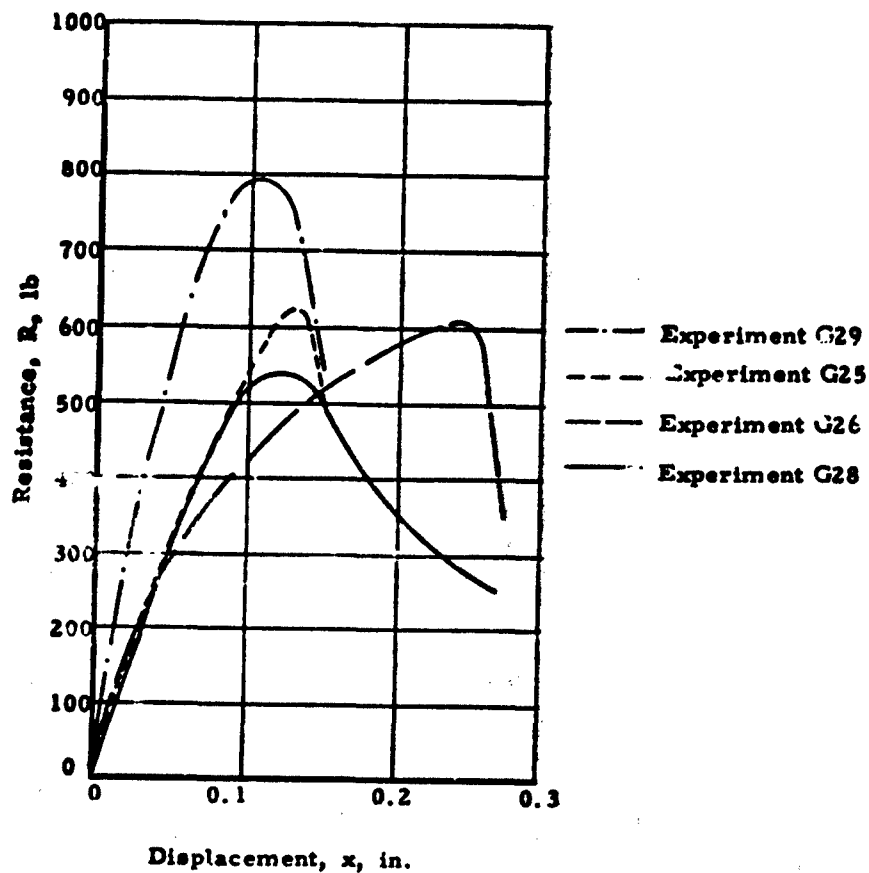
Fig. D-7 RESISTANCE-DISPLACEMENT CURVES FOR PARTIALLY
BURIED VERTICAL FOOTINGS WITHOUT STATIC
OVERPRESSURE
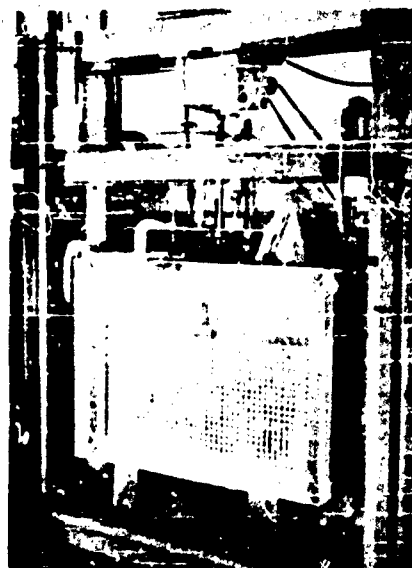
Fig. D-8 SETUP FOR STATICALLY LOADED VERTICAL FOOTINGS
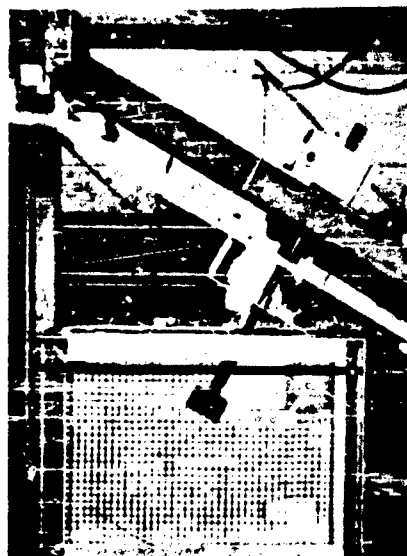
Fig. D-9 SETUP FOR STATICALLY LOADED INCLINED FOOTINGS
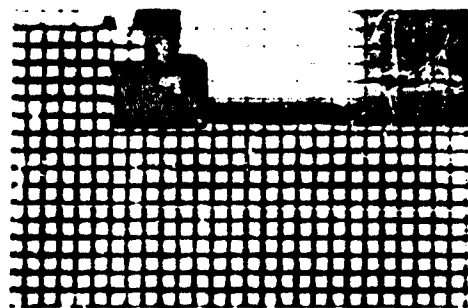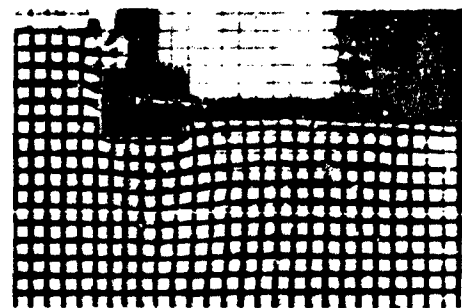
Start of Experiment | 145 sec
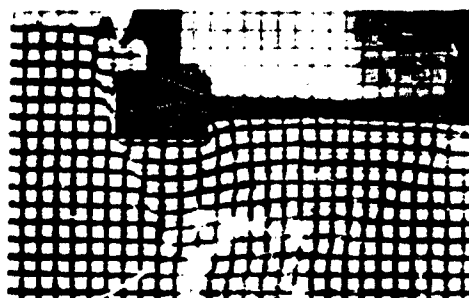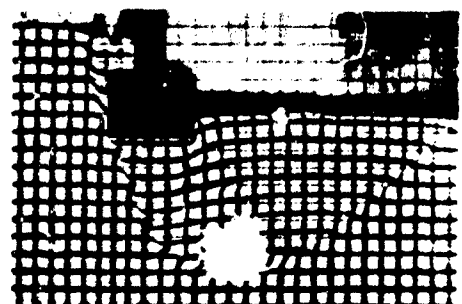
187 sec | 230 sec
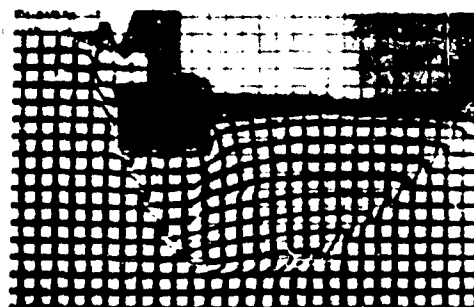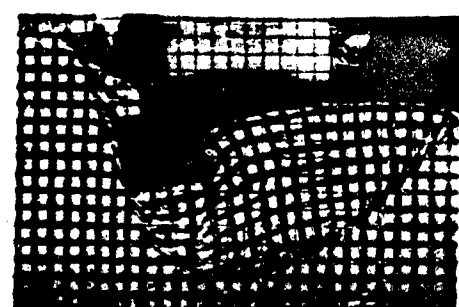
340 sec | End of Experiment

Fig. D-10 <u>SEQUENCE PHOTOGRAPHS FOR STATICALLY LOADED VERTICAL FOOTING (EXPERIMENT G28)</u>
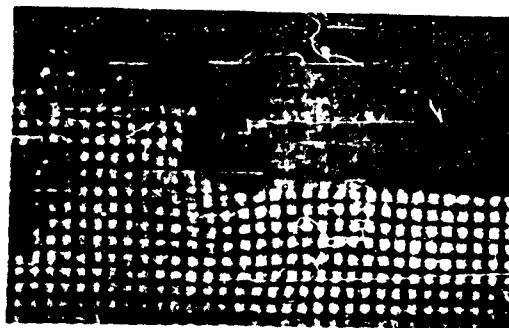
D-18
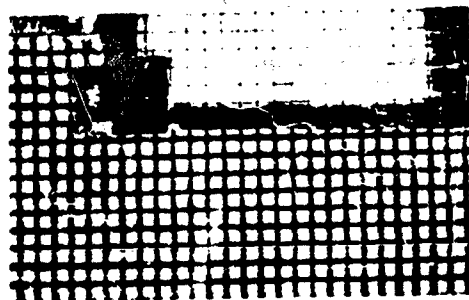
Start of Experiment   110 sec
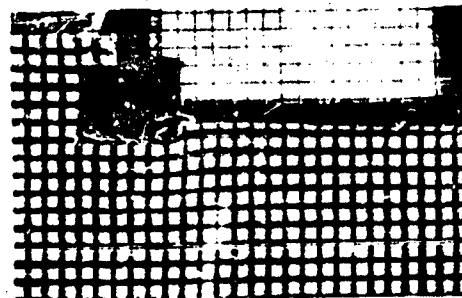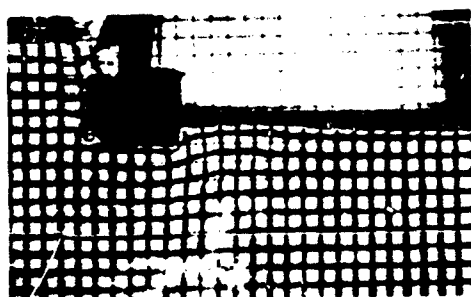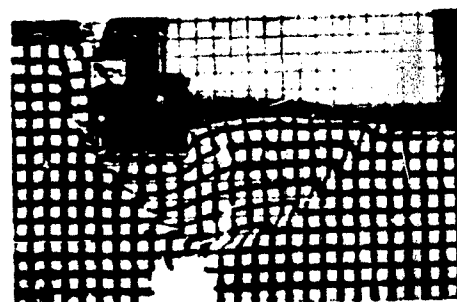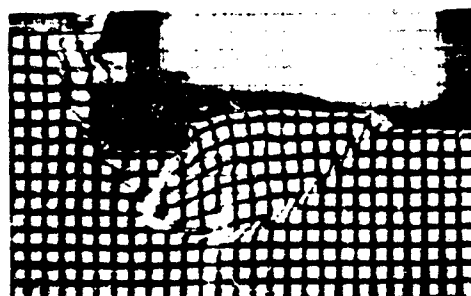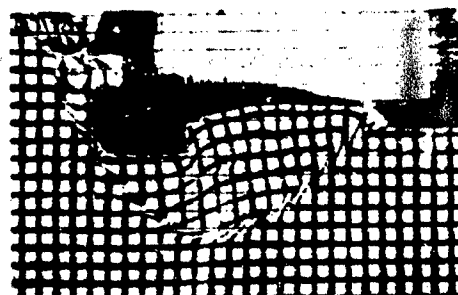
1⟨⟩ sec   275 sec

340 sec   End of Experiment

Fig. D-11 SEQUENCE PHOTOGRAPHS FOR STATICALLY LOADED
VERTICAL FOOTING, EXPERIMENT G29

D-19
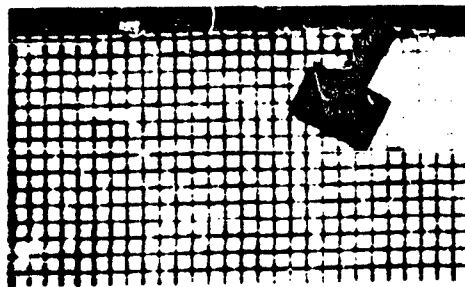
Start of Experiment
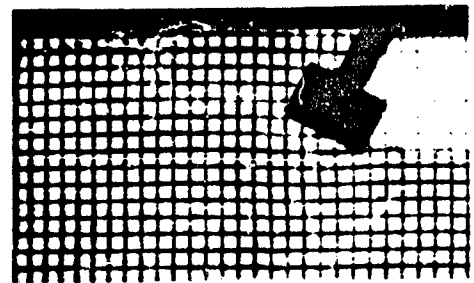
110 sec

165 sec
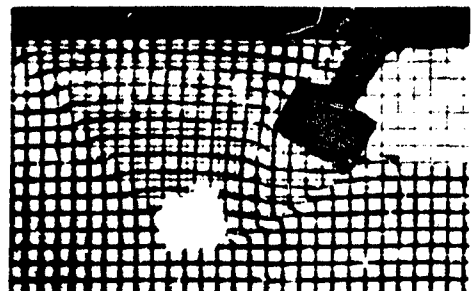
275 sec
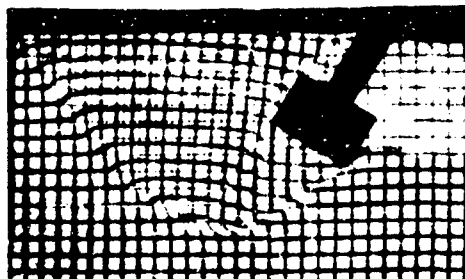
355 sec

End of Experiment

Fig. D-12   SEQUENCE PHOTOGRAPHS FOR STATICALLY
LOADED INCLINED FOOTING , EXPERIMENT G30

D-20
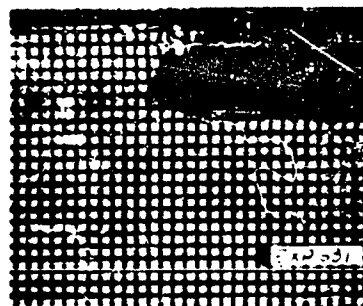
Start of Experiment
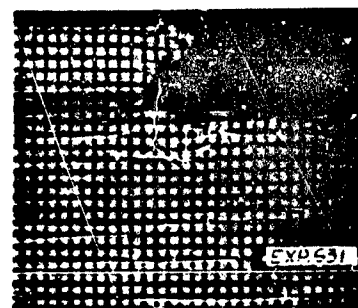
245 sec
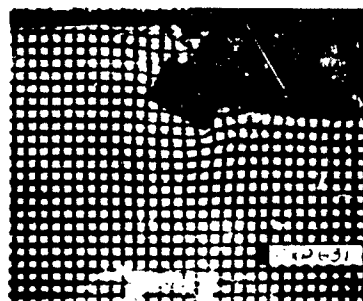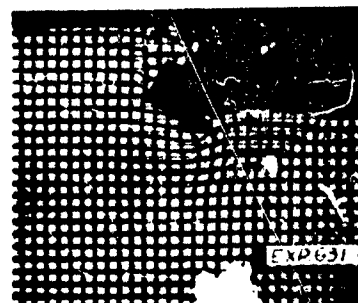
600 sec
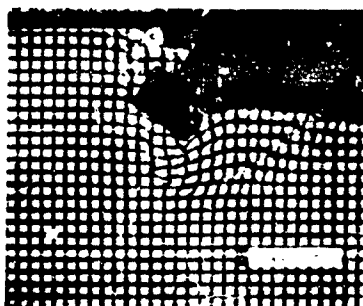
755 sec
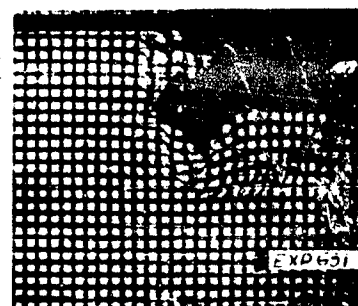
End of Experiment

**Fig. D-13 SEQUENCE PHOTOGRAPHS FOR STATICALLY LOADED INCLINED FOOTING.
EXPERIMENT G31**

D-21
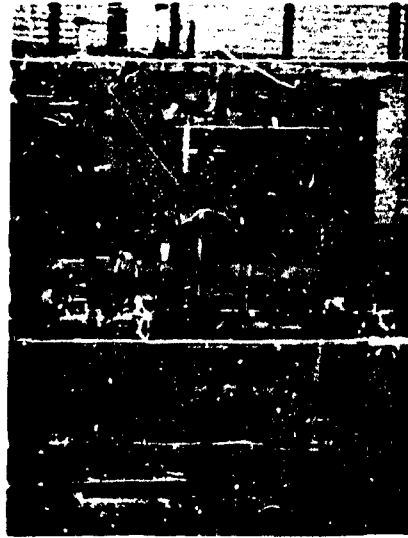
Fig. D-14 TYPICAL SETUP FOR DYNAMICALLY LOADED
VERTICAL FOOTINGS

D-22
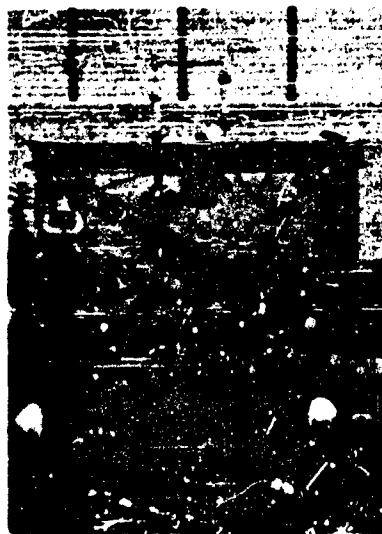
Fig. D-15 TYPICAL SETUP FOR DYNAMICALLY LOADED
INCLINED FOOTINGS
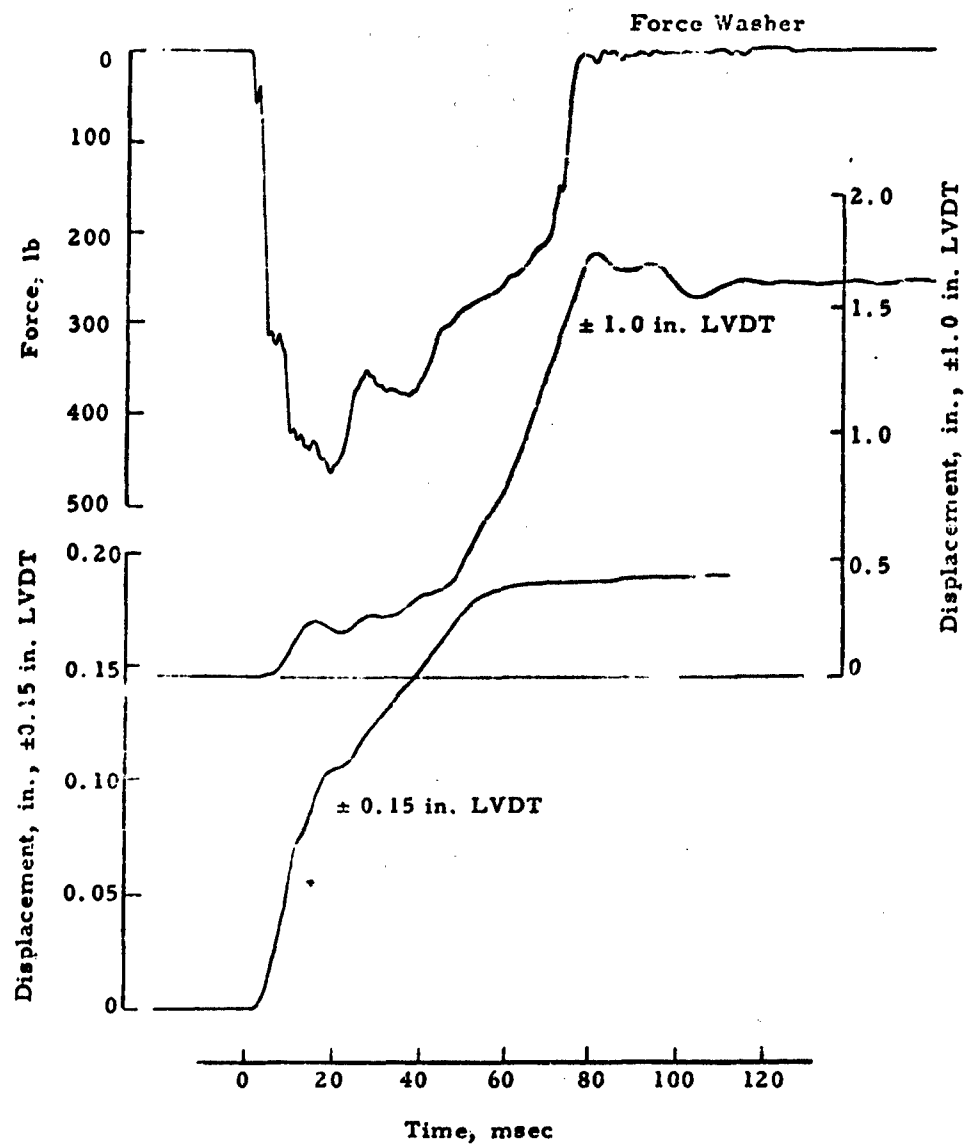
Fig. D 16 EXPERIMENT G... INCLINED FOOTING, 0 PSI
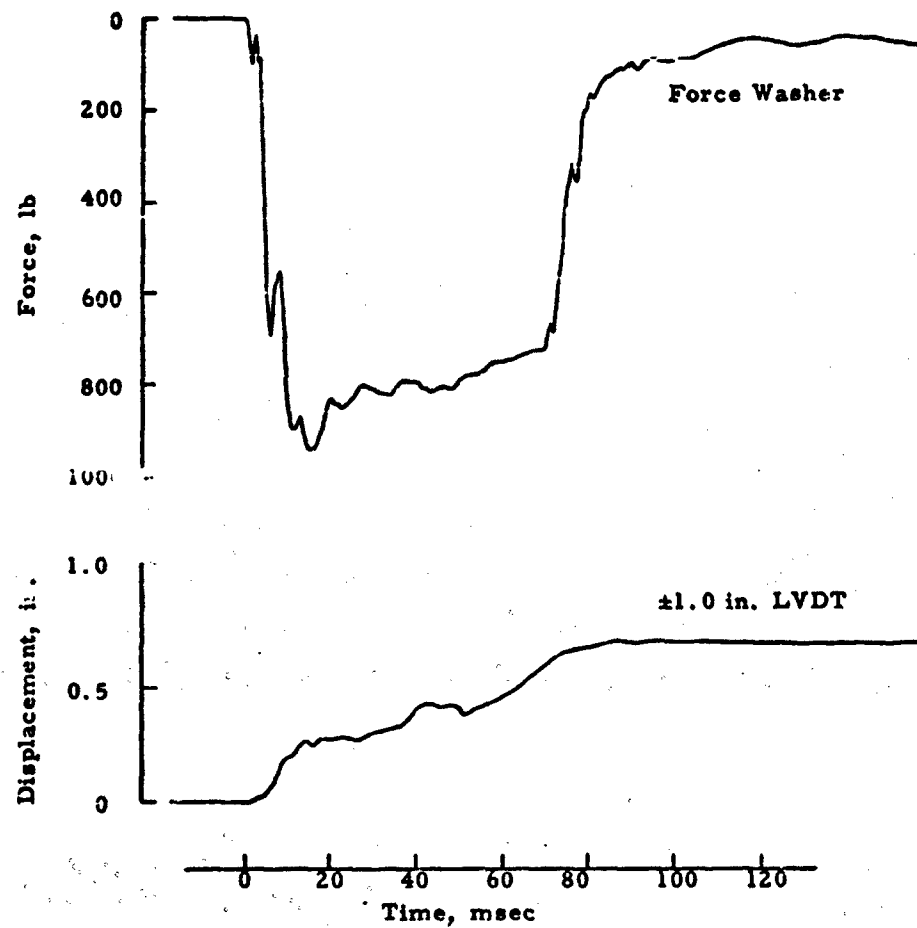
Fig. D-17 EXPERIMENT G36 (INCLINED FOOTING, 0.5 PSI)

ARMOUR RESEARCH FOUNDATION OF ILLINOIS INSTITUTE OF TECHNOLOGY

D-25
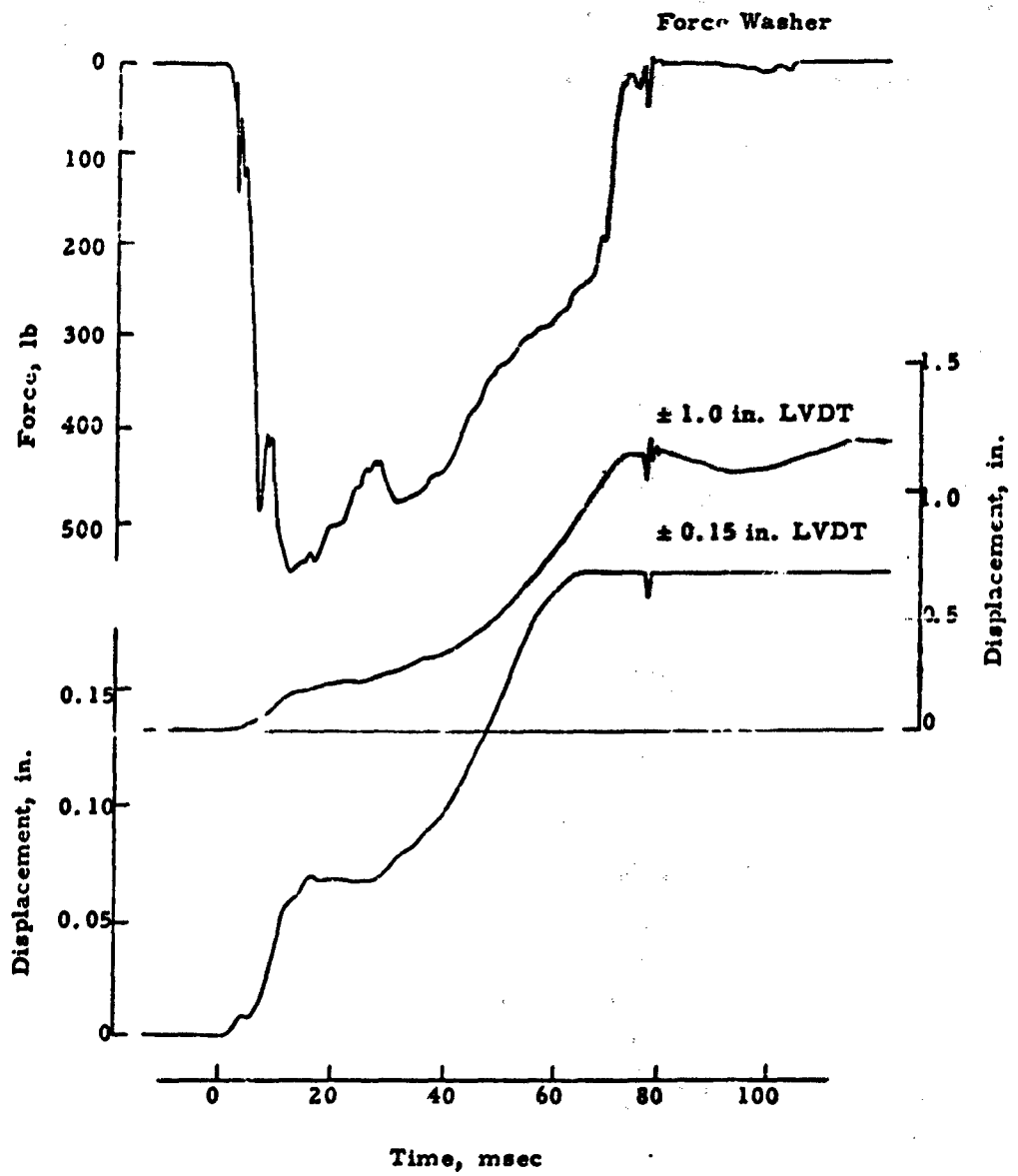
Fig. D-18 EXPERIMENT G37 (VERTICAL FOOTING, 0 PSI)

D -26
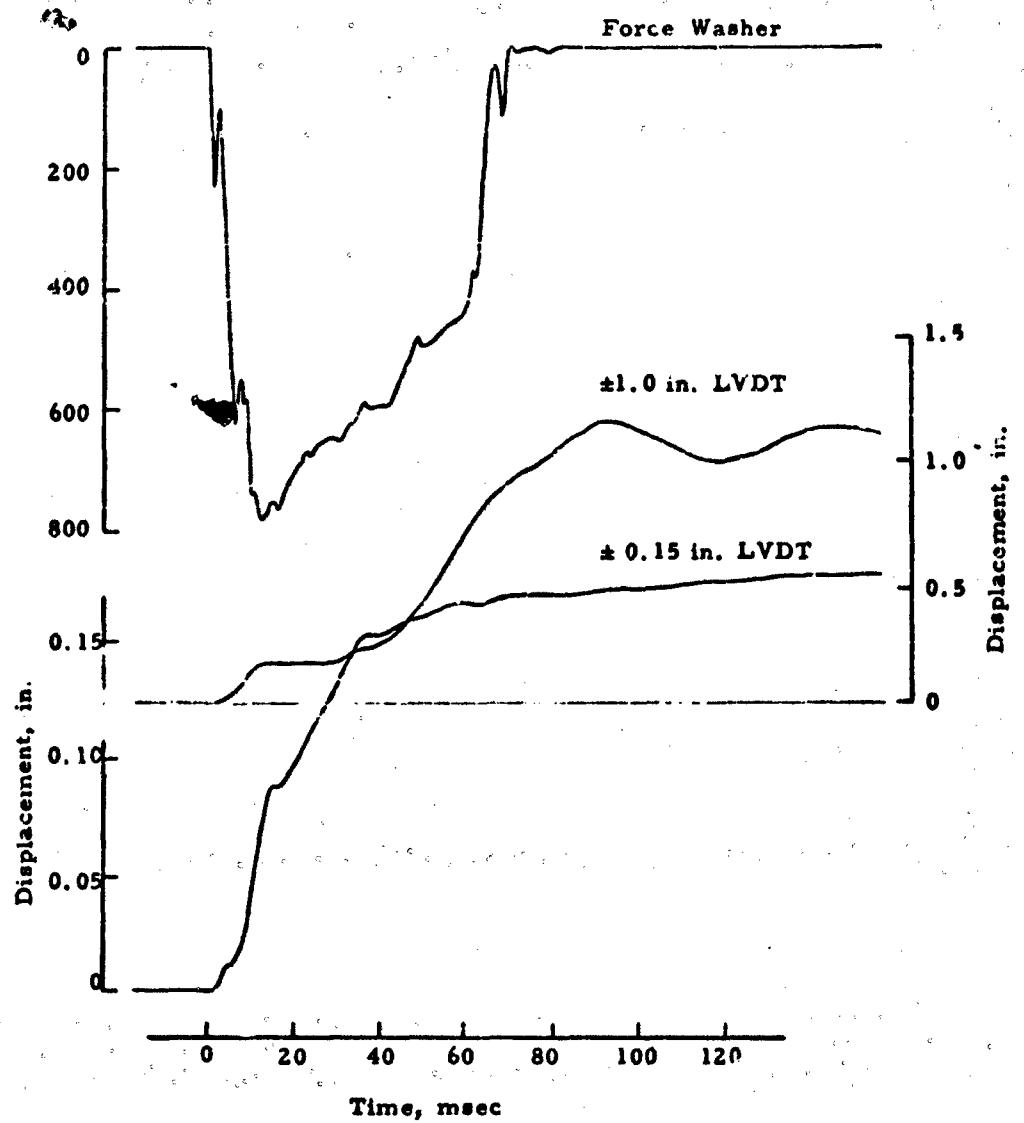
Fig. D-19 EXPERIMENT G-9 VERTICAL FOOTING, 5 FS"

Start of Experiment
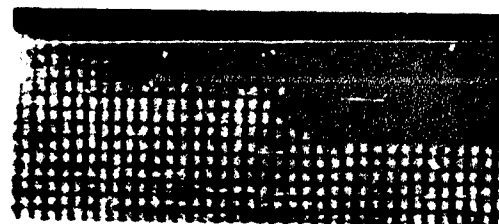
10 msec

19 msec

29 msec
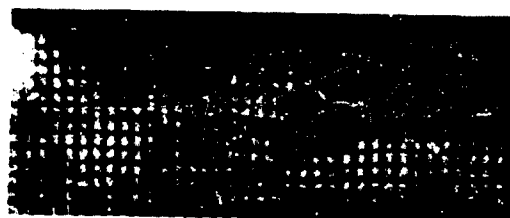
39 msec
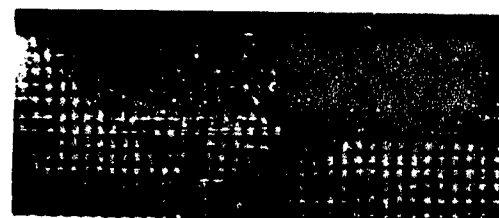
49 msec

Fig. D-20 SEQUENCE PHOTOGRAPHS FOR DYNAMICALLY LOADED
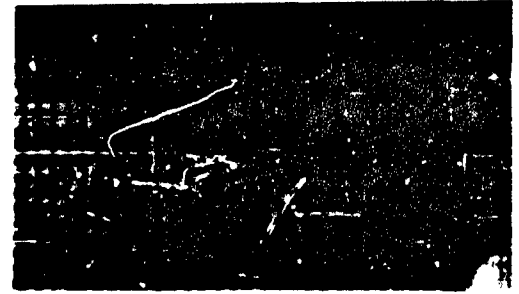VERTICAL FOOTING, EXPERIMENT G33
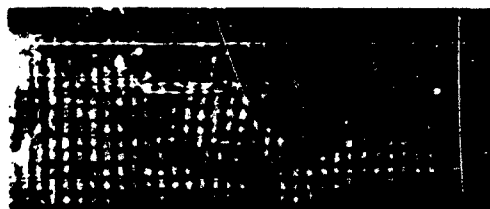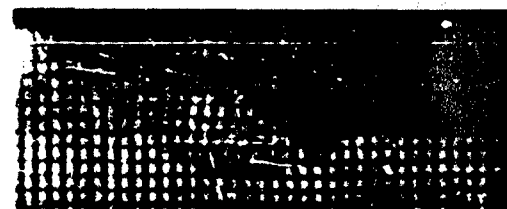
97 msec   End of Experiment

Fig. D-20 SEQUENCE PHOTOGRAPHS FOR DYNAMICALLY LOADED
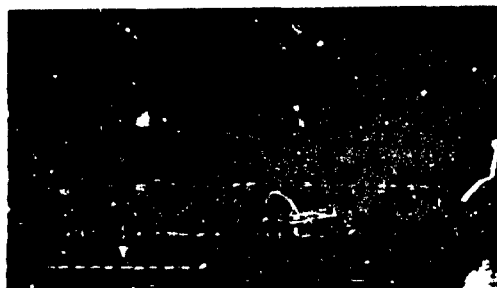VERTICAL FOOTING, EXPERIMENT G33
(cont'd)
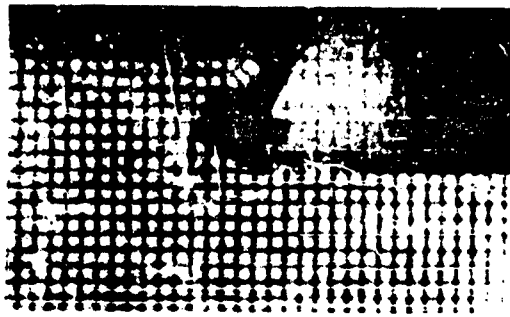
Start of Experiment
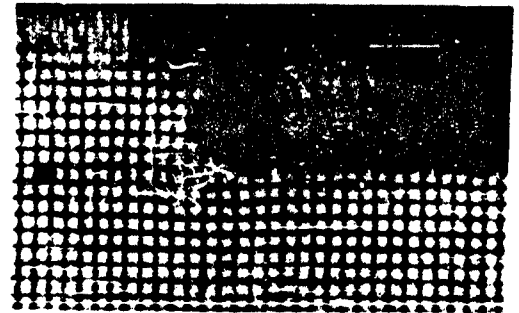
14 msec
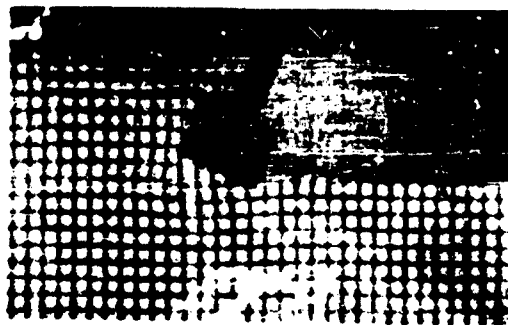
33 msec
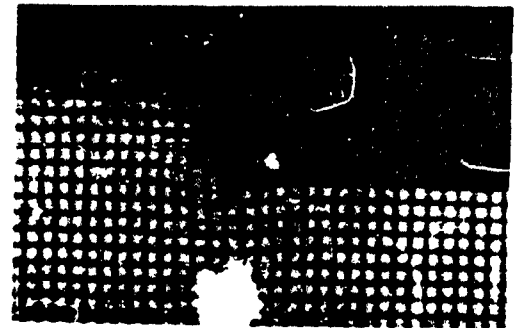
42 msec

51 msec
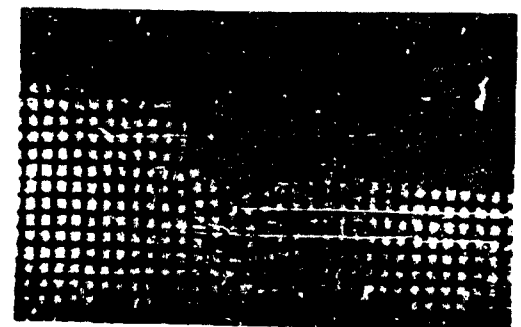
60 msec

Fig. D-21 SEQUENCE PHOTOGRAPHS FOR DYNAMICALLY LOADED
FOOTING, EXPERIMENT G36

D-30
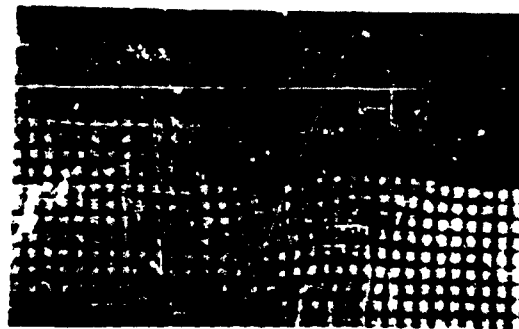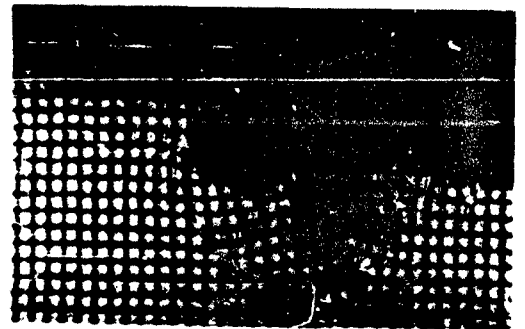
70 msec   88 msec
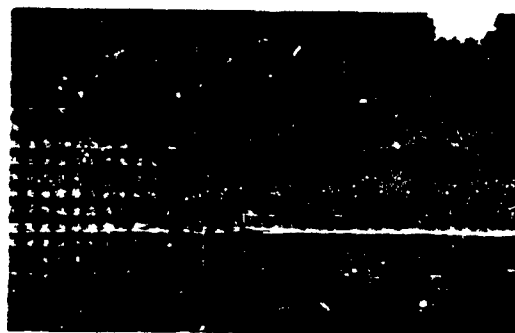
End of Experiment

Fig. D-21   SEQUENCE PHOTOGRAPHS FOR DYNAMICALLY LOADED
VERTICAL FOOTING, EXPERIMENT G36 (Cont'd)

D-31
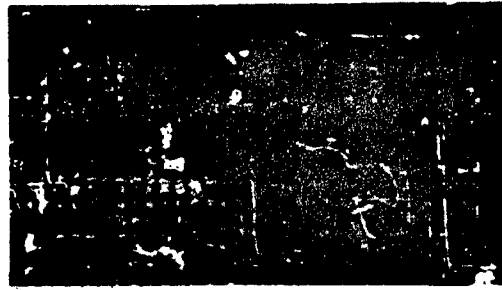
Start of Experiment   13 msec

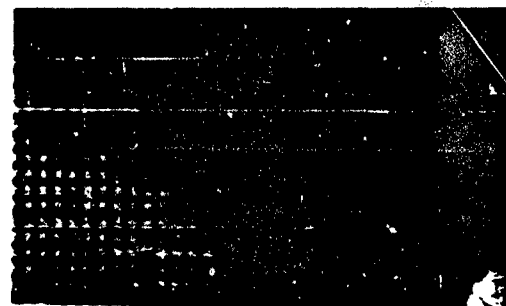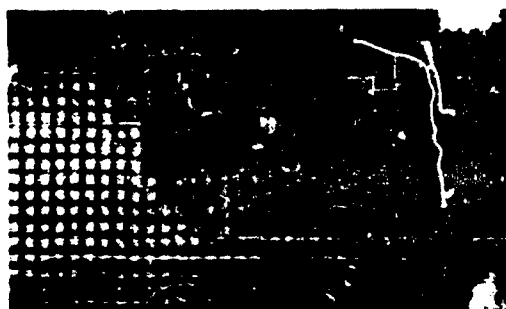30 msec   36 msec

43 msec   49 msec

Fig. D-22   SEQUENCE PHOTOGRAPHS FOR DYNAMICALLY LOADED VERTICAL FOOTING, EXPERIMENT G37
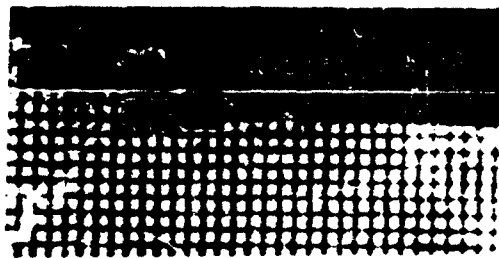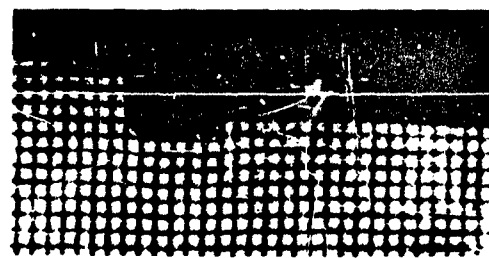
62 msec

82 msec

End of Experiment

Fig. D-22 SEQUENCE PHOTOGRAPHS FOR DYNAMICALLY LOADED
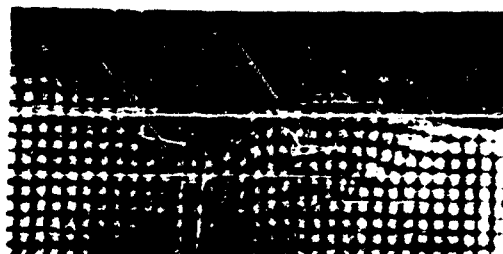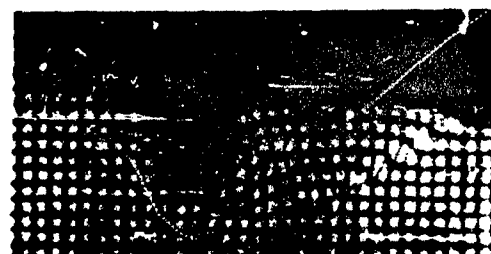VERTICAL FOOTING, EXPERIMENT G37 (cont'd)

Start of Experiment

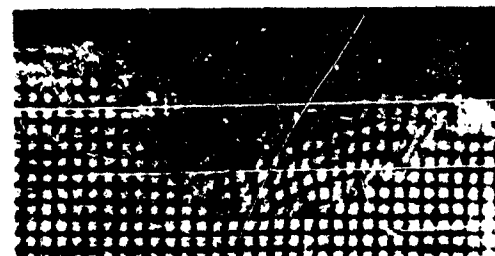16 msec

24 msec

35 msec

51 msec

67 msec

Fig. D-23 SEQUENCE PHOTOGRAPHS FOR DYNAMICALLY LOADED INCLINED
FOOTING, EXPERIMENT G39

D-34

106 msec   End of Experiment

Fig. T-23 SEQUENCE PHOTOGRAPHS FOR DYNAMICALLY LOADED
           INCLINED FOOTING, EXPERIMENT G39
                        (Cont'd)

APPENDIX E

ENGINEERING APPROACH

by

K. E. McKee

APPENDIX E

ENGINEERING APPROACH
by
K. E. McKee

Mathematical Model

The "Engineering approach", as used herein, refers to the extension of standard soil mechanics approaches to explain the behavior of footings subjected to dynamic forces. The analysis, based on one-sided behavior using a formulation similar to that used by Anderson[F-1]* was selected because of its suitability for extension to the dynamic problem. A history of this development is contained in the main body of this report.

Figure E-1 shows the model for one-sided failure of an infinitely long footing as considered for the dynamic analysis. The nomenclature introduced on this figure is summarized below:

B = footing width,

D = depth of burial of footing,

$F(t)$ = time-dependent force per unit length,

p_0 = overpressure on surface,

r = radius of circle of failure, and

θ = rotation of soil mass.

A complete nomenclature for this appendix is contained at the end of the appendix. Assuming that the location of the failure surfaces are known (i.e., that r is specified) and that the shear strength along the failure surfaces can be incorporated in terms of an equivalent resisting force acting at the center of the footing, $R_s(\theta)$ where R_s is assumed to be a function of the rotation, θ, for the known r, the dynamic equation can be written as:

$$J\ddot{\theta} + R(\theta) = M(t) \qquad \text{(Eq. E-1)}$$

---

*Superscript numbers denote references collected at the end of the Appendix.

where:

θ = rotation of soil mass

$\ddot{\theta} = \dfrac{d^2\theta}{dt^2}$ = angular acceleration of soil mass

J = rotational inertia

$R(\theta)$ = resisting moment as a function of θ

$M(t)$ = time-dependent moments

The terms in this equation can be expressed in terms of figure E-1

$$J = \frac{r\,\gamma}{g}\left[0.64397\,r^3 + \frac{D}{3}(D^2 + r^2) + 0.78540\,r\left(\frac{4r}{3\pi} - D\right)^2\right] \quad \text{(Eq. E-2)}$$

$$R(\theta) = \left(r - \frac{B}{2}\right) P_s(\theta) + \gamma\theta\left\{0.106\pi\left[r^3 + (r + D)^3 \tan\gamma\right] + \right.$$

$$\left. - \frac{D(r - B)^2}{2}\tan\lambda\right\} \quad \text{(Eq. E-3)}$$

$$M(t) = \left(r - \frac{B}{2}\right) P(t) + 0.106\,\gamma\pi\left[r^3 - (r + D)^3\right] \cdot$$

$$+ \frac{\gamma D}{2}(r - B)^2 \quad \text{(Eq. E-4)}$$

where

$$\tan\gamma = 1 - 2.332\frac{D}{r + D} \quad \text{(Eq. E-5)}$$

$$\tan\lambda = \frac{D}{r + D} \quad \text{(Eq. E-6)}$$

The only new symbol used is g for the gravitational constant, i.e., 32.2 ft per $\sec^2$ or 384 in. per $\sec^2$. It should be noted in the above development that the influence of soil shear strength and surface over-pressure are included only by implication -- the values of r and $P_s(\theta)$ depend on these parameters. Within this framework, Equation E-1, with the subsidiary equations, mathematically describes the behavior of dynamically loaded footings based on incompressible soil and the assumed type of one-sided failure.

ARMOUR RESEARCH FOUNDATION OF ILLINOIS INSTITUTE OF TECHNOLOGY

Values for $P_s(\theta)$ and r can be obtained from theoretical or experimental considerations. For certain soils and in particular for dry sand, experiments indicate that the soil strength is independent of the strain rate[F-2]. For this reason, one might anticipate that the soil below the footing might behave in essentially the same fashion for static as for dynamic load ngs. As a reasonable theoretical approach one might assume that the resistance is rigid-plastic in form with the plastic resistance equal to the static bearing capacity, P_s. Using the failure surfaces indicated on Figure E 1 and minimizing to establish the failure surface associated with the ultimate load capacity, the following equations result:

$$P_s \left[\frac{4 - \pi \tan \phi}{16 \, \gamma \tan \phi} \right] = r^2 \left[1 + \frac{D}{r} \left(\frac{1 + 2 \tan \phi}{2 \tan \phi} \right) + \right.$$

$$\left. + \left(\frac{D}{r} \right)^2 \left(\frac{1 + 2 \tan \phi}{4 \tan \phi} \right) \right] +$$

$$+ \frac{\pi}{4 \gamma} \left[\frac{c}{\tan \phi} (2r + D) + Dp_0 \left(\frac{r}{D} + \frac{\tan \phi}{\tan \phi} \right) \right]$$

(Eq. E-7)

and

$$\frac{B}{r} = \left(2 - \frac{\pi}{2} \tan \phi \right) - \frac{2}{3} \frac{\gamma r^2}{P_s} \left[(2 \tan \phi - 1) + \right.$$

$$\left. + \left(1 + \frac{D}{r} \right)^3 (1 + 2 \tan \phi) \right] - \frac{\pi \, rc}{P_s} \left[1 + \frac{P_0}{2c} \tan \phi \right] \left[1 + \left(1 + \frac{D^2}{r} \right) \right] +$$

$$\frac{nD}{P_s} \left(2 + \frac{D}{r} \right)$$

(Eq. E-8)

Equations E-7 and E-8, of course, can be solved numerically for any two parameters. For this analysis, the parameter ordinarily to be determined would be P_s and r. The other parameters, i.e., ϕ, c, γ, B, D and p_o would have to be specified. Trial-and-error solutions are, in general, necessary. The simplest method of solution requires the assumption of a value for r, which allows Equation E-7 to be solved for P_s directly. The computed value of P_s along with the assumed r are used to solve equation E-8 for B. This procedure is repeated until the desired value of B is determined, and, hence the appropriate values for P_s and r established. Extrapolation or interpolation can be used, of course, to find values when nearby values are known.

The experimental results, shown on figures 2 and 3 of the main body are typical of static test data. As pointed out earlier these experiments verify the theoretical values for the ultimate load capacity. Verification of the failure pattern by experiments is less simple to ascertain since it depends on qualitative data. Figure E-2 shows a photograph of a one-sided failure surface for a buried leg subjected to static loads. Comparison of this photograph with figure E-1 would indicate at least considerable similarity, although it should be emphasized figure E-2 illustrates static behavior while figure E-1 is here applied to dynamic as well as static behavior.

Analytic Solutions

The above development uses the shear surface location (r) and load capacity (P_s) determined by the static analysis. It should be emphasized however, that the determination of the static data should be based on the best estimate for the soil properties; i.e., the properties should be selected to incorporate the influence of the variables involved. (This would include effects such as the rate of load application.) An investigation of the influence of the various parameters was considered using an exponentially decaying forcing function of the form:

$$P(t) = P_o e^{-\alpha t} \qquad \text{(Eq. E-9)}$$

It should be noted that P_o is peak applied force. A graphical presentation of this load-time curve is given in figure E-3 for various values of α. The results presented here are based on earlier investigations by ARF[E-6, E-7] and hence detailed solutions are not included.

Figure E-4 shows the influence of variations in soil properties over almost the entire range of significance for a footing on the surface of the soil. A critical rotation of 5° was arbitrarily used in preparing this curve. It is interesting to note that, except for the limiting and impractical cases in which the soil has very little strength $(c - 0, \emptyset = 5°)$, the peak force varies by less than 10% for values of α less than 3.6. This observation is limited by the form of the forcing function, the absence of pressures on the surrounding surface, and the lack of burial of the footing.

Figure E-5 shows the effect of varying the static air pressure, p_o, acting on the surface. Again, a critical rotation of 5° was arbitrarily selected. This variation was carried out for surface footings, particular soil parameters (indicated on Fig. E-5), selected failure surface. The solutions indicate that inertial effects are of reduced significance as p_o increases. For this reason, figure E-5 is plotted as p_o divided by the static force, P_s associated with $p_o = 0$. This presentation avoids the relatively uninteresting curves which would result from applying the form of figure E-4 to these cases, and, in addition, illustrates the significant contribution to the static capacity, P_s, attributable to the surface pressure, p_o. Figure E-5 can be converted to the alternate form by multiplying the ordinates of each curve by $P_s \big|_{p_o = o}$.

The influence of depth of burial is demonstrated by figure E-6 Again a critical rotation of 5° was arbitrarily used. The distance below the surface has a major influence on both the static capacity and the inertial effects. The figure was prepared to demonstrate the increase in inertial effects with depth of burial -- these effects are definitely significant even for loads of relatively long duration. This can be shown by comparing the bottom curve $(D = 0)$ with the other curve when the

radius of the failure circle and the soil properties are held constant. Care should be taken in approximating other solutions from the results of figure E 5, since, by nature of the parameters which are held constant the footing width decreases with depth of burial (D/B = 0, 1.88 and 24.4). However, the inertial effects as well as the static capacity of a specified footing would increase significantly with depth of burial.

The above examples have been based on assuming a strength, $P(\theta)$, rigid plastic in form, having a value equal to the static bearing capacity, P_s. This assumption has the advantage of reducing the calculation time required to obtain a series of solutions, but is in no other way necessary. In the course of the research reported herein solutions have been carried out for $P(\theta)$ based on the static test data and modifications thereof and for elastic-plastic forms for $P_o(\theta)$ such as shown in figure E-7 (with A showing ideal plastic behavior and B and C indicating increasing and decreasing strength with rotation, respectively). Approximately twenty-five such solutions were carried out for various relationships between the footing capacity and displace: It should be noted that the assumption is made that the displacement can be considered in terms of the rotation or linear displacement with equal ease. Experimental results are always in terms of the linear displacement. Each solution resulted in a predicted displacement-time curve for the footing being considered. Subsequent experimental studies provided displacement-time data.

To compare the results with these data, the above procedure was reversed to obtain $P(\theta)$ or $p(x)$ from the experimental data. This approach, which will be considered in the following section, proved much more significant and provided more meaningful information than comparisons of measured and predicted displacements. For this reason no attempt is made herein to consider further prediction of displacements based on assumed or measured relationships between force and displacement.

Comparison with Experiments

Considerable quantitative data was available as a result of the controlled experiments for dynamically loaded footings. This test data provided a basis for evaluating the "engineering approach" presented above. Only limited details regarding the experimental approach are presented. Detailed reports on the experimental studies are available. [E-3, E-4, E-5, E-6]

Figure E-8 shows a typical experimental setup with the ARF pneumatic-hydraulic loader in place over a footing. Table E-1 summarized experiments from which those used for this evaluation were selected. (It should be pointed out that a considerable number of other experiments have been conducted as part of the sponsored research.) Figures E-9 and E-10 show typical sketches of the records obtained for force and displacement.

As indicated previously, the engineering approach is based on the assumption that the resistance to dynamic loads is similar to that of static loads. The initial attempts to interpret the data were therefore, based on this assumption. By using the measured dyn. force-time curve and static distance curves, it is relatively simple to calculate the displacement-time history which would be predicted by the analysis. This analytical result could then be compared directly with the measured displacement-time history. These considerations dictated the selection of the displacement as one of the quantities to be measured.

The first attempts to analyze the data obtained from the dynamically loaded three-dimensional footing were based on this approach. There is little merit in reciting the type of alteration considered to make the static resistance-displacement curve suitable. It is sufficient to say that there was no reasonable modification which resulted in calculated displacement-times verifying those recorded in the laboratory. At this stage, it became obvious that the resistance-displacement relationship for dynamic loads bore little resemblance to that for static loads and the assumption that these curves would be related to each other in some relatively simple way was shown to be wrong. The analytical approach was revised and the data evaluated in a different fashion.

ARMOUR RESEARCH FOUNDATION OF ILLINOIS INSTITUTE OF TECHNOLOGY

This evaluation used the measured force-time and displacement-time records to determine the associated resistance-displacement relationship. Carrying through this procedure required determination of the acceleration-time history from the displacement-time records. Because of the sensitive nature of this determination, the analysis was viewed with considerable trepidation. Subsequent experimental studies[E-7] making use of four accelerometers placed on the corners of the footing provided data justifying the earlier use of the measured displacement-time.

Consider a linearized equation of motion for the footings of the form:

$$m\ddot{x} + R(x) = P(t) \qquad\qquad\text{(Eq. E-10)}$$

where

m = equivalent mass,

x = vertical displacement,

$\ddot{x}$ = $\frac{d^2x}{dt^2}$ = vertical acceleration,

$R(x)$ = resistance as a function of vertical displacement,

$P(t)$ = applied vertical force as a function of time.

Note that Equation E-10 assumes a constant mass, a resistance which is dependent only on the displacement, and a force which is a function only of time. From the measured results the experiments provide $P(t)$ directly and x as a function of time. Assuming that the mass, m, can be determined, Equation E-10 can be solved for $R(x)$ using the acceleration determined from the $x(t)$ data.

$$R(x) = P(t) - m\ddot{x} \qquad\qquad\text{(Eq. E-11)}$$

This equation shows that at each instant the resistance, $R(x)$, depends on the applied force, the mass, and the acceleration.

In the first attempt to apply this approach, four experiments, P27, P28, P29 and P30 were considered in detail. These records were selected since they were similar in nature and had all produced substantial displacements. The records of these four experiments were analyzed utilizing the accelerations computed from the displacement curves. Figure E-11 shows points obtained from these analyses. The static R(x) curve, the average of the three static experiments shown in figure 3 of the main body is reproduced on figure E-11 through E-15 for comparison with the dynamic results. The fact that the points on the R(x) curves for these four experiments are so well grouped was encouraging - a single curve can reasonably be drawn through the points. On the other hand, the variations of the points from a single experiment is indicative of inconsistencies introduced by the method used in determining acceleration.

This procedure was subsequently carried out for eighteen experiments for which both the displacement and force data appeared satisfactory. Table E-2 indicates the experiments covered. Table E-3 shows an example (for Exp. P32) of calculations made. In this example, 5-msec time intervals were selected and values for displacement and force were read from the records at that interval. The mass, m, used was 0.0223 lb-sec^2/in. based on the mass of the footing added to the soil in a half cylinder having radius and lengths equal to the footing dimensions. This relatively arbitrary determination of the mass was investigated by considering possible variations - for all practical purposes, the inertial term is negligible over the range of possible values.

Figures E-11 to E-15 show the resistance-displacement curves computed in this fashion. The average static resistance-displacement is redrawn on each of these figures. The arrangement of the experiments on each of the five figures (E-11 to E-15) merely attempts to collect those having approximately the same values of the resistance. Observe that there is little resemblance between the static and dynamic curves and, more significantly, between the curves computed based on the dynamic experiments. This contrasts with the uniformity demonstrated

by the results plotted for static tests on figure 3 of the main body.

While much could be written regarding these calculated resistance-displacement curves and their meaning, it is sufficient to say that they demonstrate the inappropriateness of using the static resistance, directly or with simple modifications for a general dynamic load. The forces for the series of dynamic experiments considered in detail above had rise times of two or three milliseconds For sufficiently large rise times, the behavior is explained by the "engineering approach", since this is equivalent to the classical static analysis of soil mechanics.

A complete understanding of dynamic behavior must then depend on an improved understanding of the behavior of footings subjected to rapidly applied dynamic loads. As a result of these evaluations of the "engineering approach", one limitation certainly arises due to the assumption of a rigid soil mass. The following Appendix considers an approach taking into account the compressibility of the soil beneath the footing.

REFERENCES

E-1 Anderson, P., Substructure Analysis and Design, The Ronald
     Co., New York, 1956, p. 81.

E-2 Mass. Inst. of Technology, The Behavior of Soils Under Dynamic
     Loading, Final Report or Laboratory Studies, AFSWP 118, Aug., 1954.

E-3 McKee, K. E., Design and Analysis of Foundations for Protective
     Structures, Phase Report III, Interim Technical Report. Armour
     Research Foundation, Chicago, January 1959.

E-4 McKee, K. E., Design and Analysis of Foundations for Protective
     Structures, AFSWC-TR-59-56, October 1959.

E-5 McKee, K. E., Design and Analysis of Foundation for Protective
     Structures, Second Interim Technical Report, AFSWC-TN-61-14,
     A: ..r Research Foundation, May, 1961.

E-6 henkman, S. and McKee, K. E., Bearing Cu.ω.city of Dynamically
     Loaded Footings, Symposium on Soil Dynamics, ASTM, June, 1961.

E-7 Shenkman, S. and McKee, K. E., The Armour Research Foundation
     Pressure Vessel, report to ARF on project R5318, December, 1961.

Table E-1

DYNAMIC EXPERIMENTS ON 4-IN. SQUARE FOOTINGS

Experiment No.	Peak Force (lb)	Duration (msec)	Maximum Displacement (in.)	Time to Maximum Displacement (msec)
P1	366	1000	1	64
P2	340	1000	1	70
P3	303	1310	1	68
P4	277	249	0.99	82
P5	331	83	1	63
P6	394	70	1	66
P7	299	44	0.28	34
P6	137	25	0.04	15
P9	216	34	0.00	-
P10	397	54	0.29	51
P11	476	59	0.89	49
P24*	324	24	0.16	17
P25*	546	27	0.26	39
P27*	159	91	1.00	68
P28	148	69	0.94	60
P29	123	79	0.90	74
P30	163	66	0.93	57
P31	371	79	0.49	74
P32	112	87	0.15	18
P33	104	81	0.05	43
P34	.01	84	0.01	17
P35	104	70	0.01	14
P36	101	80	0.01	16
P37	140	71	0.01	15
P38	360	90	0.99	67
P39	334	73	0.89	63
P40	303	78	1.00	70
P41	272	72	0.96	66
P42	270	77	0.99	65
P43	272	84	0.15	64
P44	332	95	0.18	68
P45	341	122	0.15	71
P46	301	82	0.05	37

* Experiments P12 to P23 on 30-in. diameter plates are not of interest here. The records of P26 were spoiled and data is not available.

Table E-2

EXPERIMENTS USED FOR ANALYSIS

Experiment No.	Peak Force (lb)	Figure With R (x) (Fig. No.)
P7	299	17
P8	137	16
P10	397	17
P11	476	18
P25	546	15
P27	159	14
P28	148	14
P29	168	14
P30	168	14
P31	371	18
P32	112	16
P38	366	18
P39	334	17
P40	303	17
P41	272	17
P42	270	17
P43	272	17
P44	337	17

Table E-3

SAMPLE CALCULATIONS
EXPERIMENT P32

Time (msec)	Force, F (lb)	Disp., x (in)	$\dot{x}$ (in. per sec)	$\ddot{x}$ (in. per sec^2)	$\ddot{x}$ (in. per sec^2)	$m\ddot{x}$ (lb)	R F-$m\ddot{x}$
0	0	0					
			0.00232				
5	72.53	0.0116		-0.000116	-116	-2.587	75.17
			0.00174				
10	101	0.0203		+0.000120	+120	+2.676	98.32
			0.00234				
15	83.80	0.0320		+0.000228	+228	+5.084	78.72
			0.00348				
20	98.76	0.0494		-0.000348	-348	-7.760	106.52
			0.00174				
25	86.04	0.0581		+0.000468	+468	+10.43	75.60
			0.00468				
30	87.54	0.0785		-0.000236	-236	-5.263	92.85
			0.00290				
35	94.27	0.0930		-0.000116	-116	-2.587	96.86
			0.00232				
40	32.	0.1046		+0.000004	+ 4	.9	82.21
			0.00234				
45	84.05	0.1163		-0.000004	- 4	-0.089	84.64
			0.00232				
50	87.55	0.1279		-0.000348	-348	-7.760	95.31
			0.00058				
55	74.82	0.1308		+0.000232	+232	+5.174	69.0
			0.00174				
60	80.06	0.1395		+0.000004	+ 4	0.089	79.97
			0.00176				
65.	84.55	0.1483		-0.000352	-352	-7.850	92.40
			0				
70	74.82	0.1483		0	0	0	74.82
			0				
75	56.86	0.1483		-0.000352	-352	-7.850	64.71
			-0.00176				
80	11.22	0.1395		-0.002088	-2088	-46.562	57.78
			-0.01220				
85	0	0.0785					
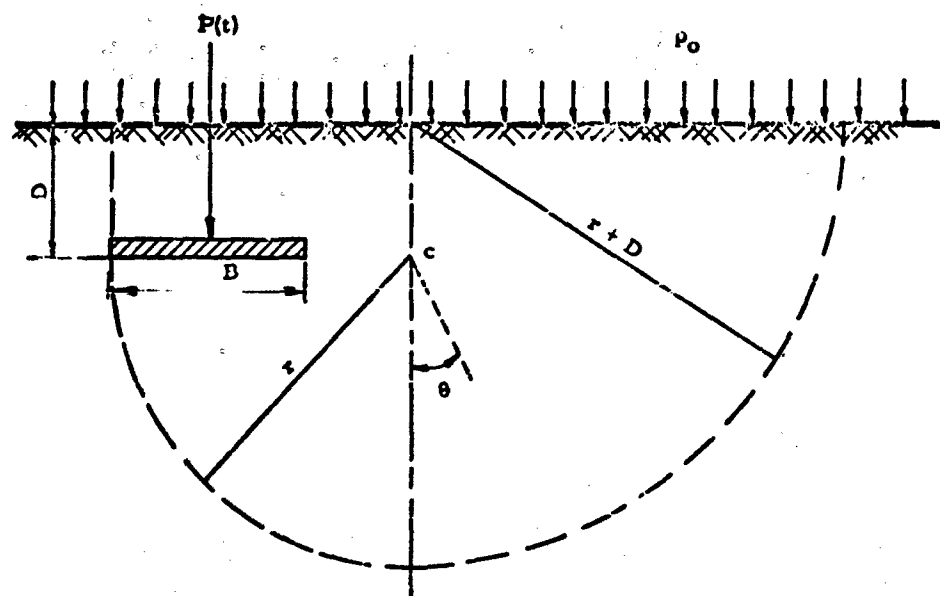
Fig. E-1 MODEL FOR DYNAMIC ANALYSIS
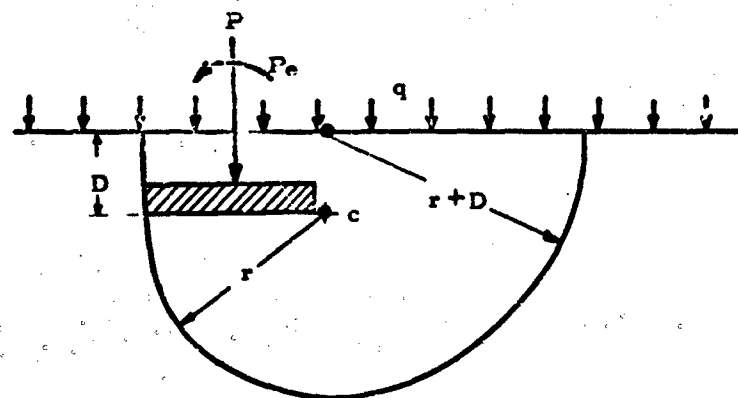
Fig. E-2 ONE-SIDED FAILURE
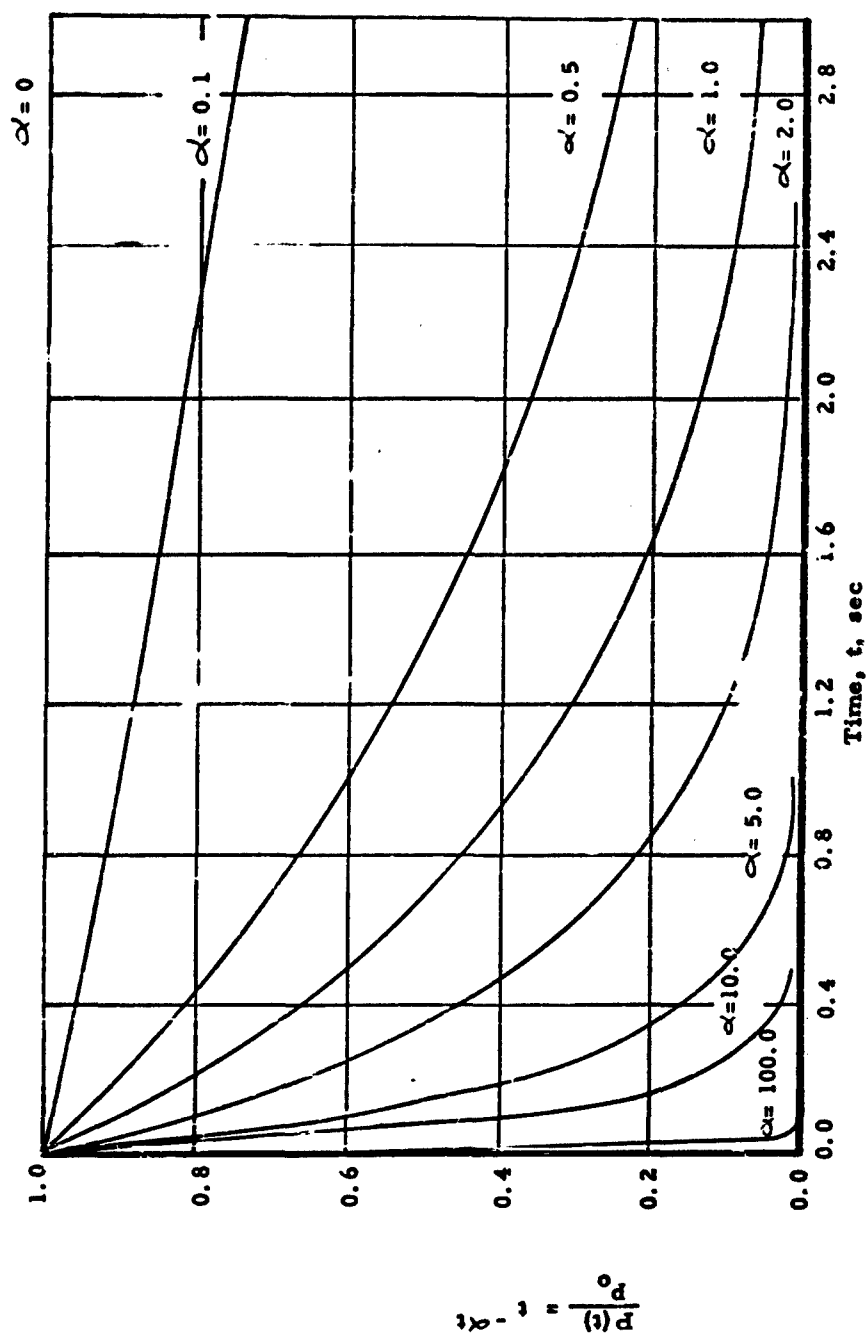
Fig. E-3 LOAD-TIME HISTORIES

$$\frac{P(t)}{P_o} = e^{-\alpha t}$$

ARMOUR RESEARCH FOUNDATION OF ILLINOIS INSTITUTE OF TECHNOLOGY

E-16

Identification of Curves					
Symbol	φ (deg)	c (psf)	r (ft)	B (ft)	P (lb)
o	5	0	1	1.24	38
▽	5	0	7	8.69	1,841
▶	5	1000	1	0.93	6,784
■	5	4000	1	0.93	27,020
□	5	4000	9	8.41	241,900
●	25	2000	7	4.58	153,200
+	40	0	3	1.36	8,359
△	40	0	15	9.00	140,000
●	40	4000	3	1.36	173,000
X	40	4000	23	8.45	2,216,000

Decay Factor, α.

P_o/P_s
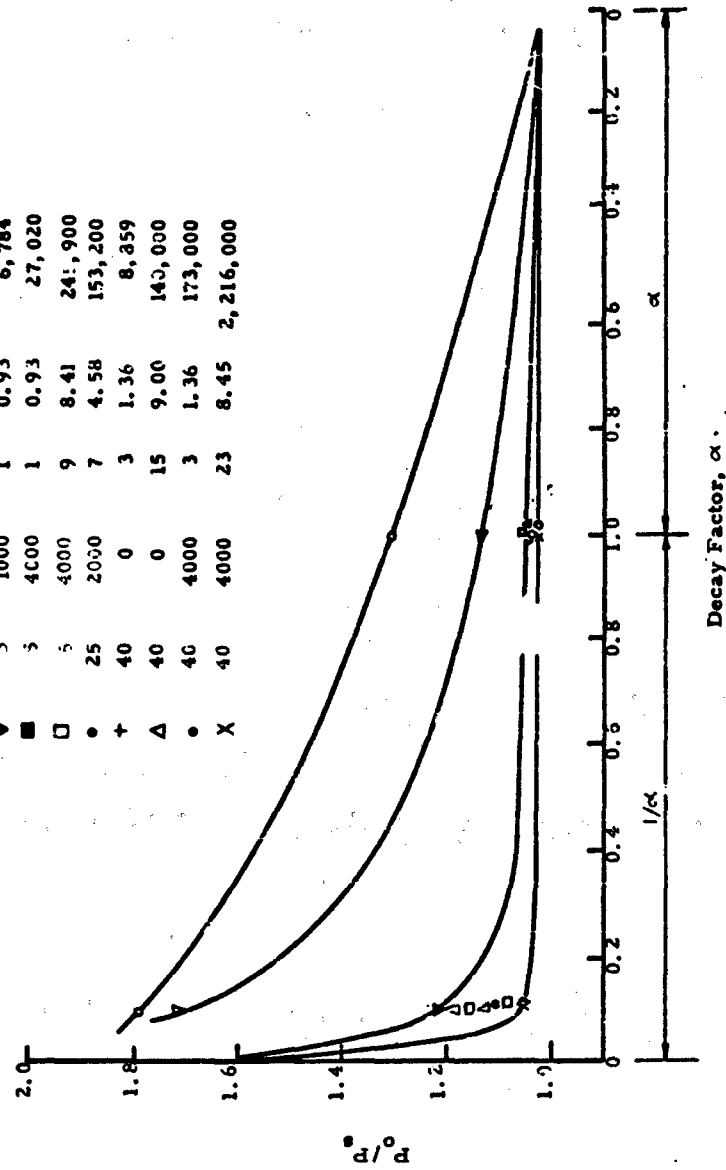
Fig. E-4 INFLUENCE OF SOIL PARAMETERS FOR SURFACE FOOTINGS (D = 0)
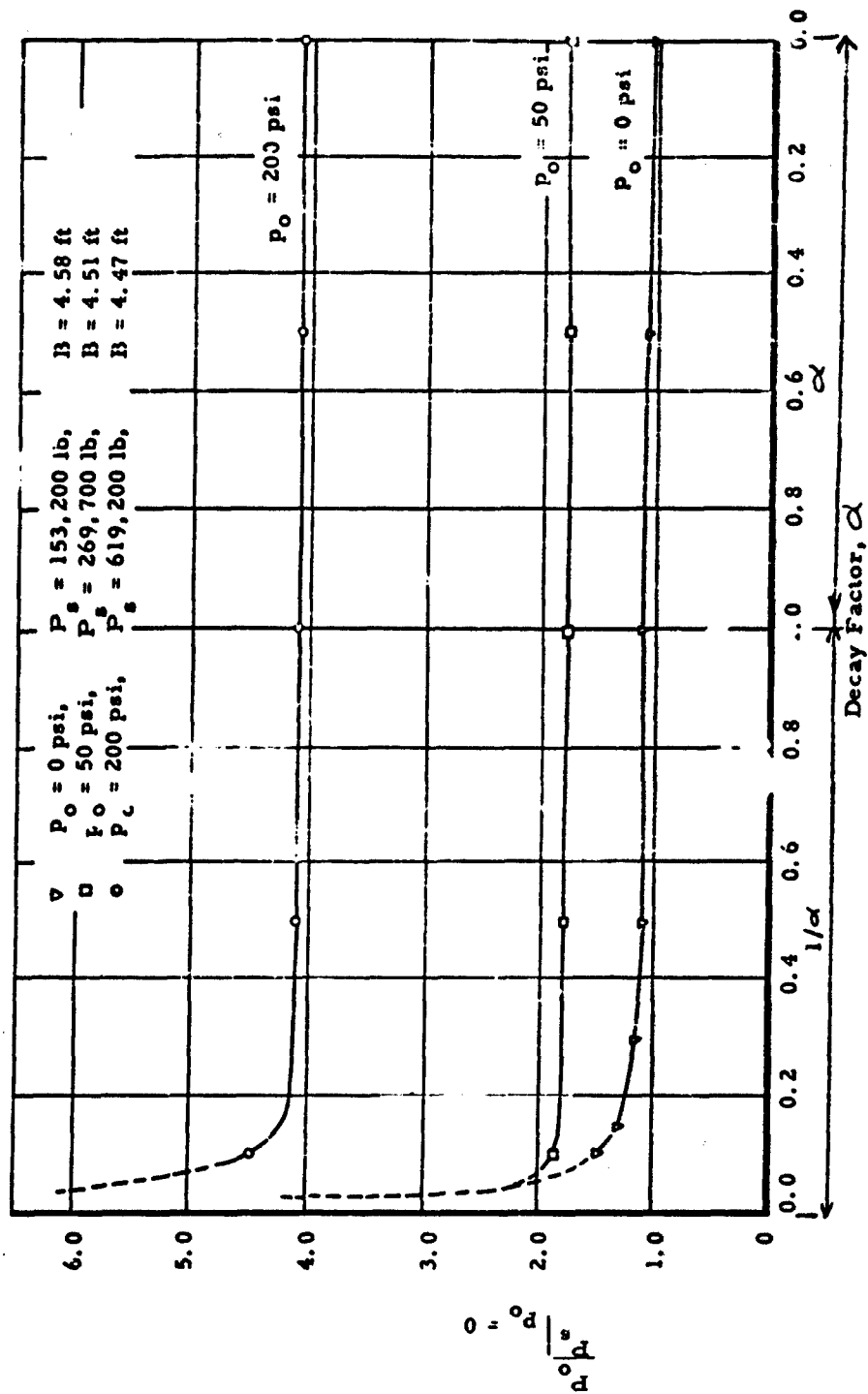
Fig. E-5 EFFECT OF STATIC OVERPRESSURE

(r = 7 ft, φ = 25°, c = 2000 psf, D = 0 ft)

ARMOUR RESEARCH FOUNDATION OF ILLINOIS INSTITUTE OF TECHNOLOGY
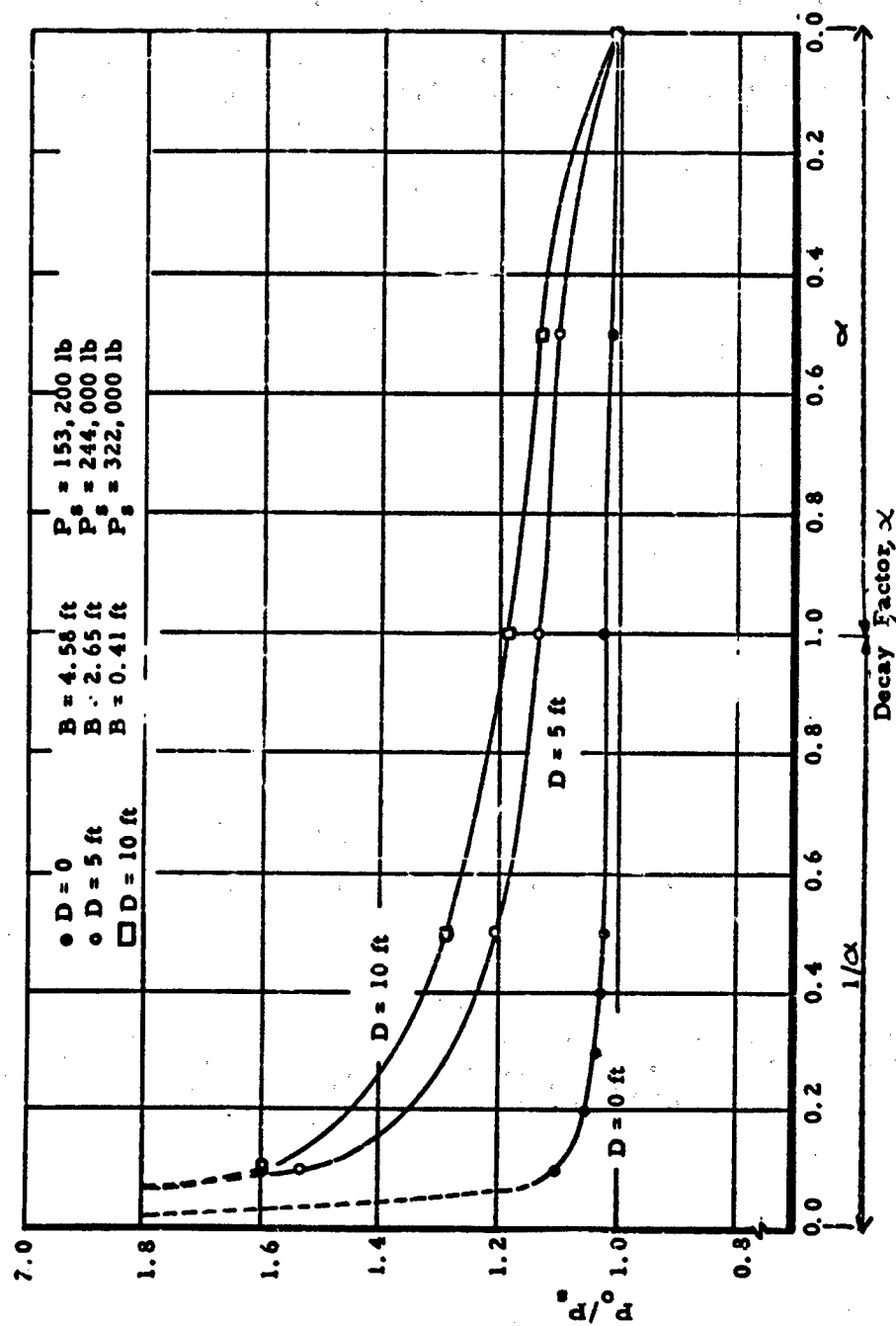
Fig. E-6 INFLUENCE OF DEPTH OF BURIAL FOR CONSTANT $\underline{r}$

$(r = 7ft, \; \phi = 25°, \; c = 2000 \; psf)$

E-19
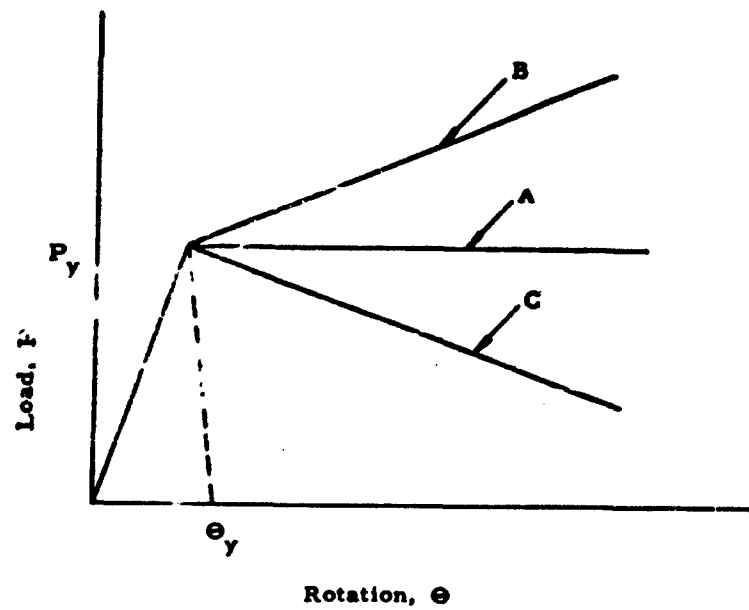
Fig. E-7 IDEALIZED ELASTIC-PLASTIC FORMS FOR $P(\theta)$
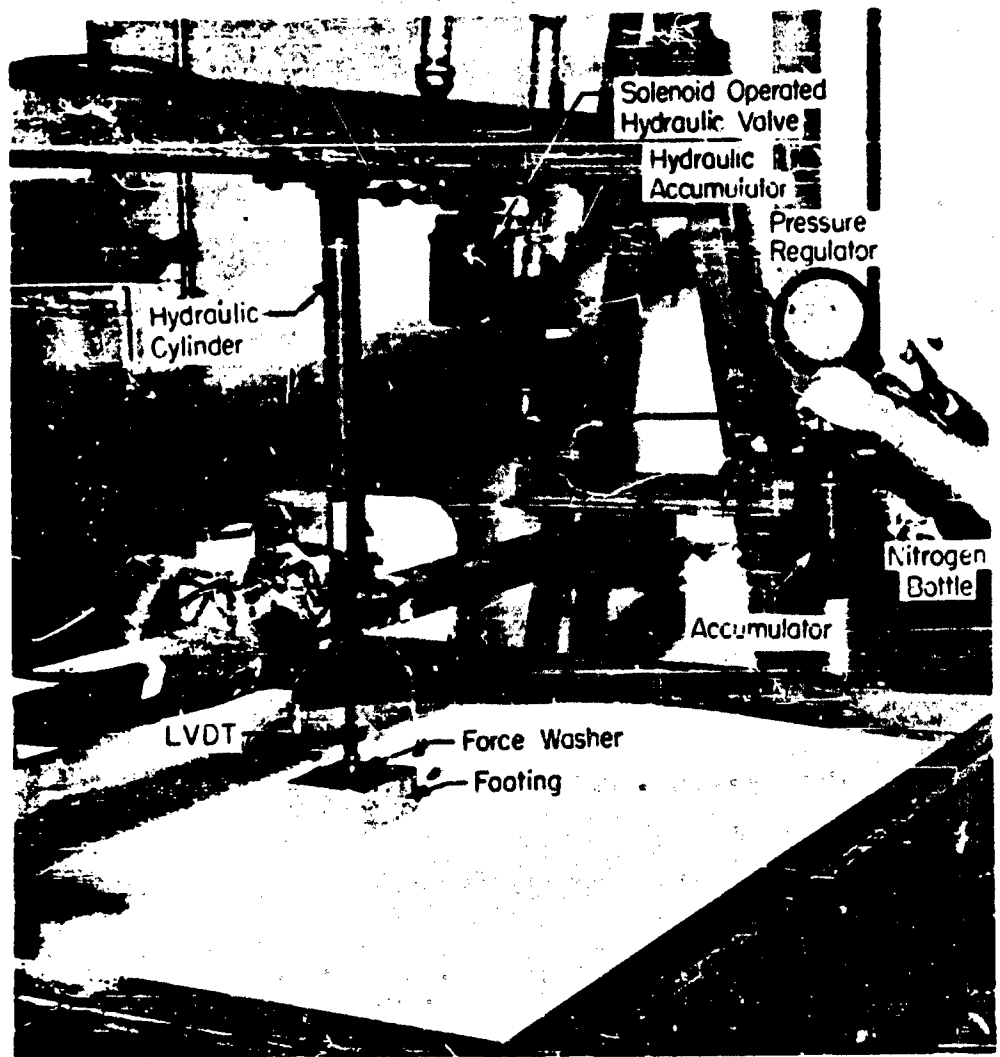
Fig. E-8 THREE DIMENSIONAL EXPERIMENTAL SETUP
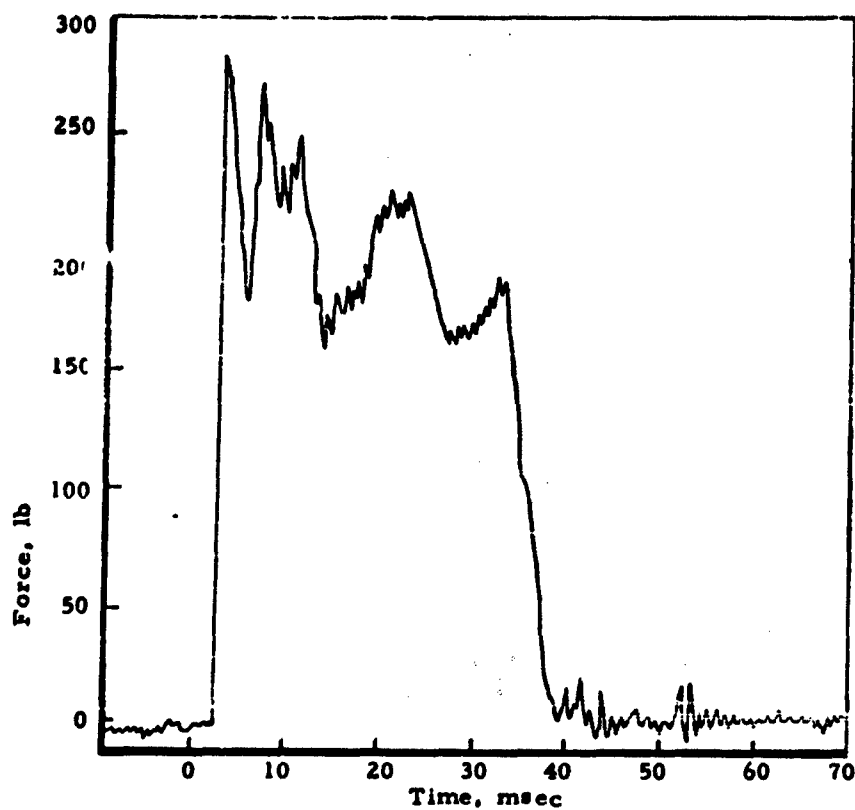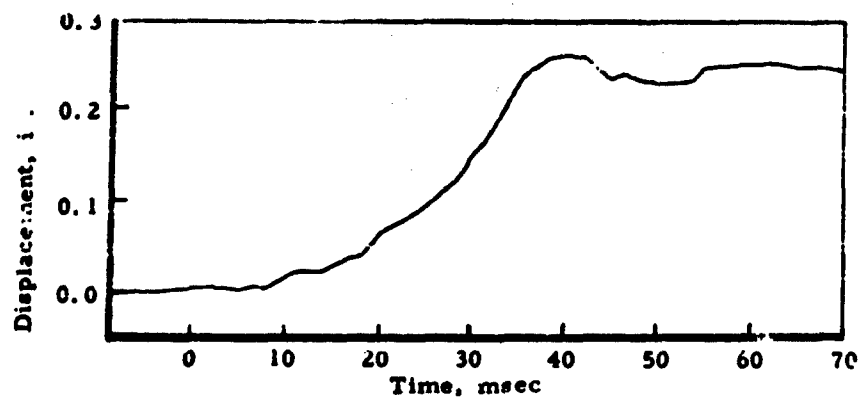
Fig. E 9 TYPICAL RECORDS FOR DYNAMICALLY LOADED
FOOTING EXPERIMENT 27

E-22

Fig. E-10 TYPICAL RECORDS FOR DYNAMICALLY LOADED
FOOTING, EXPERIMENT P27

E-23
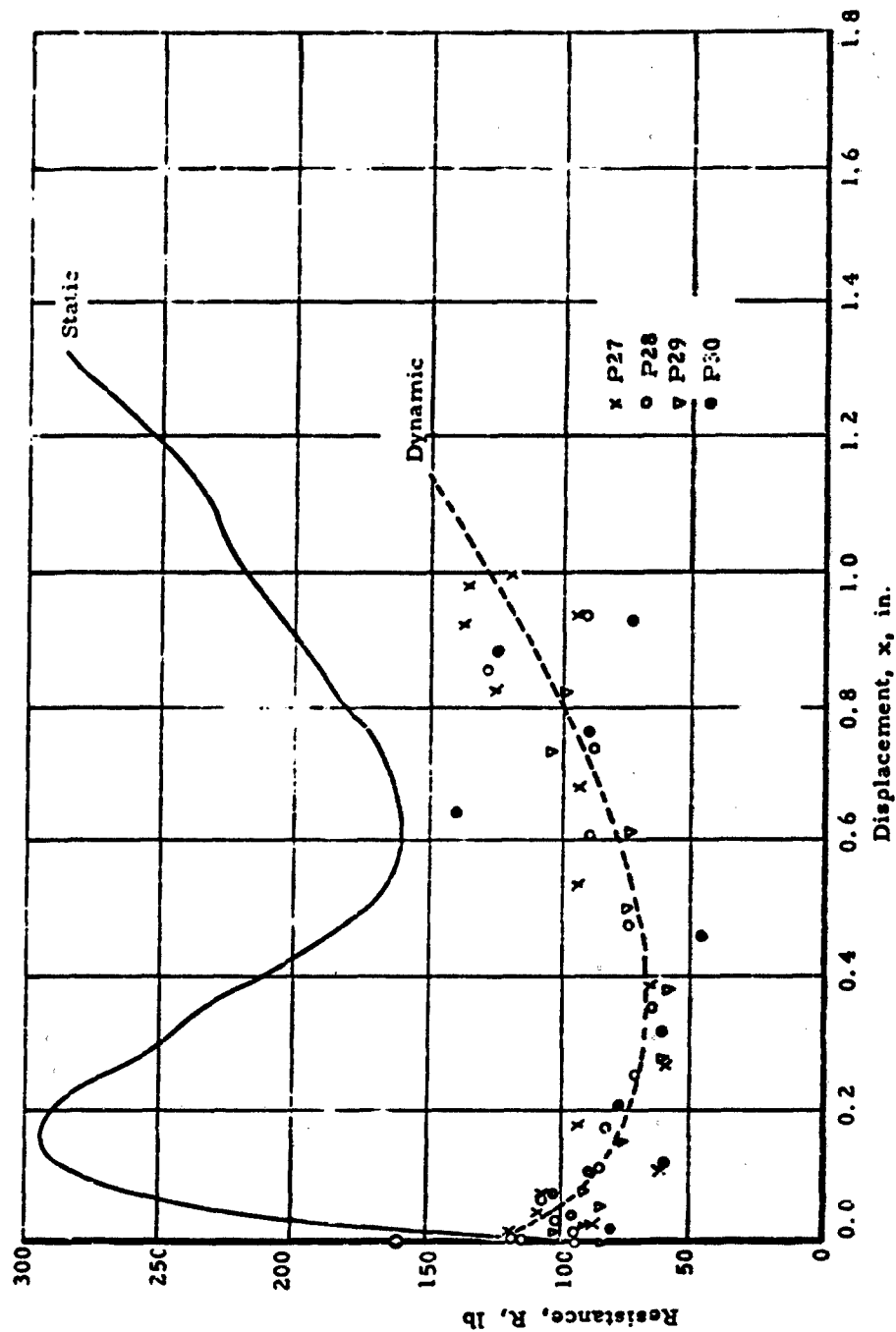
Fig. E-11 RESISTANCES FOR EXPERIMENTS P27, P28, P29, AND P30
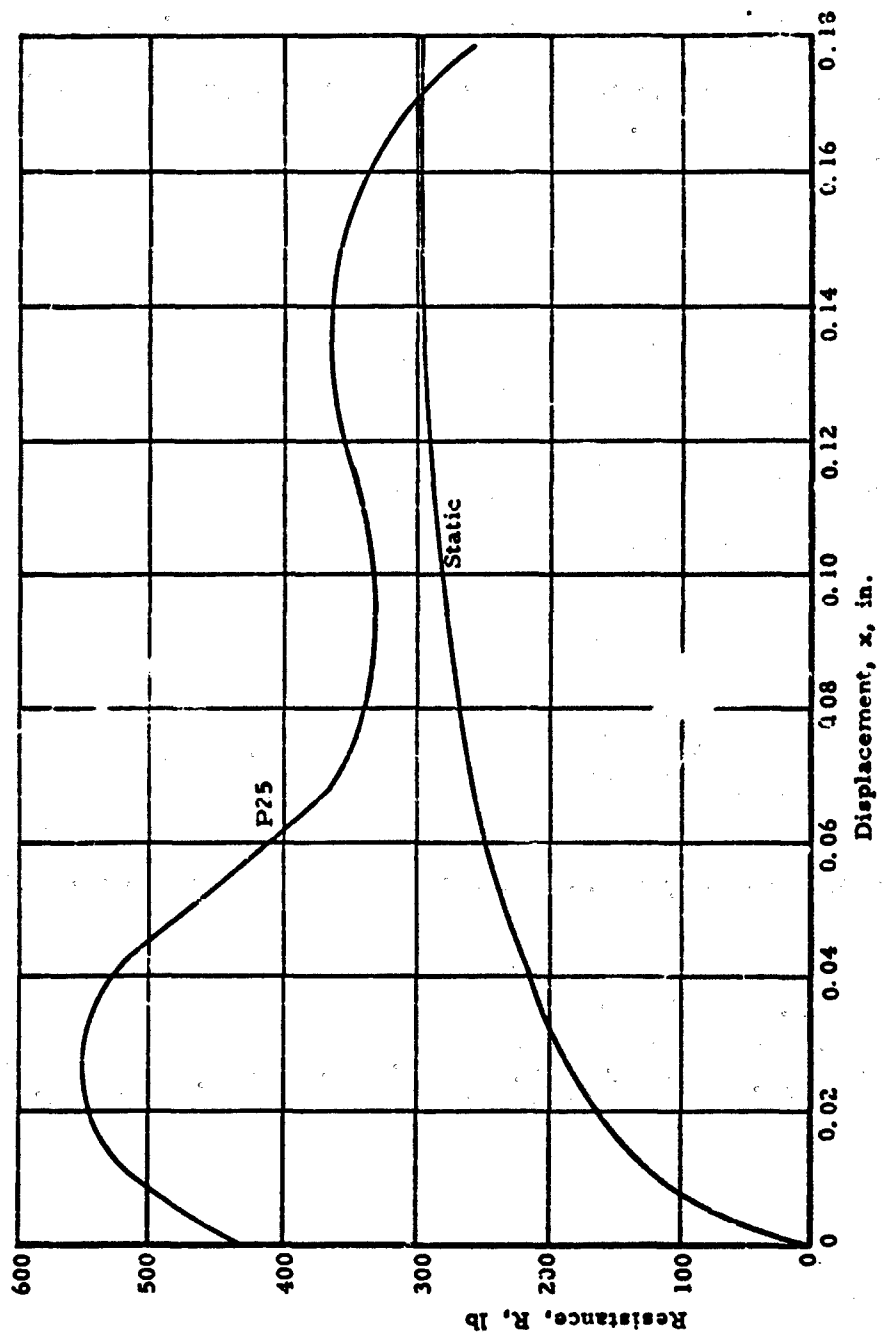
Fig. E-12 RESISTANCE FOR EXPERIMENT P25
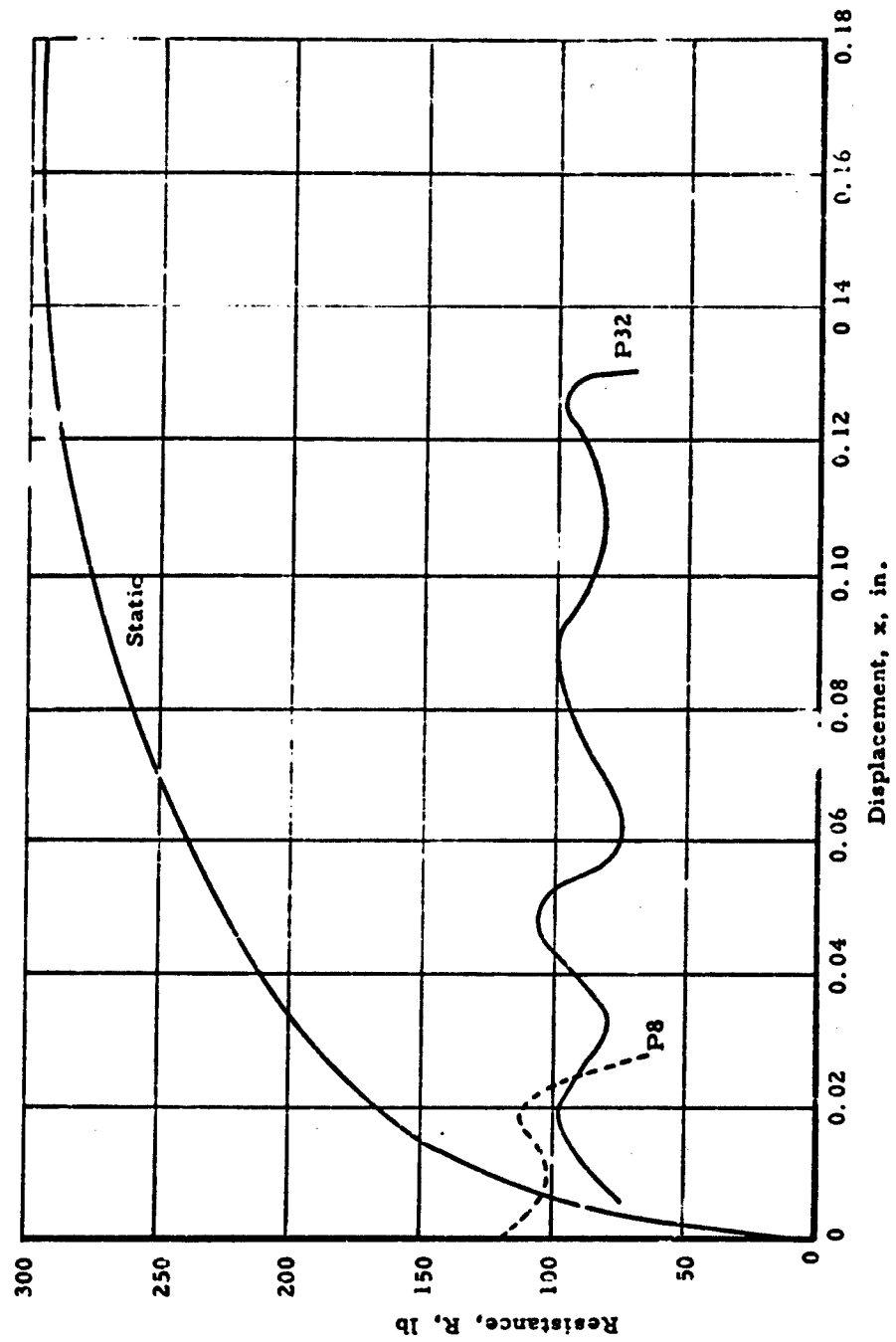
Fig. E-13 RESISTANCES FOR EXPERIMENTS P8 AND P32
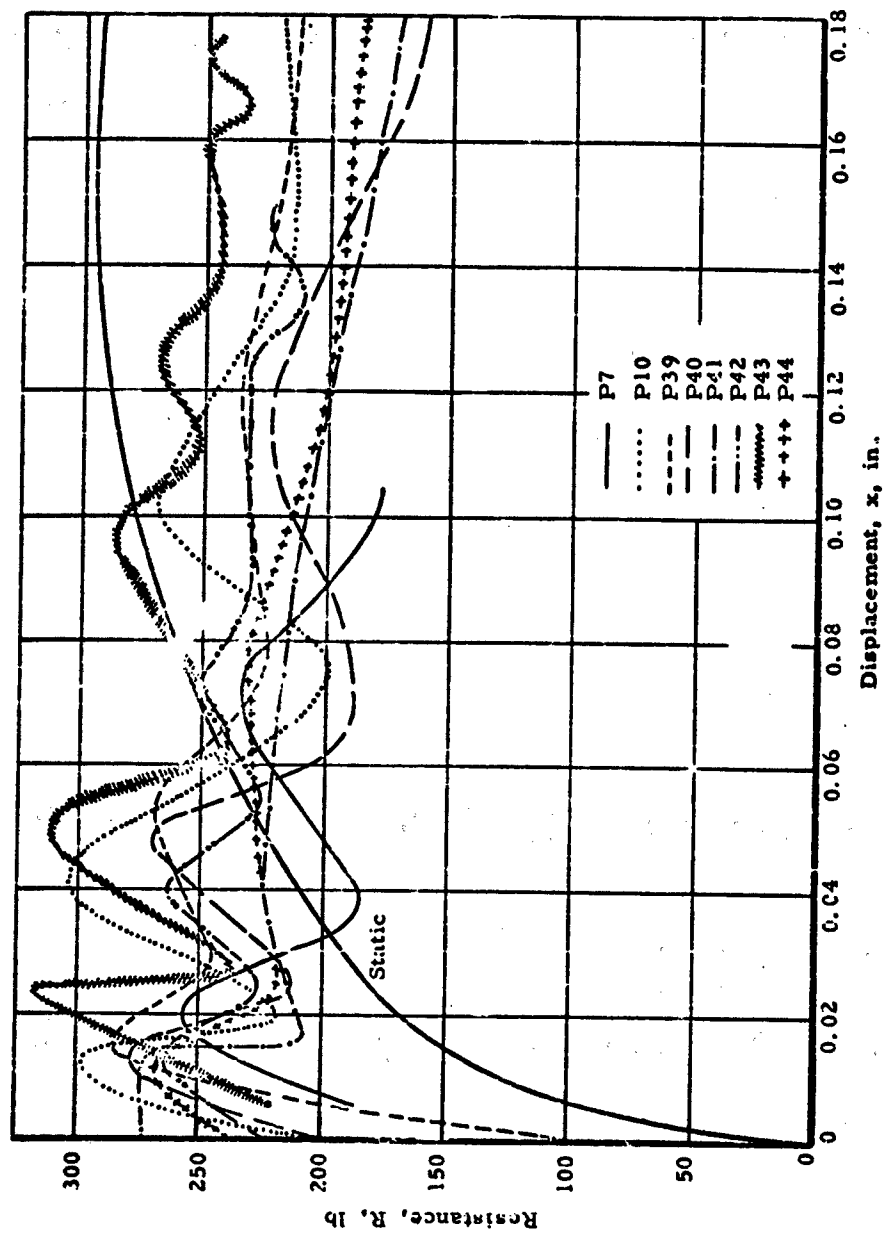
Fig. E-14 RESISTANCES FOR EXPERIMENTS P7, P10, P39, P40, P41, P42, P43, AND P44

ARMOUR RESEARCH FOUNDATION OF ILLINOIS INSTITUTE OF TECHNOLOGY

E-27
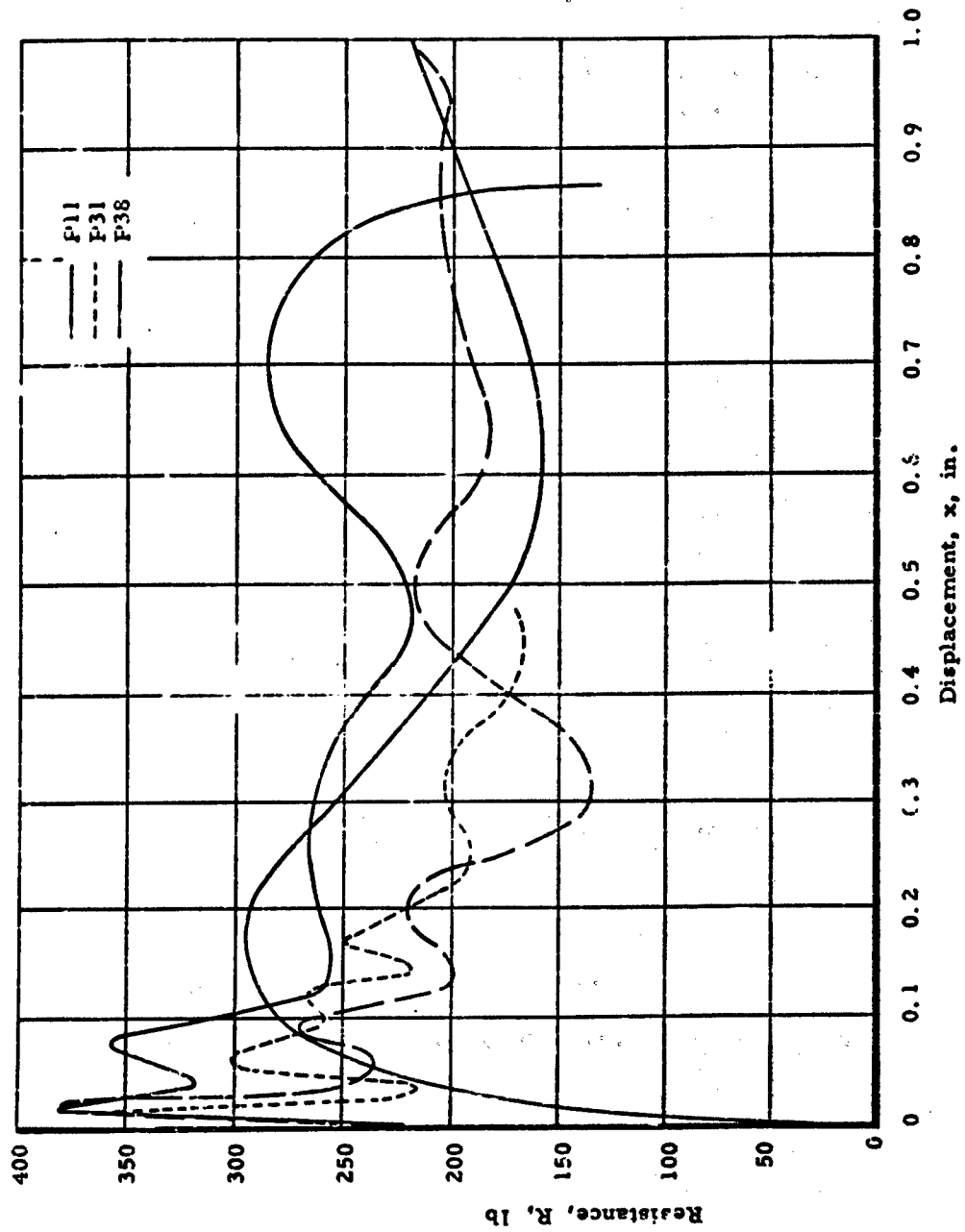
Fig. E-15 RESISTANCES FOR EXPERIMENTS P11, P31, AND P38

ARMOUR RESEARCH FOUNDATION OF ILLINOIS INSTITUTE OF TECHNOLOGY

E-28

APPENDIX   F

E FECT OF SOIL COMPRESSIBILITY

by

K E McKee

APPENDIX F

EFFECT OF SOIL COMPRESSIBILITY

by

K. E. McKee

BACKGROUND

As a result of soil compressibility, stress waves are generated in the soil below a footing loaded by a time-dependent force. An idealization of this situation would be the stress waves associated with loading a prescribed area on the surface of a half space. The only major limitation of soil properties is that they should be suitable for conducting an analysis and, of course, be related to those expected for the experimental condition. In general, the major restriction is that the soil properties should depend only on depth and be uniform at each depth.

Since any approach to this problem represents a stress wave propagation, this appendix makes use of literature relating stress wave propagation. In particular, for the materials of interest herein, i.e., soils, and for the loading of interest, i.e., a dynamic pressure applied to a portion of the surface of a semi-infinite body; the need for idealizations and simplifications becomes apparent. Before considering the specific applications which are the subject of this appendix, stress-wave propagation must be considered generally. A thorough review of stress-wave propagation with the entire development and all of the ramifications would represent a major effort. For the purposes of this report, the attempt will be made to review the state-of-knowledge in broad terms with particular emphasis on those aspects which will subsequently be used.

Interest in and theoretical solutions for stress propagation problems are far from new. Starting in the nineteenth century, classical mechanics included studies into this technical area. This interest was generated primarily by the seismologists and earthquake data supplied the bulk of the available experimental evidence. Over-all consideration of these approaches is available from a number of standard references on elasticity,

ARMOUR RESEARCH FOUNDATION OF ILLINOIS INSTITUTE OF TECHNOLOGY

e.g., Love[F-1]*, and from a large number of books on seismology; e.g., Fullen[F-2], Ewing, et al[F-3], Macchivane[F-4], or Richter[F-5]. Without in any way .... g to go over what was done in detail, certain general observations may be of interest. The range of problems which were considered is, in retrospect, astonishing. These solutions were far from inclusive and, in general, represented those cases which could be solved conveniently. The analyses were also based on simplifying assumptions which, in general, were not investigated to any major degree. Finally, the experimental data, primarily related to earthquake observations, were suitable only for evaluation and points a long distance from the source of the disturbance. This source of experimental data and the lack of knowledge relating to the material properties limited verification for the assumptions and as a result the theories were to some extent not much more than an approximation suitable for large distances from the source.

Within the past two decades, there has been substantial research, both theoreti al and experimental, relating to stress v. propagation. Davids[F-6], Keisk[F-7], and Rinehart[F-8], have summarized much of this work although certain aspects are available only in the recent technical literature. In the following paragraphs, areas of specific technical interest will be considered.

The elementary theory applies for an elastic half-space loaded over its entire surface or a bar loaded uniformly with plane cross sections remaining plane and only axial stresses. This formula results in the standard wave equation, i.e.;

$$E \frac{\partial^2 \sigma_z}{\partial z^2} - \frac{\rho \partial^2 \sigma_z}{\partial t^2} = 0 \qquad \text{(Eq. F-1)}$$

and

$$v_o = \sqrt{\frac{E}{\rho}} \qquad \text{(Eq. F-2)}$$

---

* Superscript numbers in parentheses cite references collected at the end of this appendix.

ARMOUR RESEARCH FOUNDATION OF ILLINOIS INSTITUTE OF TECHNOLOGY

F-2

or similar equations for strain or particle velocity. The general wave equation arising in connection with many physical systems and mathematical tools (generally using Fourier expansions) are available for obtaining solutions, e.g., see Miller[F-9]. One of the more significant observations resulting from this approach is that a stress wave is transmitted without change through the specimen.

An excellent discussion of the theoretical limitation of the elementary theory for elastic stress waves has been presented by Abramson[F-10]. Abramson summarizes the more exact theories that have been considered, along with the results. The various theories are compared with each other and with the available data. Because of numerical complications, solutions based on the exact theories are rare. (Use of high speed digital computers is expected to improve this situation.) Experimental research along with refined approximation solutions are, however, sufficient for a basic understanding of the phenomena.

Stress propagation through materials having nonlinear stress-strain characteristics is of particular interest for this study. Donnell[F-11] formulated in 19__ the basis for the theory of plastic stress __ves. During World War II his formulation was used independently by thr __vestigators in three countries to investigate plastic stress waves -- Rakhmatviin[F-12] in the USSR, Taylor[F-13, F-14] in the UK and von Kármán[F-15, F-16, F-17, F-18] in the USA. Since that time there have been many studies, both theoretical and experimental, in this general area. Of particular significance was the introduction of strain-rate effects by Malvern[F-19, F-20]. Recent papers by Abramson[F-10] and Lee[F-21] summarize the status of this subject. To demonstrate the basic problem, the Donnell formulation is shown in figures F-1 and F-2.

Figure F-1 shows an idealized linear stress-strain relationship with an initial slope of E_1 and subsequent slope of E_2 associated with stresses greater than σ_1. If a stress, equal to or less than σ_1 is applied, a stress wave would be propagated with a velocity of $\sqrt{\dfrac{E_1}{\rho}}$ as would be expected for an elastic stress wave. For a stress, σ, greater than σ_1 there would be two distinct stress waves propagated from the sources as shown in figure F-2.

The first wave having a stress of σ_1 is propagated at $\sqrt{\dfrac{E_1}{\rho}}$ while the second having a stress of propagates at $\sqrt{\dfrac{E_2}{\rho}}$. As shown in figure F-2 this results in a spread between the two fronts which will increase with time. This approach is obviously suitable for any material which has a slope decreasing in any fashion with increased stress. For unloading, many materials follow the initial slope, in which case the unloading portions would be expected to travel with a velocity of $\sqrt{\dfrac{E_1}{\rho}}$. Donnell's formulation explains changes in the wave shape and subsequent obliteration of all portions traveling at less than the initial velocity through the catching up of the unloading portions. Donnell's formulation, which took less than one page in Applied Mechanics in 1930, represents the basis for most studies of plastic stress waves. There is one limitation in the above which was not specifically mentioned by Donnell -- this formulation is limited to stress-strain curves where E_2 is less than E_1. A concave stress-strain curve can not be handled in this fashion. The outrunning of the second wave would be physically unacceptable. Figure F-3 shows the situation being considered. For values equal to or less than σ the stresses would be propagated with the initial velocity $\sqrt{\dfrac{E_1}{\rho}}$. For stress levels higher than σ_1 the standard approach, e.g., see White and Griffis[F-22] or Salvadori, Skalak, and Weidlinger[F-23, F-24], uses the secant modulus, as shown on figure F-3, to establish the velocity of the stress front.

The concept of a "locking material" has been adopted into a number of studies of plastic stress wave propagation. "Ideal locking materials" were introduced by Prager[F-25, F-26] as an idealization for certain classes of materials. In much the same fashion as stress-strain relationships are considered an ideally plastic (i.e., the stress remains constant with an increase in strain), Prager considers the relationship to be ideal locking with stress increasing with no increase in strain. Figure F-4 shows several of the idealizations which have been used for locking materials and obviously others could be considered. Salvadori, Skalak and Weidlinger[F-23, F-24, F-27, F-28, F-29] have used locking materials in considering stress-wave propagation in soil media. To a large extent, the

subsequent development represents applications and extensions of these studies.

MATHEMATICAL FORMULATION

The concept of a 'locking material' was selected to investigate the influence of soil compressibility on the behavior of dynamically loaded footings. As a reasonable representation for the footing problem, certain simplifications were introduced:

1. The affected soil volume is symmetrical about the vertical axis.

2. The soil is infinite in depth.

3. The problem can be reduced to one dimension i.e., expressed in terms of the vertical dimensions.

4. The soil properties are constant at each depth although they can vary with depth.

5. Lateral effects, e.g., inertia and the effect of adjacent soil is negligible.

6. Soil properties can be idealized in terms of ideal locking media.

Within these assumptions there are unlimited specific formulations which could be carried out. As a first attempt a rigid-plastic locking material was assumed (see Fig. F-5) for a column of soil extending vertically below the footing. Figure F-6 shows this column at time t and a short time later at $t + \Delta t$ based on the material properties illustrated in figure F-5. The nomenclature introduced for figures F-5 and F-6 includes:

$p(t)$ = pressure time history acting on column of soil below footing

$x(t)$ = displacement of footing as a function of time

$\dot{x}$ = $\dfrac{dx}{dt}$ = velocity of footing

$\ddot{x}$ = $\dfrac{d^2 x}{dt^2}$ = acceleration of footing

$z(t)$ = vertical location of compaction front

$\dot{z}$ = $\dfrac{dz}{dt}$ = velocity of compaction front

ϵ_c = strain associated with locking

ρ_c = mass density associated with locking

ρ_o = initial mass density

σ_o = plastic stress

Considering an element having a total depth of ℓ, the momentum at $t + \Delta t$, is:

$$M_{t + \Delta t} = \rho_c \left[z + \dot{z} \Delta t - (x + \dot{x} \Delta t) \right] \left[\dot{x} + \ddot{x} \Delta t \right] \qquad \text{(Eq. F-3)}$$

$$+ \rho_o \left[\ell - (z + \dot{z} \Delta t) \right] \dot{x}_o$$

At time, t, the momentum would be:

$$M_t = \rho_c \left[z - x \right] \dot{x} + \rho_o \left[\ell - z \right] \dot{x}_o \qquad \text{(Eq. F-4)}$$

Application of Newton's law gives:

$$p(t) - \sigma_o = \lim_{\Delta t \to 0} \frac{M_{t + \Delta t} - M_t}{\Delta t} \qquad \text{(Eq. F-5)}$$

Substitution of equations F-3 and F-4 in equation F-5 gives:

$$p(t) - \sigma_o = \rho_c \left[z - x \right] \ddot{x} + \rho_c \left[\dot{z} - \dot{x} \right] \dot{x} - \rho_o \dot{z} \dot{x}_o \qquad \text{(Eq. F-6)}$$

The conservation of mass gives: $\rho_o \dot{z} = \rho_c (\dot{z} - \dot{x})$ \qquad (Eq. F-7)

which substituted in equation F-6 gives:

$$\frac{p(t) - \sigma_o}{\rho_c} = \left[z - x \right] \ddot{x} + \left[\dot{z} - \dot{x} \right] \dot{x} - \dot{x}_o \qquad \text{(Eq. F-8)}$$

Under normal circumstances, where the initial velocity is zero, i.e., $\dot{x}_o = 0$,

$$\frac{p(t) - \sigma_o}{\rho_c} = \left[z - x \right] \ddot{x} + \left[\dot{z} - \dot{x} \right] \dot{x} \qquad \text{(Eq. F-9)}$$

Based on equation F-7, z can be expressed in terms of x :

$$z = \frac{1}{1 - \dfrac{\rho_o}{\rho_c}} \, x + c \qquad \text{(Eq. F-10)}$$

where the constant $c = 0$ since when $t = 0$, and $z = 0$, and $x = 0$. Substituting

$$z = \frac{1}{1 - \dfrac{\rho_o}{\rho_c}} \, x \quad \text{into equation F-9,}$$

$$x\,\ddot{x} + (\dot{x})^2 = \left[p(t) - \sigma_o \right] \left[\frac{1}{\rho_o} - \frac{1}{\rho_c} \right] \qquad \text{(Eq. F-11)}$$

with the initial conditions

$$x(0) = 0$$

$$\dot{x}(0) = 0$$

Since this equation can be reduced to a linear equation by substituting
$u = x\dot{x}$, it can be solved in closed form as:

$$x(t) = \sqrt{2 \left(-\frac{1}{\rho_o} - \frac{1}{\rho_c} \right) \int_0^t \int_0^{\tau} \left(p(\gamma) - \sigma_o \right) d\gamma \, d\tau } \qquad \text{(Eq. F-12)}$$

Since the stress-strain relationship allows no recovery this solution is
meaningful only so long as :

$$\int^t \left[p(\tau) - \sigma_o \right] \, d\tau \geqq 0 \qquad \text{(Eq. F-13)}$$

By considering a rigid mass at the top of the soil column as
shown on figure F-7, the effect of the mass of the footing can be introduced
into the analysis. Following the same approach used without the rigid mass
the results are

$$\frac{p(t) - \sigma_o}{\rho_c} = \frac{h \, \rho_r}{\rho_c} \, \ddot{x} + (z - x) \, \ddot{x} + (\dot{z} - \dot{z}) \, \dot{x} \qquad \text{(Eq. F-14)}$$

Since equation F-10 is again applicable this can be reduced to:

$$\frac{p(t) - \sigma_0}{\rho_c} = \frac{h \rho_r}{\rho_c} \ddot{x} + \frac{\rho_0}{\rho_c - \rho_0} x \ddot{x} + \frac{\rho_c}{\rho_c - \rho_0} (\dot{x})^2 . \quad \text{(Eq. F-15)}$$

Here again a general solution can be found as by substituting $u = \dot{x} (x + k)$ as:

$$x(t) = \left[\left\{ h \rho_r \left(\frac{1}{\rho_0} - \frac{1}{\rho_c} \right) \right\}^2 + 2 \left(\frac{1}{\rho_0} - \frac{1}{\rho_c} \right) \int_{\sigma}^{t} \int_{\sigma}^{\tau} \left[p(\gamma) - \sigma_0 \right] d\gamma d\tau \right]^{1/2}$$

$$- h \rho_r \left(\frac{1}{\rho_0} - \frac{1}{\rho_c} \right) . \quad \text{(Eq. F-16)}$$

In an attempt to introduce more realistic soil characteristics, it is desirable to consider possible variations of the yield stress with depth. If σ_0 is the value at the surface, one can postulate $\sigma_0 + f(z)$ where f is an arbit f nction representing the variation be'c the surface. The resulting e aation would be:

$$\frac{p(t) - \sigma_0}{\rho_c} = \frac{h \rho_r}{\rho_c} \ddot{x} + (z - x) \ddot{x} + (\dot{z} - \dot{x}) \dot{x} + \frac{f(z)}{\rho_c} . \quad \text{(Eq. F-17)}$$

In general, equation F-7 might also be modified so that at least ρ_0 would be a function of depth, i.e., $\rho_0 (z) \dot{z} = \rho_c (\dot{z} - \dot{x})$ (Eq. F-18)

Equation E-18 can be solved for x as a function of z and subsequently E-17 solved for z(t).   This type of solution is relatively complex to perform (it requires approximately 8 hours of calculations using a desk calculator) but offers no other difficulty. Closed form solutions do not appear to be available when either the plastic strength or initial density are functions of depth. Based on this latter observation, it should be noted that relatively complex variations with depth offer essentially the same mathematical complexity, as a simple relationship. It should also be noted that with the high speed digital

ARMOUR RESEARCH FOUNDATION OF ILLINOIS INSTITUTE OF TECHNOLOGY

F-8

computers, a numerical solution may be superior even when a closed form solution exists.

To this point only a uniform column of sand below the footing has been considered. An obvious alternate would be a column of soil increasing in size with depth. Considering the instance where the soil properties are independent of depth and there is no rigid mass, the initial development was based on a linear increase of area with depth. Figure F-8 shows the frustrum of pyramid which was considered. In essence, the development follows that used for the uniform column. The resulting equation in terms of the footing displacement is:

$$p(t) - \sigma_o = C_1 \sigma_o x + C_2 \left(1 + \frac{C_1}{2} x\right)(x \ddot{x} + \dot{x}^2) \quad \text{(Eq. F-19)}$$

where

$$C_1 = \frac{A_1}{A_o}\left(\frac{\rho_c}{\rho_c - \rho_o}\right) \quad \text{and,} \quad C_2 = \frac{\rho_c \rho_o}{\rho_c - \rho_o}.$$

Even for this linearized formulation, numerical solutions are required. Here again variation of column dimensions or soil properties with depth could be incorporated. Also, a rigid mass could be considered to be located in place of the footing.

Other formulations depend on the form assumed for the stress-strain relationships. Certain others were considered, e.g., elastic locking material, but for the purposes of this study, attention is limited to the rigid-plastic locking materials. This is done for several reasons; first, this relationship resembles those determined for soil; second, mathematical simplifications are available; and, finally, the experimental data is insufficient to justify an improved design. Here again high speed computers can simplify the requirements to obtain a satisfactory solution for more complex stress-strain relationships.

A number of solutions have been carried out based on the formulations considered above. In the following paragraphs, these results will be considered and compared with available experimental results. The attempt here then is to establish the significance of the differences between the various assumptions.

Equation F-12 is the closed form solution based on a uniform column of soil beneath the footing. Insight into this solution can be obtained by considering the load to be a step pulse, as shown in figure F-9. For a solution to exist p_o must exceed σ_o and the solution up to time t_o is:

$$x(t) = \sqrt{\left(\frac{1}{\rho_o} - \frac{1}{\rho_c}\right)(p_o - \sigma_o)\, t} \quad . \qquad \text{(Eq. F-20)}$$

For times exceeding t_o the solution would be

$$x(t) = \sqrt{\frac{1}{\rho_o} - \frac{1}{\rho_c}} \sqrt{2\left[(p_o - \sigma_o)\, t_o\, \left(t - \frac{t_o}{2}\right) - \frac{\sigma_o}{2}\frac{(t-t_o)^2}{2}\right]}$$

$$\text{(Eq. F-21)}$$

Considering a normalized dimensionless displacement for $t < t_o$

$$\frac{x}{t_o\sqrt{\left(\frac{1}{\rho_o} - \frac{1}{\rho_c}\right)(p_o - \sigma_o)}} = \frac{t}{t_o} \qquad \text{(Eq. F-22)}$$

and for $t > t_o$

$$\frac{x}{t_o\sqrt{\left(\frac{1}{\rho_o} - \frac{1}{\rho_c}\right)(p_o - \sigma_o)}} = \sqrt{\left(2\frac{t}{t_o} - 1\right) - \frac{1}{\frac{p_o}{\sigma_o} - 1}\left(\frac{t}{t_o} - 1\right)^2}$$

$$\text{(Eq. F-23)}$$

The maximum (and assuming no recovery the permanent) displacement based on equation F-13 would occur at

$$\frac{t_1}{t_o} = \frac{p_o}{\sigma_o} \qquad \text{(Eq. F-24)}$$

and would be

$$\frac{x_{max}}{t_o\sqrt{\left(\frac{1}{\rho_o} - \frac{1}{\rho_c}\right)(p_o - \sigma_o)}} = \sqrt{\frac{p_o}{\sigma_o}} \quad . \qquad \text{(Eq. F-25)}$$

ARMOUR RESEARCH FOUNDATION OF ILLINOIS INSTITUTE OF TECHNOLOGY

The dimensionless displacement versus dimensionless time is shown on figure F-10. This plot shows the behavior which would be anticipated, e.g., a linear behavior during the period of load application with the maximum displacement occurring later depending on the ratio of p_c/σ_o. This particular solution represents a gross simplification of the actual situation. Not only is the soil idealized as a column of uniform soil below the footing, but the load is idealized as a step pulse; interestingly, the results bear marked similiarities to the experimental results. Figures E-9 and E-10 show typical displacement-time curves obtained as part of the earlier experimental research conducted on this program (F-30). Improved experimental techniques for the more recent experimental studies (see Appendix C) have verified the general shape of the displacement-time histories, by use of a more sensitive LVDT (linear variable differential transformer) for the small displacements and accelerometers to serve as backup on the results. Unfortunately, these latter data were obtained only recent y and have not yet been subjected to detailed analysis. For this reason, more of the detailed evaluation whi   ve been made are car .ed out with the earlier data.

General c. mparison of the experimental results with the dimensionless plot of figure F-10 is particularly informative. Initially, there is some hesitancy, but basically the initial behavior is very nearly linear. Later experimental behavior varies significantly with the velocity increase instead of decreasing as shown on figure F-10. The more complex analytical approaches which are subsequently considered are justified to the extent that they provide a better method of predicting the observed behavior.

The most apparent factor to be considered would be the time history of the loading. If interest is restricted to the shape of the resulting displacement curve this can be done in terms of:

$$\frac{x(t)}{\sqrt{2\left(\dfrac{1}{\rho_0} - \dfrac{1}{\rho_c}\right)}} = \sqrt{\int_0^t \int_0^\tau (p(\gamma) - \sigma_0)\, d\gamma\, d\tau} \qquad \text{(Eq. F-26)}$$

for various values of σ_0. This was done for Experiment P27 and the results are plotted on figure F-11. It should be noted that no attempt is made in this presentation to calculate the actual displacement. For subsequent calculations relatively arbitrary values have been selected, i.e., $\rho_c = 0.0683$ lb per cu in. and $\rho_0 = 0.0625$ lb per cu in. The divisor for the displacement based on these values would be

$$\sqrt{2\left(\frac{1}{\rho_0} - \frac{1}{\rho_c}\right)} = \sqrt{2(1.357)} = 1.31$$

The maximum displacements are plotted on figure F-12 as a function of σ_0. The experimentally determined maximum displacement for Experiment P27 is approximately . 3 in. which would correspond to σ_0 pproximately 1.2 psi. This value of σ_0 is unrealistically low indicating a need for further evaluation of the parameters. The time-histories of figure F-11 can be compared with figure E-10 keeping in mind that figure F-11 uses a dimensionless displacement. The initial velocity based on the theoretical approach is less than the observed data for the values of σ_0 plotted - a much lower value of σ_0 would be required to justify this rate. Unfortunately lower values of σ_0 are associated with maximums occurring at later times. These results are therefore mutually contradictory with the initial velocity indicating a lower value of σ_0, and the time of maximum indicating a higher value of σ_0.

For the experimental setup the force-time history is measured above the footing. The aluminum block used for the footing therefore is a rigid mass. The influence of this rigid mass can be introduced based on equation F-16. These considerations alter the time-history of the response - they tend to account for the initially slow response and reduce the displacement at each time, assuming all of the soil parameters and

ARMOUR RESEARCH FOUNDATION OF ILLINOIS INSTITUTE OF TECHNOLOGY

forces remain the same. Limited analyses taking into account the rigid mass has been conducted. For the particular parameters selected, the mass introduced only small variations in the results. For this reason, these results have not been included, although this should not be interpreted an eliminating consideration of the rigid mass. On the contrary, this factor should be considered in future attempts to improve the analyses.

For realistic conditions one anticipates variations of soil properties with depth. Equations F-17 and F-18 provide a method for introducing variations in plastic stress and initial density with depth. These variations with depth can be introduced in as general a fashion as desired. As an example of the influence of such variations a series of solutions were carried out for a situation where the plastic strength varied linearly with depth and the initial density is independent of depth. For convenience, the stress was expressed as:

$$\sigma_0 + a(1 - \frac{\rho_0}{\rho_c})\, z = \sigma_0 + ax \qquad \text{(Eq. F-27)}$$

where "a" is a constant. As was mentioned earlier, $\rho_0 = 0.0625$ lb per cu. in. and $\rho_c = 0.0683$ lb per cu in. were used, thus $(1 - \frac{\rho_0}{\rho_c}) = 0.085$. The resulting equation is:

$$x\ddot{x} + \dot{x}^2 + x\, a\, \sigma_0 \left(\frac{1}{\rho_0} - \frac{1}{\rho_c}\right) = \left[p(t) - \sigma_0\right]\left[\frac{1}{\rho_0} - \frac{1}{\rho_c}\right]$$

$$\text{(Eq. F-28)}$$

Solution of this equation must be numerical in nature - the Ranga-Kutta method was used. Figure F-13 shows four plots for $\sigma_0 = 1.25$ psi with a = 0.25, 1.0, 10.0, and 100.0 (0.021, 0.085, and 8.5 psi per respectively). Figure F-13, which illustrates the variation for a relatively arbitrary set of parameters, is typical. Obviously the key parameter is σ_0. The value selected was based on the extrapolation from figure F-12.

In the above examples, the column of soil below the footing was assumed to be uniform in cross section. Equation F-19 provides a

solution taking into account linear variation of area with depth. Here again the Runge-Kutta method[F-31] was used. Figure F-14 shows the results for the three values of A, (i.e., the percentage change in area with depth): 5%, 15%, and 25%.

As was pointed out earlier with the number of parameters involved, there are innumerable solutions which could be obtained. More involved variations with depth or inclusion of the rigid mass could also be considered. If consideration is extended to alternate formulations of the stress-strain relationships, the possibilities are increased even more substantially.

The solutions presented above, however, are sufficient to demonstrate that consideration of soil compressibility offers a potentially useful theoretical tool for explaining the observed footing behavior. It should be emphasized that the solutions carried out to date have not been sufficient to establish suitable soil parameters. There is still much to be done, but the author believes that the feasibility of   type of approach has been demonstrated and that continuing ef   along these directions is justified.

REFERENCES

F-1. Love, A. E. H., A Treatise on the Mathematical Theory of Elasticity, 4th Edition (1927), Dover Publications, (1944).

F-2. Bullen, K. E., An Introduction to the Theory of Seismology, Cambridge at the University Press, (1947).

F-3. Ewing, W. A., Jardetzky, W. S. and Press, F., Elastic Waves in Layered Media, McGraw-Hill, N. Y., (1957).

F-4. Macelwane, J. B., Introduction to Theoretical Seismology, Part I, Geodynamics, Wiley, N. Y., (1936).

F-5. Richter, C. F., Elementary Seismology, W. H. Freeman and Co., San Francisco, (1960).

F-6. Davids, Norman (Editor) International Symposium on Stress Wave Propagation in Materials, Interscience Publishers, Inc., N. Y., (1960).

F-7. Kolsky, H., Stress Waves in Solids, Claren. Press, Oxford, (1953)

F-8. Rinehart, J. S. and Pearson, J., Behavior of Metals Under Impulsive Loads, ASM, Cleveland, (1952).

F-9. Miller, K. S., Partial Differential Equations in Engineering Problems, Prentice-Hall, (1953).

F-10. Abramson, H. N., Plass, H. J. and Ripperger, E. A., "Stress Wave Propagation in Rods and Beams", p. 114, 139, Advances in Applied Mechanics, Vol. V, Academic Press, Inc., (1958).

F-11. Donnell, L. H., Longitudinal Wave Transmission and Impact, Trans, ASME, 52, 153, (1930).

F-12. Rakhmatulin, K. A., "Propagation of a Wave of Unloading", Prikl. Mat. Mek, 9, 91, (1945).

F-13.   Taylor, G. I., The Plastic Wave in a Wire Extended by an Impact Load, British Government Report, R. C. 329, (1942).

F-14.   Taylor, G. I., "The Plastic Wave in a Wire Extended by an Impact Load", p. 457, The Scientific Papers of Sir Geoffrey Ingram Taylor, Cambridge, (1958).

F-15.   von Kármán, T., On the Propagation of Plastic Deformations in Solids, OSRD, Rept. No. 365 (1942).

F-16.   von Kármán, T., Bodnenblust, H. F. and Hyers, D. H., The Propagation of Plastic Waves in Tension Specimens of Finite Length, NDRC Report A-103 (OSRD 1946), October 1942.

F-17.   von Kármán and Duwez, P., The Propagation of Plastic Deformation in Solids, Proceedings VI Int. Congress of Applied Mechanics, 1946.

F-18.   von Kármán and Duwez, P., "The Propagation of Plastic Deformation in Solids," J. Appl. Phys., 21, 987 (1950)

F-19.   Malvern, L. E., "The Propagation of Longitu   Waves of Plastic Deformation in a Bar of Material Exhibiting a Strain-Rate Effect," J. Appl. Mech., 18, (1951).

F-20.   Malvern, L. E., "Plastic Wave Propagation in a Bar of Material Exhibiting a Strain-Rate Effect," Quar. Appl. Math. 8, (1951).

F-21.   Lee, E. H., A Theory of Wave Propagation in Anelastic Materials, p. 199-228, International Symposium on Stress Wave Propagation in Materials, Interscience Publishers, N. Y. (1960).

F-22.   White, M. P., and Griffis, L., "The Propagation of Plasticity of Uniaxial Compression," J. Appl. Mech., 15, 256 (1948).

F-23.   Salvadori, M. G., Skalak, R. A., Weidlinger, "Stress Waves in Dissipative Media," Trans. Acad. Sci., Ser. II, 21, No. 5, 427-434, (1959).

F-24.   Salvadori, M. G., Skalak, R. and Weidlinger, P., Spherical Waves in Plastic Locking Medium, Engr. Mech. Div., ASCE, Proceedings, Vol. 87, No. EM1, February 1961.

F-25   Prager, W., "On Ideal Locking Materials", Trans. Soc. Rheology, I, 169-175 (1957).

F-26.   Prager, W., Elastic Solids of Limited Incompressibility, Proceedings of the IX Inter Congress of Applied Mechanics, Brussels, 1957.

F-27.   Salvadori, M. G. and Weidlinger, P., Induced Ground Shock in Granular Media, March 1958.

F-28.   Salvadori, M G., Skalak, R. and Weidlinger, P, "Waves and Shocks in Locking and Dissipative Media." J. Eng. Mech. Div., ASCE, Proc., Vol. 86, No. EM2, April 1960.

F-29.   Weidlinger, P., On the Application of the Theory of Locking Media . Ground Shock Phenomena, The Mitre Corp ation, Bedford, Massachusetts, Sept. 1960.

F-30.   McKee, K. E., Design and Analysis of Foundation for Protective Structures, Second Interim Technical Report, AFSWC-TN-61-14, Armour Research Foundation, Chicago, May 1961.

F-31.   Scarborough, J. B., Numerical Mathematical Analysis, 2nd ed., John Hopkins Press, Baltimore, (1950).

F-32.   Andersen, P., Substructure Analysis and Design, p. 81, The Ronald Press Co., New York, (1956).

F-33.   Mass. Inst. of Technology, The Behavior of Soils Under Dynamic Loading, Final Report on Laboratory Studies, AFSWP 118, Aug. 1954.

F-34.   McKee, K. E., Design and Analysis of Foundations for Protective Structures, Phase Report III, Interim Technical Report, Armour Research Foundation, January 1959.

F-35.   McKee, K. E., Design and Analysis of Foundations for Protective
         Structures, AFSWC-TR-59-56, Armour Research Foundation, Chicago,
         October 1959.

F-36.   McKee, K. E., Design and Analysis of Foundation for Protective
         Structures, Second Interim Technical Report, AFSWC-TN-61-14,
         Armour Research Foundation, Chicago, May 1961.

F-37.   Shenkman, S. and McKee, K. E., Bearing Capacity of Dynamically
         Loaded Footings, Symposium on Soil Dynamics, ASTM, Armour
         Research Foundation, Chicago, June 1961.

F-38.   Shenkman, S. and McKee, K. E., The Armour Research Foundation
         Pressure Vessel, report to ARF on project R5318, Armour
         Research Foundation, Chicago, December, 1961.
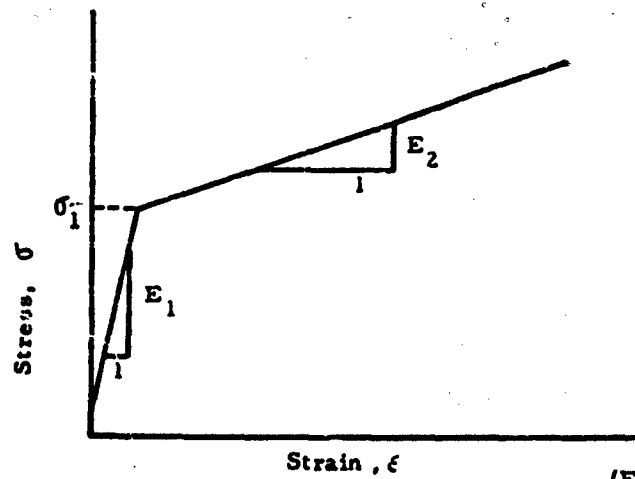
Fig. F-1 BILINEAR STRESS-STRAIN CURVE [F-11]
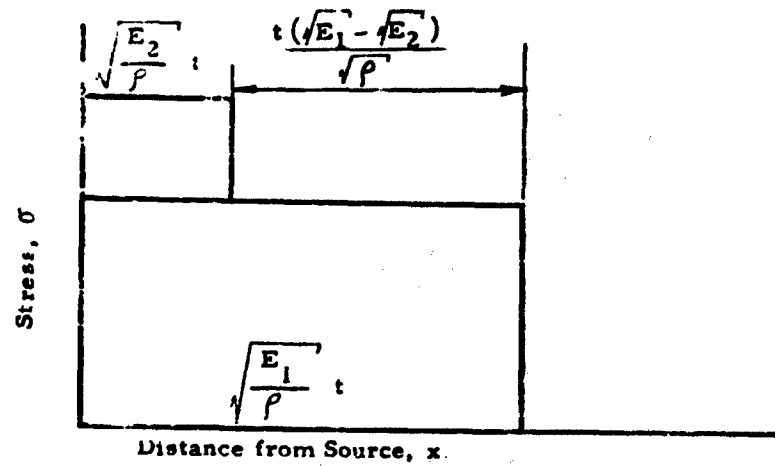
Fig. F-2 RESULTING STRESS WAVES [F-11]
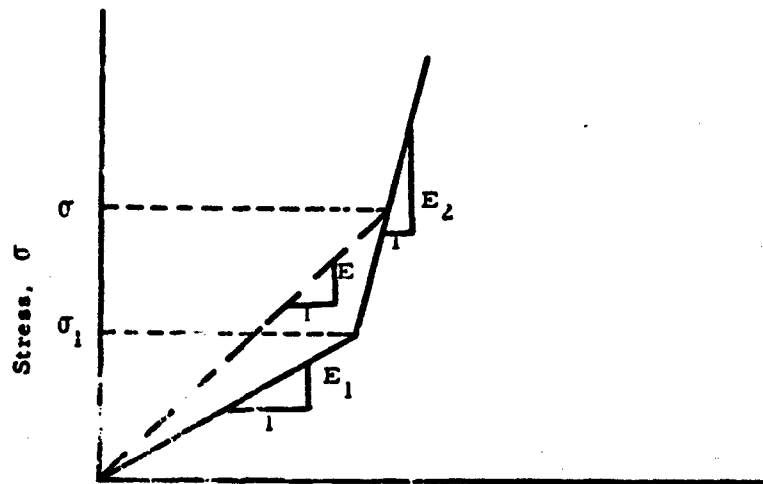
Fig. F-3 BILINEAR STRESS-STRAIN CURVE FOR
E_2 LARGER THAN E_1
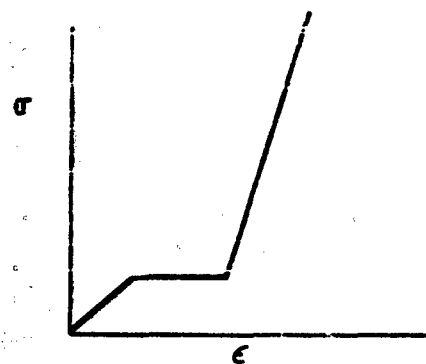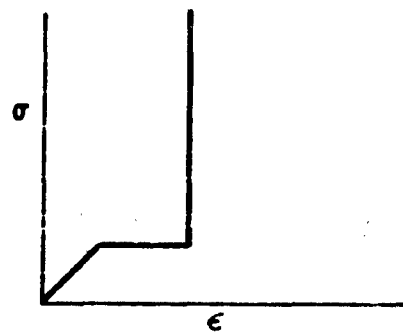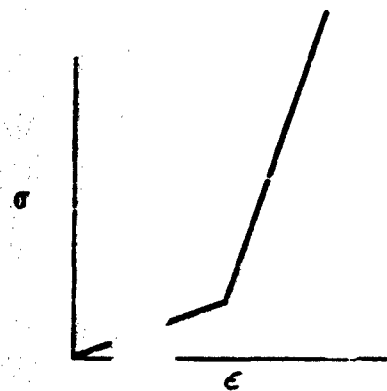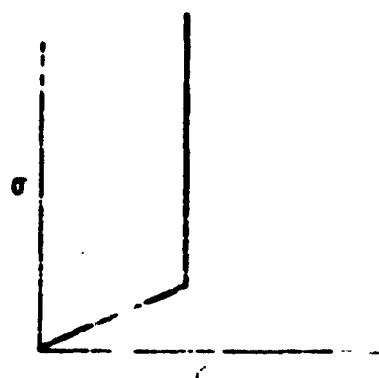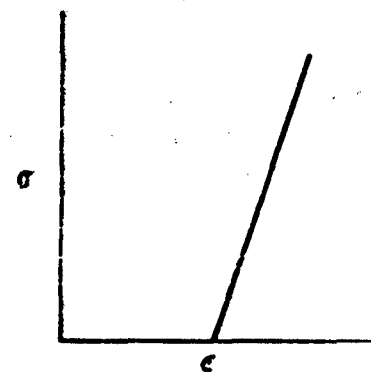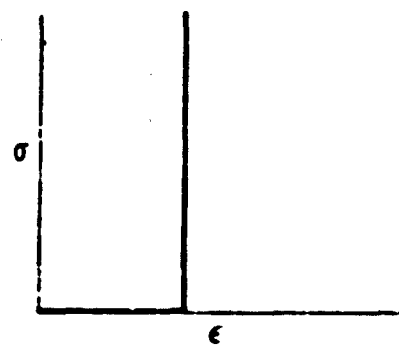
Fig. F-4 LOCKING MATERIALS
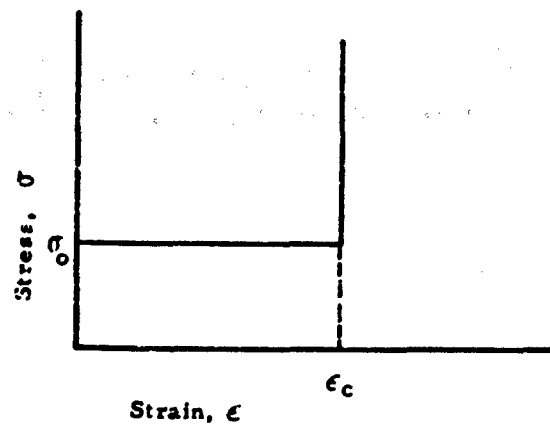
Fig. F-5 RIGID-PLASTIC-LOCKING MEDIA

(a) At Time (t)   (b) At Time t + Δt
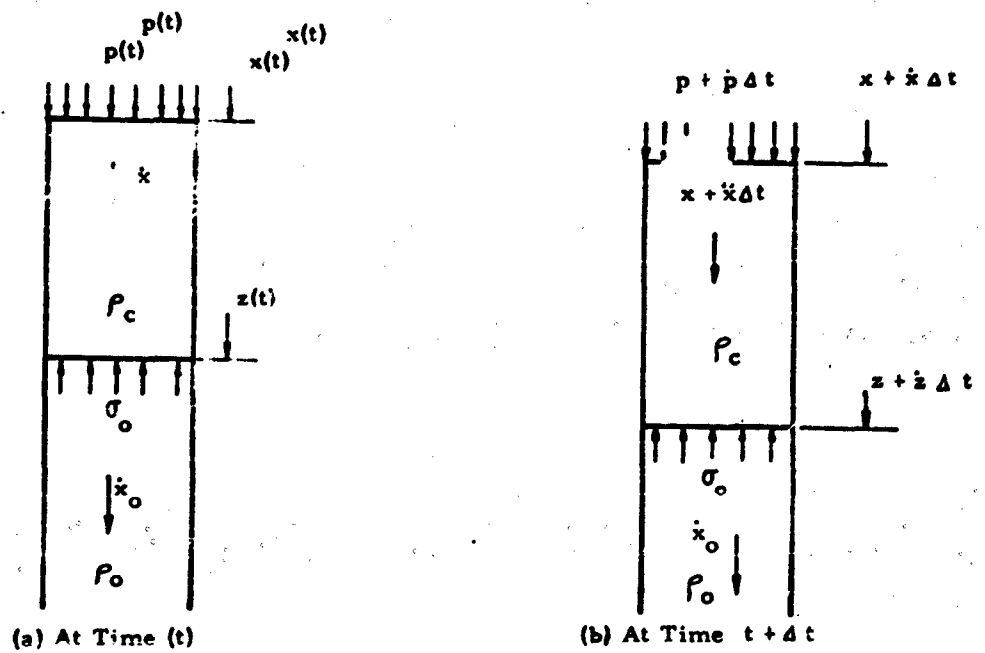
Fig. F-6 SOIL COLUMN BELOW FOOTING
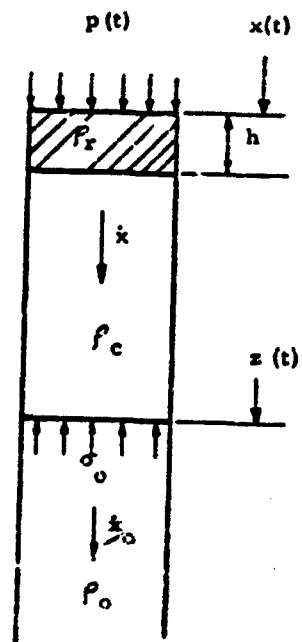
Fig. F-1 SOIL COLUMN WITH RIGID MASS
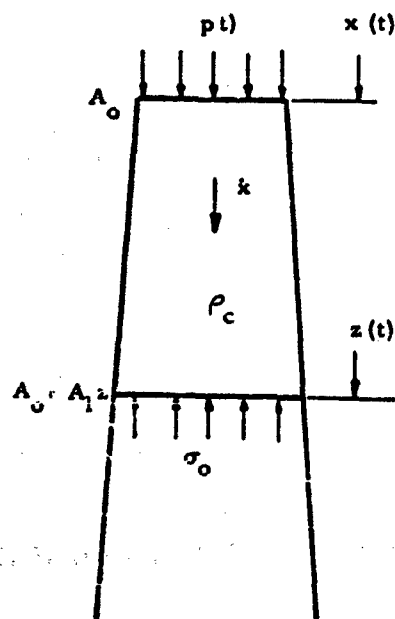
Fig. F-8 FRUSTUM OF PYRAMID AS MATHEMATICAL MODEL

Fig F-9 STEP PULSE

Dimensionless Time, t/t_o
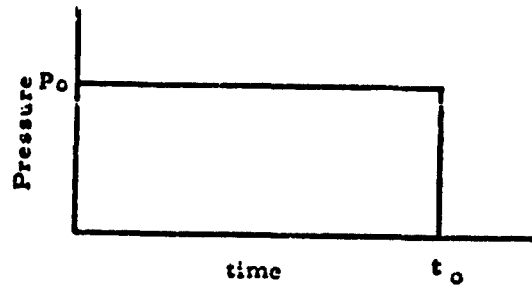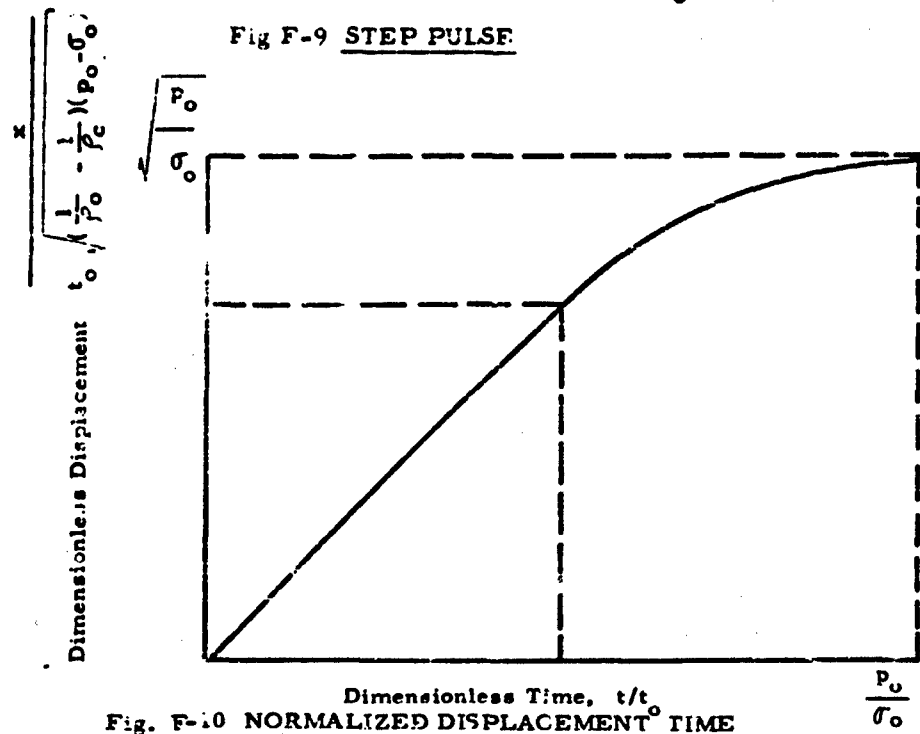
Fig. F-10 NORMALIZED DISPLACEMENT TIME

ARMOUR RESEARCH FOUNDATION OF ILLINOIS INSTITUTE OF TECHNOLOGY

F-25
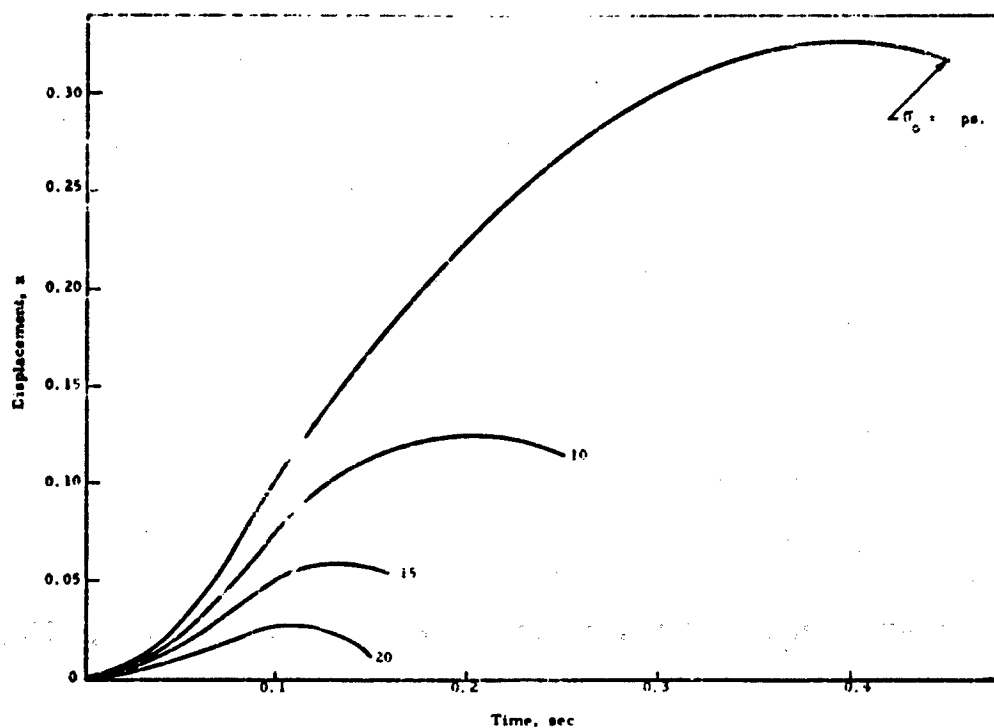
Fig. F-11 RESULTS FOR EXPERIMENT P27
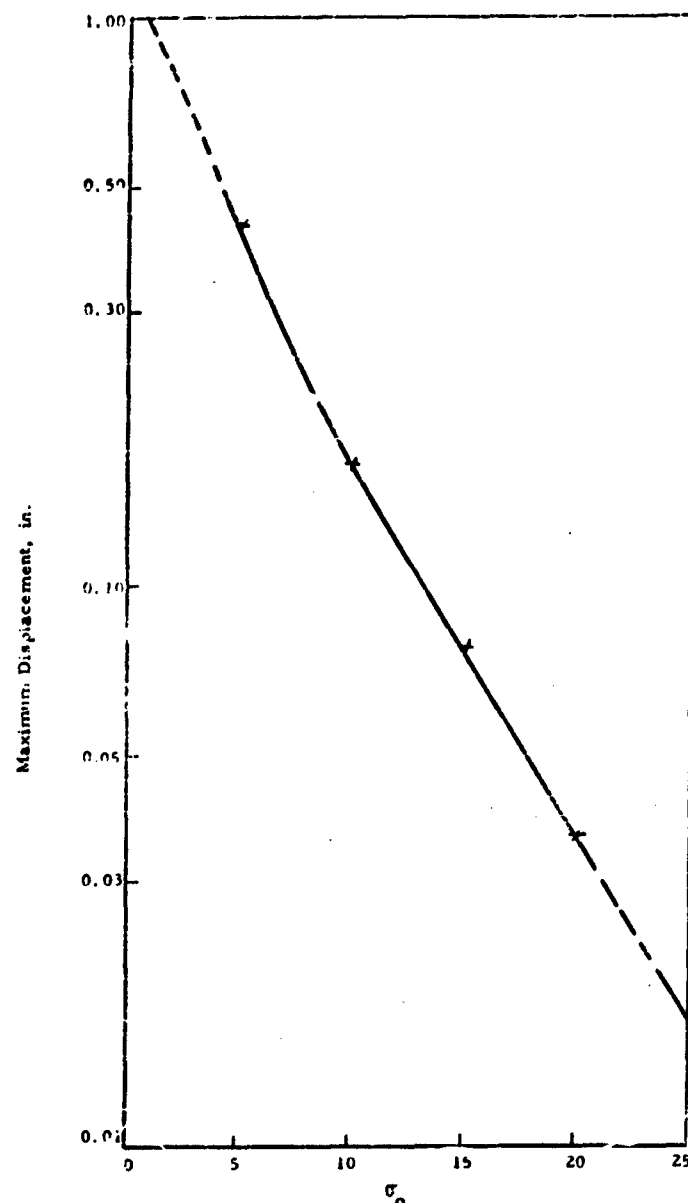
Fig. F-12 MAXIMUM DISPLACEMENTS BASED ON FIG. F-11
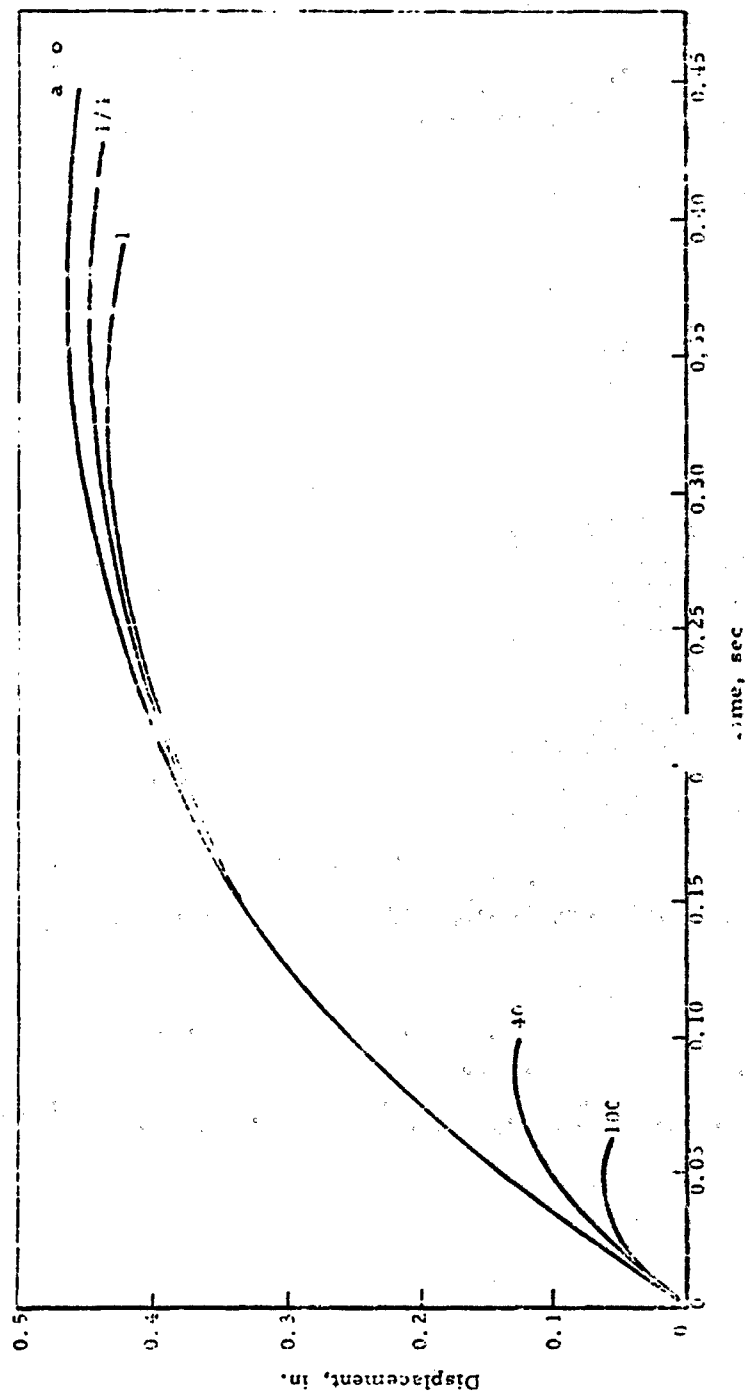
Fig. F-13 VARIATION OF STRESS WITH DEPTH FOR σ_c = 1.25 PSI
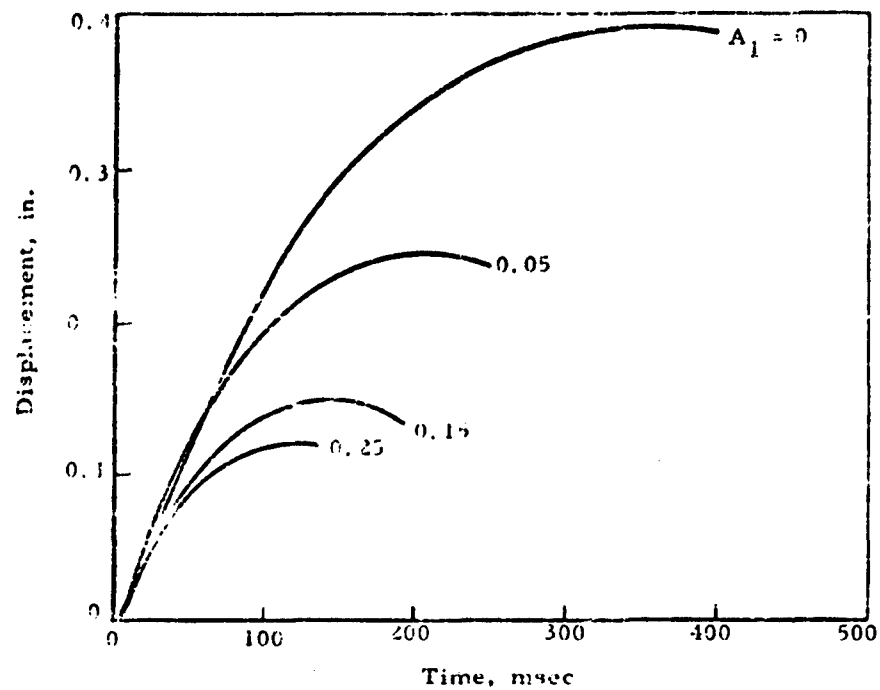
Fig. F-14   LINEAR VARIATION OF AREA WITH DEPTH
For C_0 = 1.25 PSI

TDR-62-1

DISTRIBUTION

No. Cys

HEADQUARTERS USAF

1   Hq USAF (AFOCE), Wash 25, DC
1   Hq USAF (AFCEI-ES), Wash 25, DC
1   Hq USAF (AFRDR), Wash 25, DC
1   Hq USAF (AFOIN-3-3), Wash 25, DC
1   USAF Dep IG for Insp (AFCDI-B-3), Norton AFB, Calif
1   USAF Dep IG for Safety (AFINS), Kirtland AFB, N Mex
1   AFOAR (BRONN), Bldg T-D, Wash 25, DC

MAJOR AIR COMMANDS

1   AFSC (SCT), Andrews AFB, Wash 25, DC
1   AFLC, Wright-Patterson AFB, Ohio
1   ACC, Maxwell AFB, Ala

AFSC ORGANIZATIONS

    A CRL, Hanscom Fld, Bedford, Mass
       (CRRA)
1   (CRZG)
2   ASD (ASAPRL, Tech Doc Library), Wright-Patterson AFB, Ohio
1   BSD (BSR), AF Unit Post Office, Los Angeles 45, Calif

KIRTLAND AFB ORGANIZATIONS

    AFSWC, Kirtland AFB, N Mex
1   (SWEH)
24   (SWOI)
1   (SWRS)

ARMY ACTIVITIES

1   Director, Ballistic Research Laboratories, (Library), Aberdeen Proving Ground, Md
1   Commanding Officer, US Army Engineers, Research & Development Laboratories, Ft. Belvoir, Va
2   Office of the Chief, Corps of Engineers, US Army (Protective Construction Branch), Wash 25, DC

DISTRIBUTION (con't)

No. Cys

Director, US Army Waterways Experiment Sta, P. O. Box 60, Vicksburg, Miss

1   (WESRL)

1   (WESSE)

NAVY ACTIVITIES

1   Chief, Bureau of Yards and Docks, Department of the Navy, Wash 25, DC

1   Commanding Officer and Director, Naval Civil Engineering Laboratory, Port Hueneme, Calif

OTHER DOD ACTIVITIES

2   Chief, Defense Atomic Support Agency, Blast and Shock Division, Wash 25, DC

1   Commander, Field Command, Defense Atomic Support Agency (FCWT 3), Special Weapons Publication Distribution, Sandia Base, N Mex

10   ASTIA (TIPDR), Arlington Hall Sta, Arlington 12, Va

OTHER

1   American Machine and Foundry Company, ATTN: Dr. G. Neidhardt, 7501 North Natchez Avenue, Niles, Ill

1   Mr. Paul Weidlinger, Consulting Engineer, 770 Lexington Avenue, New York 21, NY

1   University of Missouri, School of Mines and Metallurgy, ATTN: Dr. Clark, Rolla, Mo

1   Purdue University, School of Civil Engineering, ATTN: Dr. G. A. Leonards, West Lafayette, Ind

1   University of Illinois, ATTN: Dr. N. M. Newmark, 207 Talbot Laboratory, Urbana, Ill

1   University of Illinois, ATTN: Dr. H. O. Ireland, 207 Talbot Laboratory, Urbana, Ill

1   Massachusetts Institute of Technology, Department of Civil and Sanitary Engineering, ATTN: Dr. Robert V. Whitman, Cambridge 39, Mass

1   St. Louis University, ATTN: Dr. Carl Kisslinger, 3621 Olive Street, St. Louis 8, Mo

1   Armour Research Foundation, Illinois Institute of Technology, 3422 South Dearborn Street, Chicago 15, Ill

TDR-62-9

DISTRIBUTION (con't)

No. Cys

1	University of Massachusetts, Department of Civil Engineering. ATTN: Dr. Merit P. White, Amherst, Mass
1	University of New Mexico, Department of Civil Engineering. ATTN: Dr. Eugene Zwoyer, Albuquerque, N Mex
1	OTS, Department of Commerce, Wash 25, DC
1	Official Record Copy (SWRS)

TABLE OF CONTENTS